UNIVERSITY OF CALIFORNIA
RIVERSIDE

Watershed Transport Processes of Anthropogenic Litter

A Dissertation submitted in partial satisfaction
of the requirements for the degree of

Doctor of Philosophy

in

Environmental Sciences

by

Win C Cowger

September 2021

Dissertation Committee:
Dr. Andrew Gray, Chairperson
Dr. Hoori Ajami
Dr. Chelsea Rochman
Dr. David C. Volz

The Dissertation of Win C Cowger is approved:

_____

_____

_____

_____

Committee Chairperson

University of California, Riverside

Acknowledgments

I am indebted to my family, friends, mentors, mentees, and nonprofit groups without whom this dissertation would not have been possible. Thank you mom for always supporting me to pursue my dreams and telling me to go to college. Thank you Jim for incorporating my love for waste management into your life and for keeping on until the day you passed. Thank you Doug for teaching me to be brave and resilient and stick it out through the tough times. Thank you grandparents for supporting me financially and emotionally throughout the years. Thanks aunts uncles and cousins for watching over me like parents and older siblings throughout the years and saving my life on a few occasions. Thanks Arnie and Rory for setting a high bar of excellence in everything you have done for me to try to mirror throughout my life. Thank you Faith and Sheana for encouraging me and reminding me to be the best I can. Thank you Tori for being my partner throughout all of graduate school and showing me how to have an epic adventure.Thank you friends who keep me smiling, always have my back, and treat me like family. Thank you Andy for taking a chance on a wide-eyed kid with wild dreams of revamping the foundations of science and for teaching me to write concisely and thoroughly. Thank you committee for pushing me to take my science deeper and fuller. Thank you reviewers for being thorough in your reviews, I learned so much from your recommendations. Thank you mentees for implementing some of these wild projects with enthusiasm and for teaching me to be a better mentor. Thank you to all the nonprofit groups and individuals within who took notice of me, gave my work

a purpose, and gave me opportunities beyond my wildest dreams. Without each and every one of you, this dissertation wouldn't have been possible.

This research was supported primarily by UCR's Chancellor's Distinguished Fellowship and an NSF Graduate Research Fellowship. Additional support was provided by the National Marine Sanctuaries, NOAA Marine Debris, UCR's GSA Travel Grants, SETAC North America, and UCR's Undergraduate Learn and Earn Grant.

Copyright Acknowledgements

The text and figures in Chapter 2, in part or in full, are currently under review for publication as “Litter transport, accumulation, and source dynamics on urban roadsides of the Inland Empire, California” in Environmental Research Letters.

The text and figures in Chapter 3, in part or in full, are submitted as “Trash Taxonomy Tool: Harmonizing Classification Systems Used to Describe Trash in Environments” to Science of the Total Environment.

The text and figures in Chapter 4, in part or in full, are submitted as “What the Flux? Floating Macroplastic Concentration-Discharge Relationships Reveal Source and Transport Processes” to Water Resources Research.

The text and figures in Chapter 5, are a reprint of “Microplastic Spectral Classification Needs an Open Source Community: Open Specy to the Rescue!” published in Analytical Chemistry (93) 21 p 7543-7548. W. Cowger created the software and led the writing of the manuscript. Z. Steinmetz led the development and deployment of the Open Specy CRAN package, advanced the code base, advised on development priorities, and drafted and revised the manuscript. O. Herodotou provided technical assistance for web deployment of Open Specy. All others contributed equally by beta testing and validating Open Specy, advising on development priorities, and drafting and revising the manuscript.

The text and figures in Chapter 6, in part or in full, are a reprint of the material as it appears in “Concentration Depth Profiles of Microplastic Particles in River Flow and Implications for Surface Sampling” published in Environmental Science and Technology 55 (9) p 6032-6041. The co-authors James Guilinger, Brandon Fong, and Kryss Waldschlager helped in acquiring and analyzing data. The co-author Dr. Andrew Gray supervised the study and conceived of the fundamental equations and study design. All authors edited, revised, and approved the final version of the manuscript.

Dedication

To my father, Jim Cowger, who never gave up.

ABSTRACT OF THE DISSERTATION

Watershed Transport Processes of Anthropogenic Litter

by

Win C Cowger

Doctor of Philosophy, Graduate Program in Environmental Sciences
University of California, Riverside, September 2021
Dr. Andrew Gray, Chairperson

From abandoned vehicles to tiny plastic particles, anthropogenic litter ends up in the environment and damages ecosystems and economies. River ecosystems are highly impacted by anthropogenic litter and transport litter from land to the ocean. Managers, in particular, need information on watershed litter source and transport processes to make best management decisions. However, approaches to estimating anthropogenic litter fluxes are highly uncertain. In chapter two, we monitored litter accumulation on roadsides in the Inland Empire, CA. We determined that human transport was the primary process transporting litter from the sale location to the roadsides we studied. We quantified litter accumulation rates along roadsides as 1170 (917-1447) $kg^{1}km^{-1}year^{-1}$ and established a harmonization tool in chapter three for comparing our results to other studies. Litter from roadsides is one source of macroplastics in river stormflow along with direct dumping and litter already within the channel. In chapter four, we investigated the sources of macroplastic in the Santa Ana River and tested the hypothesis that

discharge controled macroplastic concentration. The particle size distribution of macroplastic particles (validated with the methodology in chapter five) did not respond to hydrologic transport mode (i.e. stormflow vs lowflow) suggesting that macroplastics in riverflow were primarily sourced from the stream channel. We found that the relationship between discharge and macroplastic concentration was nonmonotonic, and there were path-dependent effects causing variability. We estimated annual macroplastic flux in the Santa Ana as 18.2 (2.9-222.2) metric tonnes per year. Within the channel, microplastics (small plastic particles < 5 mm) can be influenced by turbulence to create concentration depth profiles. In chapter six, we tested the hypothesis that microplastics are transported via a predominant concentration depth profile, commonly assumed in other studies. We found that microplastics can be transported in any transport mode and that misapplication of transport mode assumptions to monitoring and modeling approaches increase uncertainty or systematic bias by multiple orders of magnitude. Overall, these studies support the advancement of the science and management of anthropogenic litter by bringing us closer to accurately monitoring and modeling a watershed mass balance of anthropogenic litter, and its plastics constituents.

Table of Contents

List of Figures

Chapter 2

Chapter 3

Chapter 4

Chapter 5

Chapter 6

Appendix A

Appendix C

Appendix D

List of Tables

Chapter 3

Chapter 5

Chapter 6

Appendix B

Chapter 1: Introduction

1.1 Impact of anthropogenic litter on the watershed environment

Anthropogenic litter causes economic, environmental, and human health issues. Anthropogenic litter on coastal beaches negatively impacts tourism if unmanaged[1]. Plastic is ubiquitous in our air and water and can be up to 84% of the anthropogenic litter items observed in the environment[2]. Plastic debris has proliferated in our oceans[3,4], causing habitat damage[5,6], wildlife endangerment[7,8], impeded navigation[9], and significant economic losses[10]. Aquatic life, from bivalves to whales, can be harmed by ingesting plastic of all sizes[11]. Larger particles present a physical hazard from entanglement and blockage of the digestive tract [7]. Smaller particles are expected to present more significant hazards due to their ability to enter and damage tissues[12]. Widespread contamination[13], ease of ingestion, and toxicity of inherent and adsorbed compounds[14] heighten the potential for bioaccumulation and impacts to both marine life and human health[15,16].

1.2 Management of anthropogenic litter

The Resource Conservation and Recovery Act of 1976 created waste management as we see it today in the United States by requiring regional planning of waste management and closing open landfills[17]. However, some waste still escapes management and ends up in our waterways. The Clean Water Act requires that streams in the United States are monitored to assess potential

pollution from a wide range of contaminants, including anthropogenic litter[18]. In California, the state adopted “The Trash Ammendments” in 2015[19] which regulate anthropogenic litter greater than 5 mm in length in rivers (macro-litter). Once a waterbody is determined "impaired" (polluted), responsible entities must develop plans for rectification by either installing trash capture devices in their storm drains or demonstrating the equivalency using a combination of other mitigation strategies (e.g., public education, street sweeping, river booms, and manual cleanup, and trash capture devices in storm drains.) Remediation of anthropogenic litter in United States' waterways costs hundreds of millions of dollars annually[20,21].

While some remediation of anthropogenic litter is necessary to undo environmental damage, prevention is key to avoiding damage[22]. Educational campaigns[23], improved labeling on products[24], waste bin placement[25], and signage[25] have been shown to prevent anthropogenic litter to varying degrees. In California, policy actions on preventing plastic macro litter include the straw ban[26] and plastic bag ban[27]. Other similar bans are underway across the country. As efforts to prevent macro-debris have progressed, concerns over microplastic impairment have risen[28]. Recent regulations have targeted one type of microplastic, a ban on small plastic particles used in cosmetics (microbeads) (AB 888). There is a critical need by managers and policymakers to understand the sources and transport of anthropogenic litter to develop the best remediation and prevention practices and assess their effectiveness[29].

1.3 History of watershed transport research on anthropogenic litter and open questions

Plastic pollution research today is exponentially growing[30]. Plastic pollution sampling began in 1972 when Edward Carpenter noticed plastic on the Sargasso Sea surface and was catalyzed in 2001 when Charles Moore drew public attention to marine plastic pollution[31,32]. Today plastic pollution in the ocean is increasing[33]. Studies have concluded that the primary source of marine plastic pollution is land-based and transported to the ocean via rivers[34,35]. However, relatively few studies have been conducted in freshwater systems compared to marine systems[36].

A major objective of anthropogenic litter research is to establish strategies for removing anthropogenic litter from the environment and stopping it from getting there in the first place. A watershed mass balance for anthropogenic litter would facilitate assessing and prioritizing these management efforts on land[37]. The basic function for the watershed mass balance states that the change in storage within a watershed must be equal to the fluxes into the watershed subtracted by the fluxes out of the watershed. Fluxes of anthropogenic litter into the watershed include: littering, dumping, and other forms of unsound waste handling[38]. Fluxes of anthropogenic litter out of the watershed environment include: river anthropogenic litter flux[35] and cleanup[39]. Early anthropogenic litter watershed mass balance models have proven uncertain by multiple orders of magnitude due to incomplete understandings of the fluxes into and out of the watershed[40].

Baseline research on terrestrial anthropogenic litter fluxes in Southern California highlights the current understanding of watershed transport dynamics. Kim et al.[41] described anthropogenic litter transported from roadways to rivers through storm drains during runoff events. Van et al.[42] found a correlation between plastic concentration on Southern California beaches and storm event occurrence, suggesting an increased plastic flux during stormflow when discharge is higher. Moore et al.[43] conducted the first study of plastic flux in Los Angeles streams, where they found varying microplastic concentrations with stream depth, suggesting that microplastics have a variety of concentration depth profiles. Open questions remain about how litter gets to roadways, whether discharge can be used to predict anthropogenic litter concentration, and how to predict plastic concentration depth profiles.

While research on anthropogenic litter transport processes advanced, large methodological gaps were revealed which hampered comparisons between studies and accurate characterization of anthropogenic litter. Studies worldwide were creating unique classification schemes for anthropogenic litter (e.g. paper, plastic, glass) without a strategy for merging those classes with other studies that may have used slightly different words[44]. This presented an opportunity to develop a relational database and software tool for harmonizing trash classes. Microplastic analysis began to adopt Raman and FTIR spectroscopy as the gold standards for

identifying polymer composition of plastic in samples [45]. However, the commercial software available was prohibitively expensive and innaccurate[46]. This presented an opportunity to develop affordable and accurate software for FTIR and Raman spectral analysis of plastic samples. While conducting the primary research in this dissertation, we advanced these methodological components to support our research and the broader scientific community.

1.4 Translating sediment transport fundamentals to anthropogenic litter

While flux-based anthropogenic litter monitoring in rivers first began in the 1990s[47,48], suspended loads of 'natural' mineral and organic sediments have been monitored in rivers for over a century[49,50]. Fundamentals of natural sediment transport dynamics seem to apply to anthropogenic litter transport[51,52], which is expected since anthropogenic litter is composed of particles of a wide range of shapes and sizes similar to natural sediment. However, the majority (> 99%) of mineral sediments found in streams display a narrow range of particle densities, most of which are greater than water[53], unlike plastic density which varies from 0.03 – 2.2 g^1ml^{-1} [51,54]. Other anthropogenic litter factors like shape[55] and rigidity[56] can also differ from mineral particles. Anthropogenic litter must always be initially sourced from human activities, but mineral sediment sources are naturally ubiquitous. These and other differences may compromise the generalizability of mineral transport equations. By studying the watershed transport of anthropogenic litter, we will develop a more robust understanding of particle transport as a whole.

1.5 Overview of research objectives and hypotheses

In the chapters of this dissertation, we advance current knowledge gaps in the scientific understandings of watershed transport processes of anthropogenic litter and establish new methodologies for improving study comparability and accuracy. In chapter 2, we assess the sources and transport of litter accumulation along roadsides in the Inland Empire. In chapter 3, we introduce and discuss a method we developed for making the results found in chapter 2 comparable with other studies. In chapter 4, we assess sources of macroplastic and their concentration discharge relationships in Santa Ana riverflow. In chapter 5, we introduce and discuss a method we developed for accurately characterizing plastic material types of the macroplastic particles found in chapter 4. In chapter 6, we improve plastic flux estimation for fluvial systems by expanding the theory of particle concentration depth profiles to microplastic particles using the Rouse profile equation.

Chapter 2: Litter generation on roadsides

2.1 Abstract

Urban areas are the primary source of human-made litter globally, and roadsides are a primary accumulation location in urban areas. The goals of this study were to investigate how litter arrives at roadsides and determine the accumulation rate and composition of roadside litter. We monitored select roadsides in the Inland Empire, California, for litter abundance (count) and composition (material, item, and brand type) primarily during periods with little rain. Receipt litter with time and sale location information was used to investigate whether wind, runoff, or human travel were dominant transport agents. Only 9% of the receipts could have experienced runoff, and wind direction was not correlated to the receipt transport direction. However, human travel and receipt transport distances were similar in magnitude and distribution, suggesting that the displacement of litter from the place of purchase was predominantly affected by human travel during dry periods. The median distance receipts traveled from the sale location to the litter observation location was 1.6 km, suggesting that most sources were nearby to where the litter was found. Litter accumulation rates were surprisingly stable (mean 40349 (33255-47865) pieces^{1}km^{-1}year^{-1} or 1170 (917-1447) kg^{1}km^{-1}year^{-1}) despite our repeated cleanups and the COVID-19 stay-at-home orders. A new approach was employed to hierarchically bootstrap litter composition proportions and estimate uncertainties. The most abundant materials were plastic and paper.

Food-related items and tobacco products were the most common item types. The identified branded objects were from the primary manufacturers (Philip Morris (4, 2-7 %), Mars Incorporated (2, 1-3 %), RJ Reynolds (2, 1-3 %), and Jack in The Box (1, 1-3 %)), but unbranded objects were prevalent. Therefore, identifiable persistent labelling on all products would benefit future litter-related corporate social responsibility efforts. Future studies should also investigate transport during wet periods, when runoff may be a more effective transport agent. High-resolution monitoring on roadsides can inform urban litter prevention strategies by elucidating litter source, transport, and accumulation dynamics.

2.2 Introduction

Urban areas are the primary sources of anthropogenic litter that damages aquatic and terrestrial environments[34,35,39,57]. The source of all anthropogenic litter is at the production location[58]. Production lines transform litter into various forms and transport it to a sale location. Consumers purchase the litter from the sale location and transport it further[38]. At any point across this system, there can be a loss of litter to the urban environment. Roadsides are the primary litter accumulation location within urban areas[38]. In the United States, the major roadside litter supply processes are suspected to be individual littering, illegal dumping, and improper household waste disposal[59]. Although these mechanisms are typically associated with consumer actions, the entire supply chain and governing bodies need to be engaged to solve litter pollution[22]. Producers can create more reusable or less

harmful products[60], and governments can pass ordinances to regulate products and improve waste management strategies[22].

After humans mismanage litter and it escapes into the environment, it can be transported by wind[61] or runoff[62] to other locations or removed by cleanup activities or degradation. Litter observed during roadside monitoring campaigns will reflect an integration of these processes. Recent policy research has highlighted the importance of local action[63] and source identification[64] on ending litter accumulation. A strategy for identifying which sources are pertinent to a region could be a critical decision-making tool. Receipts are a novel piece of litter that often have location and time information about the sale location they originated from. The first goal of this study is to use receipt trajectories to unravel the relative importance of runoff, wind, and human transport mechanisms and describe the proximity of litter sources to litter observations.

Identifying prevention strategies to end the accumulation of roadside litter is a critical step for improving urban environmental quality and avoiding the financial costs of cleanup[65]. A common observation in littering behavior research is that people are more likely to litter in littered areas[66]. We hypothesized that removing litter from roadsides to keep them clean would decrease litter accumulation throughout the study duration. During the COVID-19 pandemic other studies observed increases in the proportion of personal protective equipment and sanitary products[67,68] and decreases in other types of pollution, e.g. air[69]. The second goal

of this study is to examine the role of frequent cleanup in reducing litter accumulation and the impact that the COVID-19 pandemic had on litter.

Roadside litter composition is critical to describing litter properties (which inform hazard and fate assessment) and identifying litter sources. Typically, material type (resource) and item type (shape) compositions are assessed to describe litter. Brand information directly ties litter to a corporation that produces it and is less often measured[70–72]. Litter composition is often reported as a total proportion of litter classes (material, item, brand types) without any uncertainty metrics[73]. Information about brands can be used to hold producers accountable and improve environmental conditions through corporate social responsibility initiatives[74]. Corporate social responsibility initiatives are voluntary and mandatory actions by corporations to improve social and environmental quality. Corporate social responsibility initiatives could benefit from advancing tools that facilitate converting brand information to manufacturers and quantifying uncertainty in brand proportions observed on litter in the environment. Recently, a new relational and hierarchical classification system (Trash Taxonomy) was developed to thoroughly assess litter composition by material, item, and brand, but it has not been used in the peer-reviewed literature[75]. The third goal of this study is to assess gaps in current litter classification strategies and quantify the uncertainty of litter composition proportion estimates.

2.3 Methods

This study monitored roadside litter in the Inland Empire, California, using high-resolution surveying of litter accumulation and composition. We aim to assess transport, accumulation, and source dynamics of litter to inform policy and litter management.

2.3.1 Survey region

The Inland Empire includes San Bernardino County and Riverside County, California, United States (Figure 2-1). The topography of the area includes mountains and valley regions, and major land uses are natural vegetation (>90%), developed (2-5%), and agricultural (1-4%) areas[76]. The climate is Mediterranean with 50 cm of average annual precipitation, primarily falling as rain from October through April, and hot dry summers with little to no rain. The region has a mean population density of 60 people^{1}km^{-2}, median poverty rate of 41%, and median traffic density of 543 (vehicles-km^{1}hr^{-1}km^{-1})[77–79]. The Inland Empire has a robust waste management system that includes municipal and private street-side collection of three recovery streams (landfill, recycling, and yard waste), street sweeping, litter capture devices in storm drains and rivers, as well as regular and ad-hoc cleanups by municipal employees and community members.

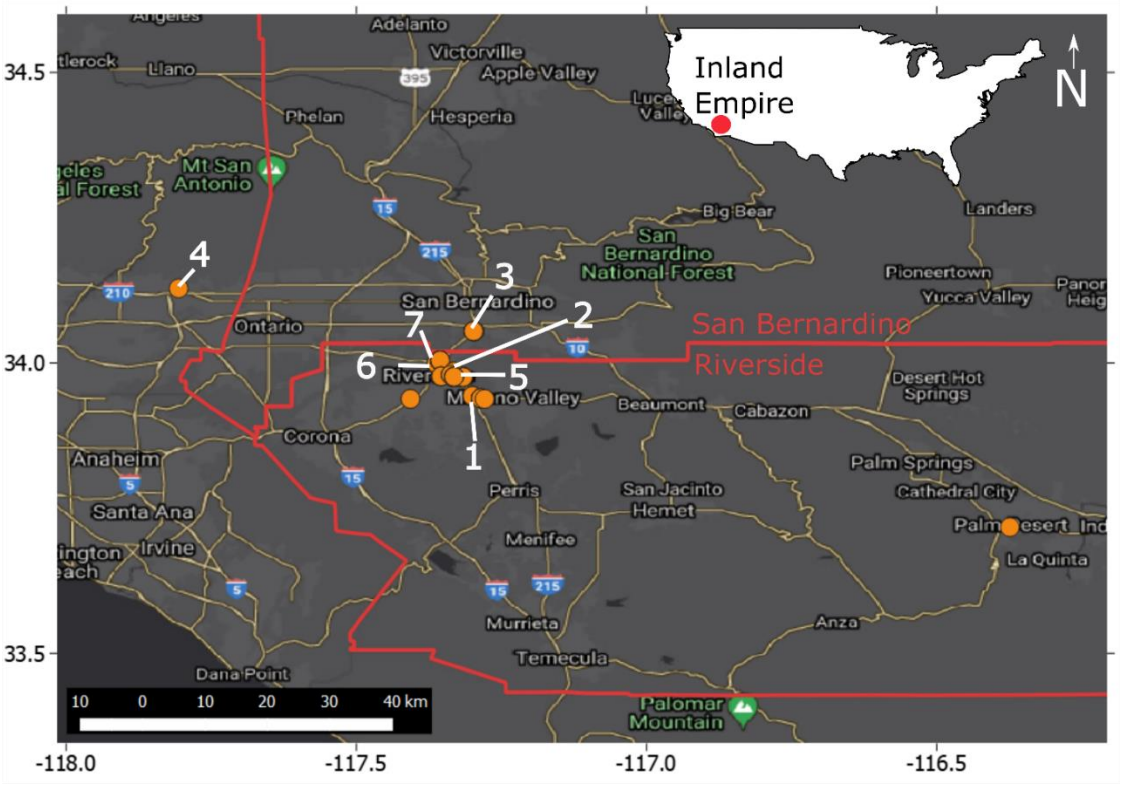

Figure 2-1: Monitoring locations site numbers are labeled on the map and orange dots show locations where receipts were found. We used all receipts found in this study, but not all study locations met the standardization criteria for monitoring locations. That is why some receipts do not have a site label. Riverside and San Bernardino counties boundaries are in red (the Inland Empire). A red dot is placed on the inset map of the United States where the Inland Empire is located. Numbers on the borders are latitude and longitude coordinates.

2.3.2 Survey methods

Eighteen researchers each surveyed a unique ~100 to 1000 meter length of roadside for litter 1-3 times per week for two to four weeks in 2018 or 2019 in the following Inland Empire cities: Riverside, Moreno Valley, Loma Linda, San Dimas, and Palm Desert (Figure 2-1). Both sides of the road were surveyed at each site, including the curb, sidewalk, and back sidewalk margin. Private property was not

entered. Site length depended on litter abundance, and researchers were instructed to survey until approximately 100-300 pieces of litter were observed during their first survey. This strategy was used to ensure a low likelihood of non-detect. Each researcher recorded the site conditions, observations, and any changes to the methodology. To maintain safety, researchers generally stayed on the sidewalk out of the road. Observations indicated that most litter was concentrated near the sidewalk curb and along the back sidewalk margin.

Before beginning surveys, all surveyors were trained in person during a 1-hour session and joined a group called Our Clean Community in Litterati, a crowdsourcing litter app[80] for data collection. Although we used the Litterati application in this study, Open Litter Map[81] or geolocated images on any phone could produce the same results.

During each survey, all litter (> 1 cm length) was recorded and removed from the study location. Litterati was utilized to photograph litter and record the material, item, and brand type. Location (± 7 m), date, and time (Figure 2-2). Digital images of each object were taken at a location within 1 m of where the object was found (Figure 2-2A) while ensuring branding marks were visible in the image (Figure 2-2C). Receipts were flattened so that all information on the receipt was viewable in the image (Figure 2-2A). If multiple objects of the same type or fragments from a single object were found, those objects were logged together in one image. Bags full of litter were not deconstructed, but loose piles of litter were. Large or

hazardous objects were left at the site and only photographed on first observation. Images were retaken if blurry. Trash classes were recorded in the app during cleanup. Material and item types were categorized in Litterati (Figure 2-2C) using the most up-to-date version of the Trash Taxonomy[75]. When a litter class did not exist in the Trash Taxonomy, a new class was created to describe the litter. Brands were recorded when found on an object.

Post survey, each researcher delineated their study area on a map using Google Maps (Figure 2-2B). Litter location accuracy was calculated as the mean distance from all points recorded outside the study area to the surveyed boundary (Figure 2-2B). Each researcher cleaned their data by removing duplicate or inaccurate images, correcting incorrect tags, noting when multiple objects were in one image, and identifying any data points that were not for this study. In total, eighteen locations were surveyed, and 146 receipts were found.

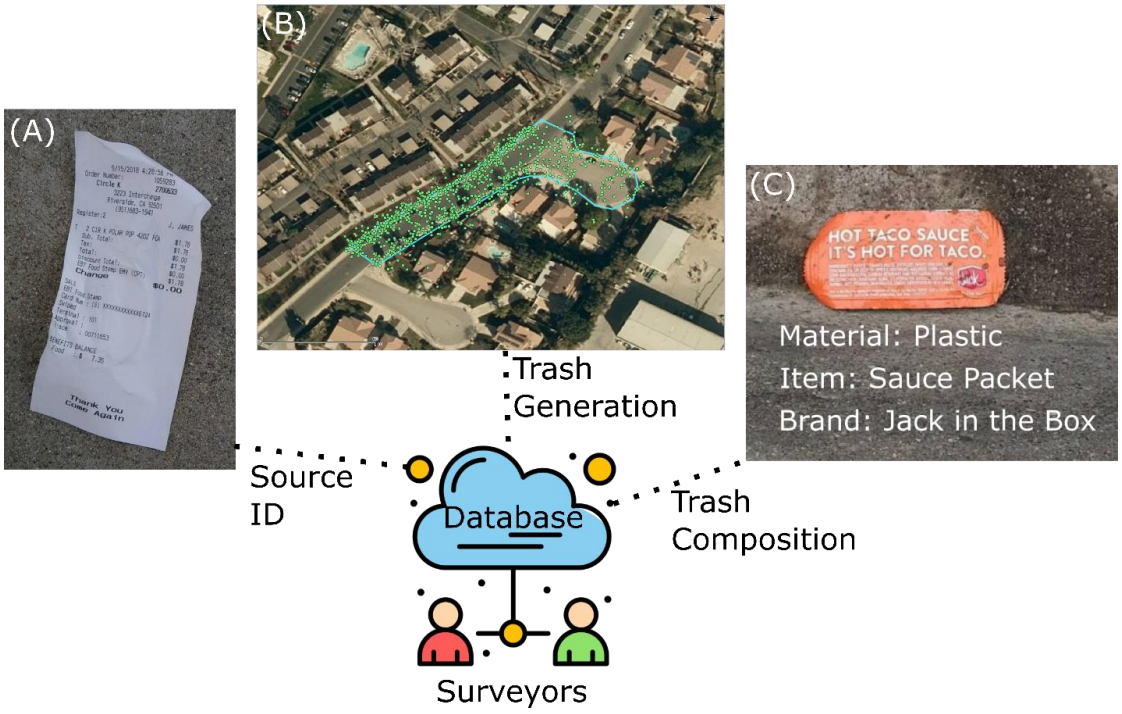

Figure 2-2: All data from surveyors were compiled in a centralized database using Litterati. A) When receipts were found, they were laid out flat to ensure readability. Source identification in this study was described using the information on receipts found during the study. B) All litter observations for Site 7 are presented. Every piece of litter has a geographic coordinate and a timestamp. Survey boundaries (blue outline) were provided for each monitoring location. Litter accumulation rates were computed using the observations at each site on each day. C) During the survey, we described the material, item, and brand type of every piece of litter found and recorded images of the pieces of litter. This data was used to interpret litter composition.

Data were archived by Litterati and accessible through their data portal[80], including images, user input labels, time stamps, latitude, and longitude coordinates of every piece of litter (Figure 2-2). Further refinement of the data resulted in two datasets structured for our specific study objectives. The first dataset (Receipt dataset) includes 146 receipts found at all eighteen of the survey locations. Receipt observations were extracted from the total dataset by searching the tags for the

keyword "receipt". Of the 146 receipts, 72 had both time and location information for the sale transaction, 85 had at least location information, and 75 had at least time information. The second dataset (Monitoring dataset) focused on data from survey locations with similar quality control procedures to compare and combine litter accumulation and composition data across sites.

2.3.2.1 Receipt dataset

We calculated transport metrics for receipts including time and distance traveled and corresponding precipitation, wind, and human transport metrics. Receipt travel distances were calculated as Haversine distance (straight line) from the latitude and longitude coordinates where the object was found to the address listed or nearest possible location. Haversine distance was divided by the time between when the receipt was created and when it was found to determine the transport rate (m^1day^{-1}). We compiled wind (mean daily wind direction, mean daily wind speed) and precipitation (total daily) data for the entire observation period from a weather station (KRAL) near the center of our study region using the Midwestern Regional Climate Center's cli-MATE application[82]. Mean daily wind directions were vector averaged with daily wind speed for the receipt's potential duration in the environment to estimate the vector mean wind direction the receipt could have experienced. We acknowledge that a single weather station cannot represent spatial variability of wind direction and speed. However, meteorological stations are limited in the study region and gridded climate products are prone to large

uncertainties. The receipt transport direction was calculated as the straight direction from the address on the receipt to where the receipt was found. Receipts with distances were collected from 2018-09-16 to 2019-11-18, and all were found in Riverside and San Bernadino counties. Data on human trip distances from 2019-01-01 to 2019-12-31 in San Bernardino and Riverside Counties were acquired from the Bureau of Transportation Statistics[83]. These data were created using smartphone tracking data and aggregated daily to the county level. Trips were defined as movements with a stay of longer than 10 minutes. The trip distances for each day were aggregated in scaled histogram bins. We made the data continuous by randomly sampling the histogram bins with uniform probability distributions ranging from the smallest to largest value for the bin.

2.3.2.2 Monitoring dataset

The monitoring data passed final data cleaning and quality assurance protocols before being used in statistical analysis. All surveyors included in the monitoring dataset needed to have cleaned their data and removed trash from their entire site at some point during the study to ensure high quality and comparable data. Only 7 of the 18 locations met this criterion and the others were excluded. When multiple objects occurred in one image, the image metadata was copied to create additional entries for different litter types. One site was unable to be fully cleaned during the first two days of the study, so the data for those first two days were omitted from the monitoring dataset. A technical malfunction in the app disrupted data logging

at one site during one survey, but the litter was manually tallied outside Litterati and added to the database without a timestamp or latitude and longitude information. One site was surveyed on two separate occasions. First, a year before the COVID-19 pandemic and second, during the 2020 stay-at-home orders issued by California Governor Gavin Newsome effective March 19, 2020. The activity of walking around the neighborhood (essential for conducting this study) was permitted by the stay-at-home order. The stay-at-home order continued throughout the second survey period.

Datasets were reconciled to the Trash Taxonomy tables using Open Refine[84] and reconcile-csv[85], and socio-geographical information was added to them. We identified the Census tract for survey locations using the Census web explorer. Demographic and environmental data were extracted for each location by merging Census tracts with the 2015 Census tract planning database[78] and CalEnviroScreen 3.0 dataset[79]. Population density was calculated by dividing the population in the tract by the tract area. Road length was calculated in Google Earth by tracing the centerline of the road in the monitoring area. At monitoring locations, mean population density was 1617 people^{-1}km^{-2}, median percent of people in poverty of 38%, median traffic density of 1529 (vehicles-km^{1}hr^{-1}km^{-1}), containing only urban land use areas (residential and mixed commercial-residential). Road widths ranged from 10 m to 25 m, and road lengths ranged from 121 m to 483 m.

Litter accumulation rates were calculated for each date by dividing the number of litter observed by the total number of days since the previous survey and by the length of the surveyed road. We also computed the litter mass accumulation by conducting a literature review to find the average mass of each litter object[72,86,87]. When a reasonable estimate for an object's mass was unavailable, we used the suggested 82.5 g estimate[86]. The mass conversion table was applied to every found object to compute mass accumulation rates similar to the count accumulation rates.

Litter composition was assessed using the Trash Taxonomy. Data were merged to the most up-to-date Trash Taxonomy material, items, and brand alias, and hierarchy tables. This procedure makes the data compatible with the 69 other litter surveys incorporated in the Trash Taxonomy. Litter composition was computed for each survey day by dividing the total number of pieces observed for an individual category by the total number of pieces observed.

2.3.3 Statistical analysis

2.3.3.1 Origins and transport processes

We tested three potential litter transport mechanisms: runoff, wind, and people. If precipitation occurred between when the receipts were created and found, we considered runoff a possible transport mechanism. Receipts that had time difference data (75) were used for precipitation analysis. If the vector mean wind

and receipt transport directions were correlated by circular correlatio [88] (absolute value of correlation > 0.2 and $p < 0.05$), we would consider wind a possible important transport mechanism. Receipts that had time and location data (72) were used in the wind direction correlation analysis. We also implemented a spoke plot[89] for visualizing circular correlations, which was not implemented elsewhere in R to our knowledge. The cumulative distributions of litter transport distances and human trip distances were assessed for similarities and differences for the 85 receipts with location data. Quantiles were derived for the receipt and human transport distance distributions at 0.01 – 0.99 for a 0.01 step size, and an ordinary linear regression was performed between the two $\log_{10}$ transformed distributions to assess the offset and goodness of fit.

2.3.3.2 Litter accumulation rates

The effect of persistent cleanup as an intervention to litter count accumulation was tested by plotting each survey site's litter accumulation time series and assessing the change in litter accumulation over each study duration using linear regression. We expected greater than a 50% difference in mean litter accumulation rate between pre-COVID-19 and during COVID-19 stay-at-home. The significance of differences were assessed using overlap in 95% confidence intervals. Mean litter accumulation confidence intervals were generated by bootstrapping (resampling with replacement, n = 10,000). Post hoc power analysis was conducted in R to determine what shifts in the mean litter accumulation rate could be visible if future

repeat studies were conducted. The mean litter accumulation rate from all monitoring observations, the total sample size, and the sample standard deviation were used in a t-test power analysis to determine the Cohens d effect size which would be necessary to achieve a power of 0.8 and a p value of 0.05 if the same study were repeated.

2.3.3.3 Litter composition

Differences between litter class proportions were assessed statistically using confidence intervals calculated using bootstrapped (resampling with replacement, n = 10,000) mean proportions for each survey. Sunburst plots were generated with the plotly package[90] and the data.tree package[91] to hierarchically display clustered proportions and their confidence intervals. Any material or item class with a mean proportion less than 10% was considered non-essential to display. Any brand class with a mean proportion of less than 1% was considered non-essential to display.

2.3.3.4 Data availability

All data and source code for data analysis and figure creation is provided open access (CC BY 4.0) with version control history on GitHub (https://github.com/wincowgerDEV/OurCleanCommunity). For original raw data from sources published beyond this study, please see references linked throughout the text.

2.4 Results

2.4.1 Origins and transport processes

Three plausible mechanisms could transport receipts in the Inland Empire: runoff, wind, and people. The median receipt transport rate was 290 m^1day^{-1}, and 50% of the data fell between 147 m^1day^{-1} and 1497 m^1day^{-1}. Although we do not have estimates of litter transport rates over land due to wind or runoff, we suspect the transport rates observed were much faster than those processes. Nevertheless, we rigorously tested the likelihood of wind and runoff transport. Based on the precipitation data during the receipt's potential duration in the environment, we determined that 68 out of 75 receipts (91 %) did not experience any precipitation (Figure 2-3A). We compared the vector mean wind direction during the receipt's potential duration in the environment to the mean transport direction using circular correlation (Figure 2-3B). The Pearson's product moment circular correlation indicated no correlation between wind direction and receipt transport direction (correlation -0.1, p value 0.357). The receipt transport distances followed a similar cumulative distribution function (log normal) to the human trip distance but were offset to smaller distances (Figure 2-3C). Of the 85 receipts with sale locations found in the Inland Empire, the maximum transport distance was 136 km and the minimum was 27 m (three times as large as the estimated mean location uncertainty (7 m)) (Figure 2-3C). Half of the receipts originated from less than 1.67 km away from where they were found. Linear regression fit to log_{10} transformed

data between the paired quantile values revealed that the offset between receipt and human trip distances increased by 1.1 times per unit of human trip distance and had a y-intercept of -0.9 (Figure A-1).

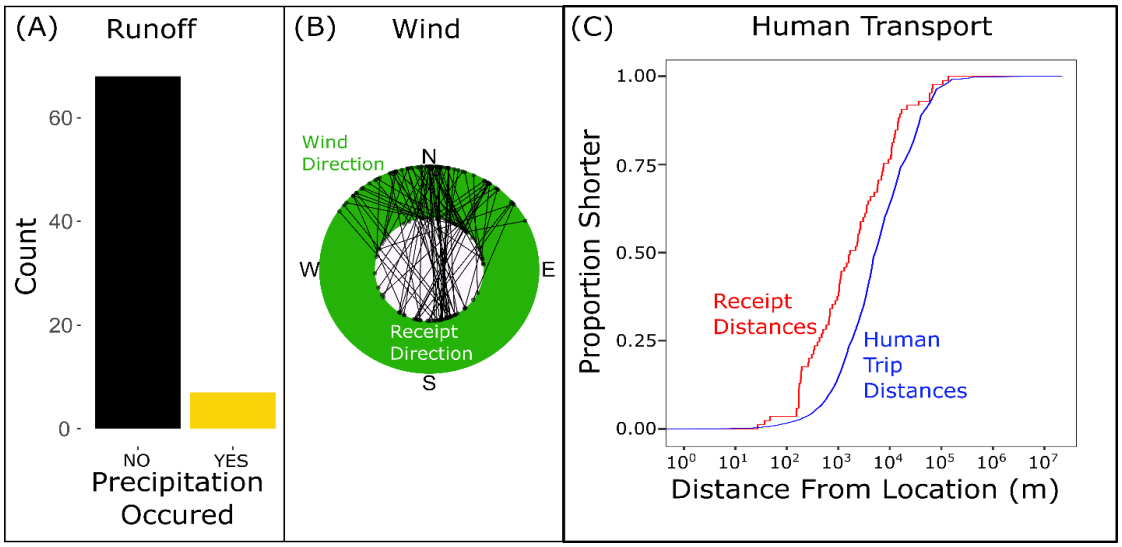

Figure 2-3: A) Precipitation occurring during the receipts potential time in the environment. YES stands for the receipt could have experienced precipitation, NO means the receipt couldn't have experienced precipitation. We found precipitation could not be a dominant process transporting the receipts. B) A spoke plot displaying the circular correlation between direction receipts came from (inner circle), and vector mean wind directions (outer circle). North (360º) is up. The lines connecting the points represent the paired directions for a single receipt. The plot can roughly be interpreted as similar directions when the line does not cross the central circle and different directions when the line does cross the central circle. The Pearson product moment circular correlation is -0.1 and p-value 0.36. There is no correlation between wind direction and receipt travel direction. C) ECDFs of distance to receipt address (red) and the human trip travel distance (blue) from the Bureau of Transportation. Receipts were slightly shifted to lower distances than the trips. Human travel appears to be the most probable mechanism for the majority of observed receipt transport.

2.4.2 Litter accumulation rates

The majority of monitoring sites had relatively stable litter accumulation rates throughout the sampling period (Figure 2-4). Most observations at sites were within half an order of magnitude of one another (Figure 2-5). We did not find a steady drop in the litter accumulation rate at any monitoring locations (Figure 2-4). Instead, trends in litter accumulation rates seem random throughout each survey and none were significant (Figure 2-4). Power analysis revealed that a Cohen's d effect size of 0.45 (small-medium effect) amounting to a shift of 37% from the current mean accumulation rate of the full monitoring dataset (Figure 2-5) would be required to attain a power of 0.8 and p value of 0.05 for future repeat studies.

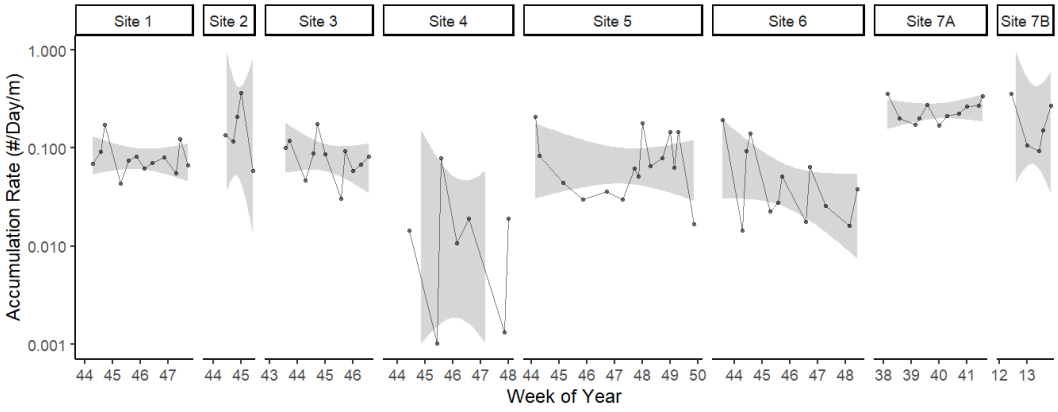

Figure 2-4: Litter accumulation rates for each monitoring observation (count per day per meter). Site name is indicated on the top axis. The total count observed during each sample date and a plot showing comparisons between sample days are indicated in the supplemental information (Figure A-2). Sample dates (x-axis) were reported as week numbers for the year and differed between sites. Confidence intervals (95%) for linear regressions were plotted for the time series to assess the effectiveness of persistent cleanup on litter generation. None of the sites show significant decreasing signals in litter accumulation.

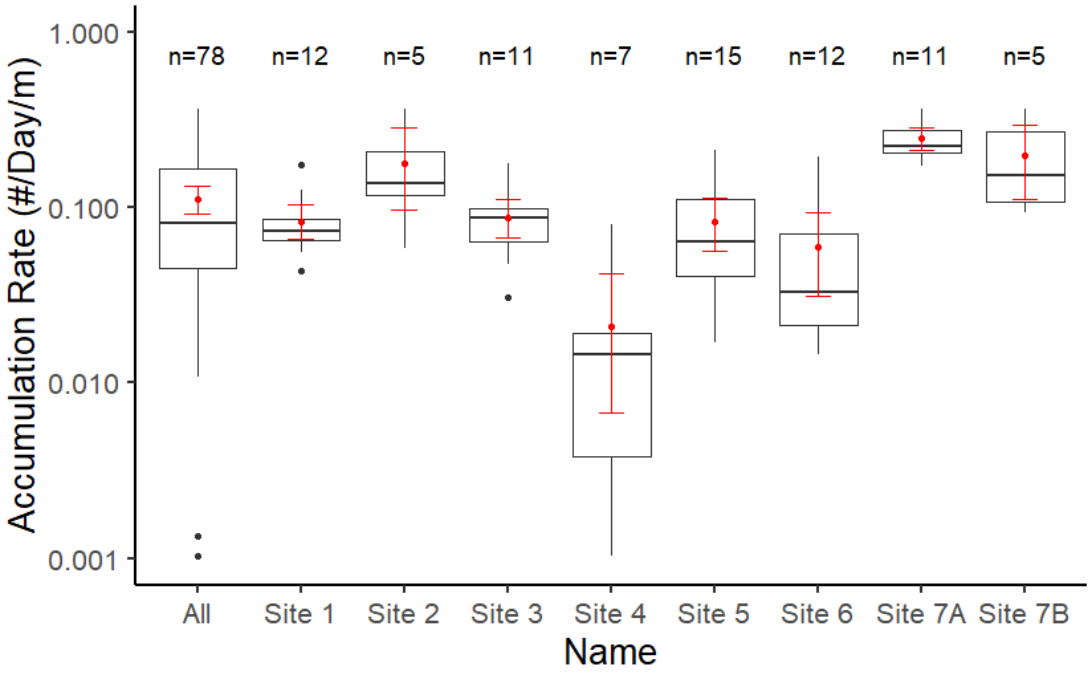

Figure 2-5: Differences in median litter accumulation rate. X axis is the site name. Y axis is the litter accumulation rate in count per day per meter. Boxplots show the median line and notched 95% confidence intervals. Number of observations are indicated above each boxplot. Site 7A was before COVID-19 and 7B was during COVID-19 stay at home. Red error bars and red points correspond to the mean and bootstrapped confidence intervals for each. The total count of study days for each location is shown at the top.

We observed a small decrease (20 %) in the mean litter accumulation rate during COVID-19 stay-at-home orders at Site 7 (0.2, 0.11-0.29 $\#^{1}m^{-1}day^{-1}$) compared to before COVID-19 (0.24, 0.21-0.26 $\#^{1}m^{-1}day^{-1}$), but the means were not significantly different. Site mean litter accumulation rates varied over an order of magnitude, ranging from 0.021 to 0.25 $\#^{1}m^{-1}day^{-1}$. Across surveys, most of the litter accumulation rates fell within a factor of four (0.045 - 0.166 $\#^{1}m^{-1}day^{-1}$) (Figure 2-5). The total mean annual accumulation rate is estimated to be 40349 (33255-

47865) pieces^{1}km^{-1}year^{-1} or 1170 (917-1447) kg^{1}km^{-1}year^{-1} for the region, similar to the city of Riverside estimate of 2855 kg^{1}km^{-1}year^{-1}[92].

2.4.3 Litter composition

The most common material types found in the litter surveys were plastic (mean proportion: 56, 53-59 %) and paper (33, 30-35 %) (Figure 2-6A). Food-related items (38, 35-42 %) and tobacco-related items (14, 11-17 %) were the most abundant litter item types (Figure 2-6B). Correspondingly the top four brands were all cigarette and food producers: Philip Morris (4, 2-7 %), Mars Incorporated (2, 1-3 %), RJ Reynolds (2, 1-3 %), and Jack in The Box (1, 1-3 %) (Figure 2-6C). The majority of objects were unbranded (66, 62-70 %), and there were also many brands (13, 11-15 %) that were identifiable but could not be merged with the Trash Taxonomy.

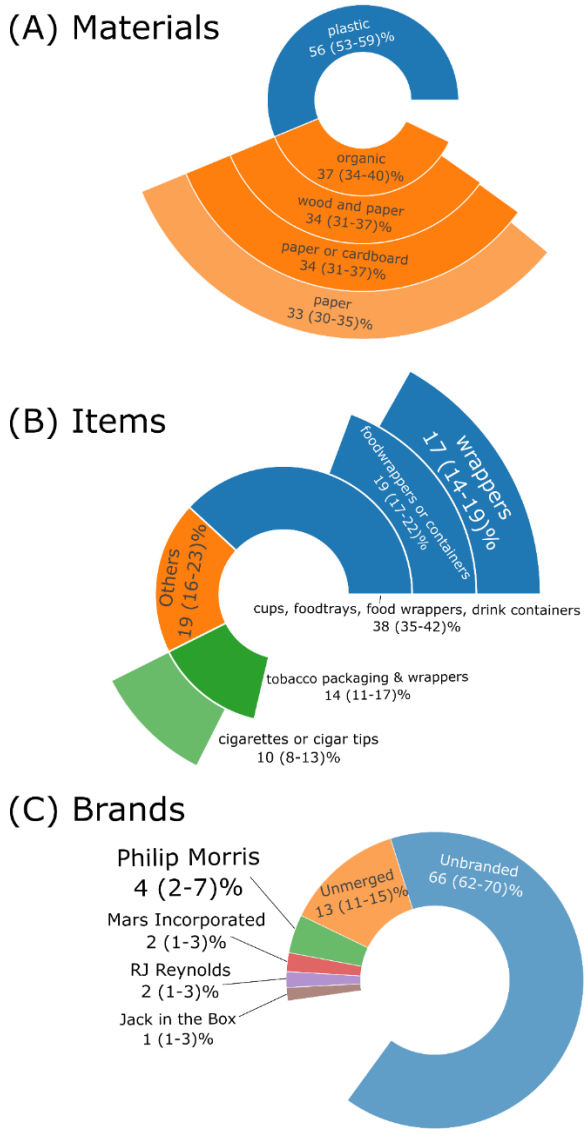

Figure 2-6: Sunburst plots show the relative composition of litter clustered by the hierarchy from the Trash Taxonomy. Each category lists the percent composition of that category to all litter found during the study, and uncertainties around the mean percent were bootstrapped (resampling with replacement, n = 10000) and listed. A) shows the material composition, any category less than 10% of the total was removed from the figure for visualization. B) Shows the item types, any category less than 10% of the total composition was removed from the figure. C) Shows the manufacturer names, any category less than 1% was removed from the figure.

2.5 Discussion

2.5.1 Origins and transport processes

We found that human trips were likely the primary transport mechanism of the receipts in our study sites. There is an offset between human trip distances and litter transport, which is likely due to the differences in the calculation of human trips (travel path) and receipt transport distances (as the crow flies), and the acquisition and/or deposition of litter within a given trip rather than at the trip endpoints. Receipt addresses were slightly further away than the nearest potential receipt address on average (Figure A-3). This result supports the observation that litter item purchase occurs at convenient locations along personal and work commutes. Human trip distance distributions could be a good proxy for estimating litter transport distances using quantile regression (Figure A-1). Although this research focuses on receipts in the Inland Empire, we expect that these metrics apply to similar litter morphologies on roadsides in the United States with similar human trip distributions, climate, and waste management practices.

Most of the receipts found on roadsides in this study originated less than a 1.6 km away. Local action has been proposed as a strategy to combat litter accumulation[63]. If local actions in the Inland Empire targeted prevention of receipt-like litter from sale locations within 1.6 km to litter hotspots, they would likely account for half of the sources supplying the litter.

2.5.2 Litter accumulation rates

We were surprised by the persistence of litter accumulation rates despite our efforts to keep the sites clean and COVID-19 stay-at-home orders. Litter behavior studies have noted that keeping areas clean has some effect on the aptitude of people to litter, but that effect is generally small[66], so we may not have had a long enough study period to detect it. Although only a small number of observations (6) were collected during stay-at-home orders, these data (and the prevalence of essential goods in the composition i.e., food items) point toward the idea that litter accumulation may be tied to essential everyday activities continued during the stay-at-home order. Pon and Becherucci[93] found that litter standing stock on roadsides in Brazil was stable throughout the seasons of the year without removing any of the litter, similar to the first observations of standing stock at Site 7, which were both around 200 pieces (Figure A-2). Litter accumulation may be generally balanced by litter removal at these monitoring locations.

We are concerned and delighted by the stable litter accumulation result. We are concerned that cleanup may never lead to prevention in the Inland Empire. However, as the cleanup did not impact the litter accumulation, this method will allow us to test other intervention strategies. Future repeat studies should expect the occurrence of an intervention capable of producing a shift in the mean accumulation rate greater than ± 37% or collect more data to be able to quantify a statistically robust effect.

2.5.3 Litter composition

Plastic, food items, cigarette products, and brands with high market prevalence are also known to be the most prevalent litter objects in environmental compartments around the world[70–73]. Solutions have been proposed to decrease single-use plastic product availability and engage corporations through corporate social responsibility initiatives[74]. The approach we have developed for measuring the uncertainty in the proportion of objects attributed to manufacturers should assist in developing effective corporate social responsibility strategies. We would like to see the most prevalent manufacturers of litter found in the Inland Empire take an active role in decreasing the abundance of their waste in our region, and future studies could employ this monitoring technique to measure their efficacy.

Unmerged and unbranded categories were prevalent, not useful, and resulted from a limitation of our current classification capabilities for litter. Unmerged categories are not currently in the Trash Taxonomy and should be added to the Trash Taxonomy in future work. Most objects were unbranded and therefore nearly untraceable to their producer. This discrepancy hampers corporate social responsibility initiatives for the producers of unbranded products. We advocate for improving material fingerprinting and branding policies that increase the identifiability of manufacturers who created the products[94].

2.6 Conclusions

In this study, we advance science relevant to government entities, individuals, and corporations so that all can work together to end litter by advancing the science of litter transport processes, accumulation rates, and composition in the Inland Empire of California. This study was the first of its kind to conduct high-resolution surveys of litter accumulation rates on roadsides and identify human transport as a primary mechanism for litter transport. However, this study was conducted primarily during dry conditions when runoff could not play a role in litter transport. Future studies should evaluate the roll of runoff in litter transport by surveying roadside litter, and downstream litter accumulation points during periods of precipitation. Roadsides are a significant input of litter to the environment, and this work reports a methodology for monitoring litter on roadsides and measuring the efficacy of interventions to litter accumulation there. The hierarchical litter composition and uncertainty analysis used here has vast implications for thoroughly interpreting litter compositions and brand composition assessment which could be instrumental in driving future corporate social responsibility initiatives. Removing litter from the studies locations made our efforts impactful in its own right, although this intervention did not reduce littering as we expected.

Chapter 3: Trash Taxonomy

3.1 Abstract

Despite global efforts to monitor, mitigate against and prevent trash pollution, no harmonized trash classification system has been widely adopted worldwide. This impedes the merging of datasets and comparative analyses. We undertook this study to 1) assess the state of trash classification, 2) develop a harmonized framework of relational tables and tools, and 3) inform practitioners about challenges and potential solutions. We analyzed 68 trash survey lists to assess similarities and differences in classification. We created comprehensive harmonized hierarchical tables and alias tables for item classes and material classes. On average, the 68 survey lists had 20.8% of item classes in common and 29.9% of material classes in common. Multiple correspondence analysis showed that the 68 surveys were not significantly different from one another regarding organization type, ecosystem focus, or substrate focus. We built the Trash Taxonomy Tool (TTT) web-based application with query features to give researchers access to tools at wincowger.shinyapps.io/trashtaxonomy. The TTT provides practitioners with tools that can allow for integration of datasets and maximization of comparability. Use of the TTT will facilitate analyses for 1) assessing trends across space and time, 2) identifying targets for mitigation, 3) evaluating the effectiveness of prevention measures, 4) informing policymaking, and 5) holding producers responsible.

3.2 Introduction

It is widely recognized that the impacts of mismanaged trash on environmental systems pose substantial risks to ecosystems worldwide, including aquatic ecosystems where it can kill marine life through ingestion and entanglement[95] and transport invasive species[96,97]. Surveys of trash in streams, beaches, sea, and other environmental compartments are conducted to assess those risks[18], plan mitigation[98], determine prevention priorities, and inform policymaking[99]. Trash surveys often include information about trash classes (e.g., bottle, plastic, cigarette), their abundances, and site descriptions. Trash mitigation through cleanup and capture is sometimes necessary to reduce the risks of mismanaged trash. For example, the California State Legislature now requires municipalities to manage trash flowing to streams via urban stormwater[19] to achieve levels that do not adversely impact aquatic habitats. There are a growing number of efforts to control trash at its source, such as placing bans on single-use plastic items, which have relied on trash survey data for prioritizing banned items[100,101]. Trash surveys are essential to addressing anthropogenic trash pollution, but global trash classification is neither standardized nor harmonized.

Trash classification systems are often developed with specific use cases or objectives in mind. Trash survey developers often try to minimize the number of classes they use to reduce complexity while focusing on the classes most relevant to their management questions. This approach decreases training requirements

and execution times. For example, a trash survey on a beach may explicitly list derelict *fishing gear* as a class, while other surveys may specify unique classes to fishing items, such as *fishing poles and fishing wire*. In this example, *fishing gear* cannot be easily split into *fishing poles* and *fishing wire* classes without those being explicitly listed on the trash survey[102]. So, while the structure of these surveys may serve individual objectives, some datasets cannot be readily used together or compared, even when those differences are only semantic.

Standardization and harmonization between existing trash surveys will allow trash monitoring data to be readily used together. Harmonization involves developing taxonomic frameworks that facilitate relational and comparative operations between established and new surveys. Hierarchical and alias frameworks assist the harmonization of surveys that employ different levels of detail. For example, Vriend et al.[44] developed a framework for harmonizing river trash monitoring strategies, outlining six hierarchical levels of trash classification: 1) organic/inorganic, 2) material, 3) polymer classes, 4) polymer type, 5) item type, and 6) the raw sample. JRC (Joint Research Centre) recently developed a hierarchical framework for their survey lists to allow heterogeneous surveys to be combined and analyzed[103]. There is a growing interest expressed by policymakers and managers in developing a standardized survey list by harmonizing those already widely used[104]. Standardization involves prescribing one survey list or a set of survey lists for different use cases. JRC (Joint Research Centre) and

OSPAR (Oslo/Paris Convention) created standardized trash survey lists focusing on European ecosystems and surveys. The OSPAR surveys have been successfully applied to other regions. Additionally, creating a standardized framework will improve computer vision technology by lessening labor-intensive image labeling. The challenge of standardizing and harmonizing heterogeneous datasets can be overcome by developing a schema matching tool and relational database structure[105]. Relational tables describe the relationships between data sets, and schema matching tools assist in combining datasets. By using both standardization and harmonization methods, it is possible to achieve a trash taxonomy system that can be used to describe survey classes that already exist, evaluate how they are related, and develop new lists optimized for given applications and cross-study comparability.

This study aims to 1) develop and describe the use of a universal trash taxonomy framework of relational tables and schema matching tools, and 2) use the trash taxonomy to assess the current state and future of trash classification, trash survey types, and their comparability. To provide potential users with definitions we operationalized in this study, we present a glossary of terms used (Table B-1).

3.3 Methods

3.3.1 Developing Relational Tables

3.3.1.1 Approach and Assumptions

We compiled 68 English-language survey lists from various countries and organizations, including government, research, nonprofit, and academic groups that describe trash survey types for freshwater and marine environments. Throughout this report we italicize class names when referring to trash classes. Three groups of classes were found across most of the surveys, which describe trash in terms of materials (the resource used to make the item, e.g., *plastic* or *paper*), item (description of the form of the object, e.g., *bottle* or *fragment*), and brand (the logo or manufacture's name identified on the item). We also recognized two relational systems within the data: alias (synonymous words, e.g., *cap* and *lid*) and hierarchy (words that are parents or nested as children, e.g., *spoon*, *fork*, and *knife* nested under utensils). We developed relational tables for comparing words used within and between these structures.

This primary assumption within this framework is that the trash classes used in each survey fully define each study object, which means that there are no differences between surveys in the definitions of a given class. An example of a violation of this assumption would be two surveys that define *fragment* based on size, but with different criteria: *fragment* = particles > 1 mm versus *fragment* =

particles < 5 mm. These surveys would classify different sets of objects using the same word. There are other types of information held within the methodological distinctions in definitions that we did not investigate further (e.g., color, shape, size) unless the methodological limitation was encoded in the class name (e.g., rope diameter <1 cm). This study compared the relationships between the words used to describe trash and how they relate to one another based on professional experience with trash nomenclature.

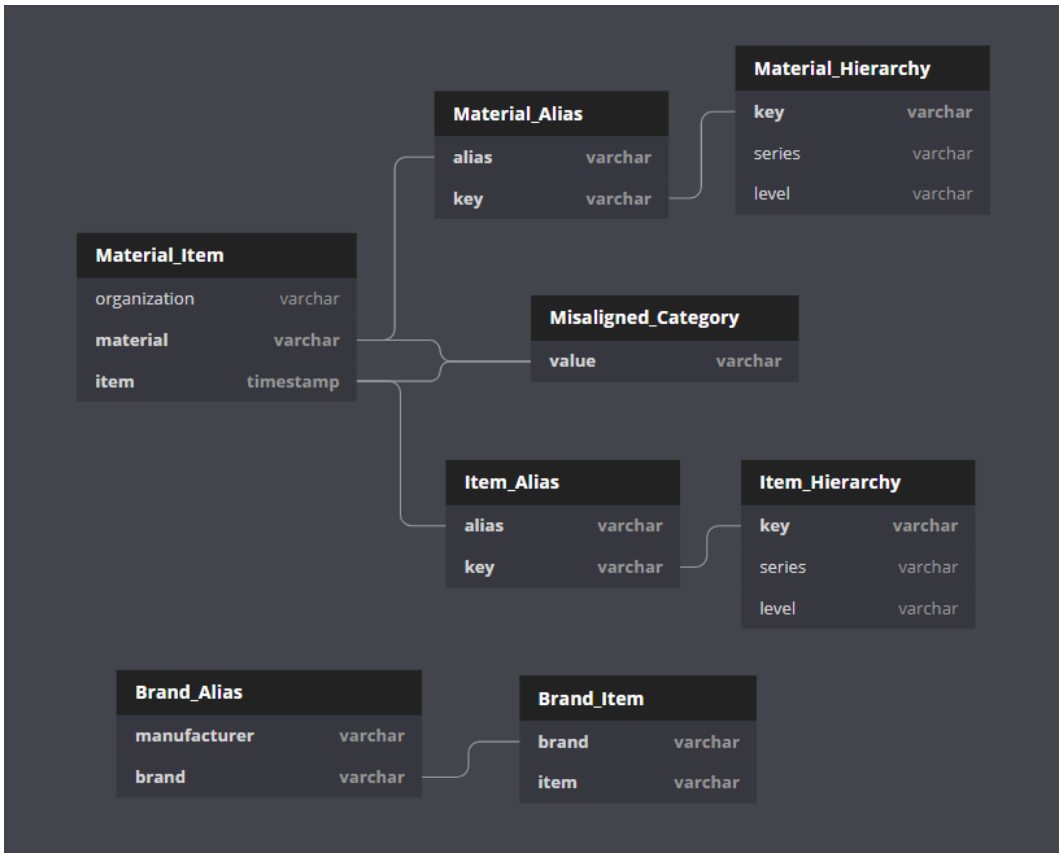

Figure 3-1: Visual representation of relational tables and how they can be linked to one another. This database can be accessed in an interactive version at https://dbdiagram.io/d/5f3d9342cf48a141ff557dfe

3.3.1.2 Material-Item Relational Table

We compiled a table listing the materials and items described by each organization's classification system we reviewed for our study. Each row represented a unique material-item relationship (e.g., *plastic* and *straw* being listed in a row together). Sometimes it was unclear whether a class described a material class or an item class (e.g., *disposable fork*, typically made of plastic). These classes were placed in the item class, and the material class was not inferred to avoid introducing bias and adding words not used explicitly in the surveys.

3.3.1.3 Misaligned Class Table

We identified misaligned classes as classes that did not fit within the material, item, or brand classes. If the class was too ambiguous or did not describe trash in environments, we added it to a separate document called the misaligned class table. Some examples of misaligned classes include c*onstruction materials*, *fishing gear*, and *tree*. The misaligned classes were omitted from the material-item relationship table because they neither described material nor item classes.

3.3.1.4 Alias Tables

We developed alias tables for material, item, and brand classes independent of one another (Figure 3-1). For the item and material alias tables, all words that were found to have the same meaning were linked using rows in a table where the first column defined the prime word, which is used as a key for joining to the hierarchy

(Figure 3-1), while all other columns were defined as aliases. Break Free From Plastic, a nonprofit organization promoting a global movement to create a future free from plastic pollution, developed the brand alias table by researching the manufacturers who own the brands found during their annual Brand Audit in 2018 and 2019[102]. This table is formatted with recurring manufacturer classes in one column corresponding to each brand owned by that manufacturer. In the alias tables, prime words can be merged with the hierarchical tables and vice versa (e.g., *fork* and *forks* will be under the same alias).

3.3.1.5 Hierarchical Tables

Additionally, we developed hierarchy tables for item classes (Figure 3-2) and material classes (Figure 3-3). These tables specify the hierarchical position of prime words through multi-level grouping (e.g., the utensils class encompasses forks, knives, spoons, and straws; *plastic* in materials includes *foam* and *soft plastic*). The hierarchy tables only describe the prime words from the alias tables since those words are equivalent to the other words used to describe trash. Hierarchical groups were sometimes obvious. For example, one survey we reviewed used the class *glass/ceramic* while another split the classes into two *glass* and *ceramic*. In other cases, the relationships were more nuanced. For example, *organic* is a more general material description that includes materials like *wood* and *cloth*.

3.3.1.6 Database Query Tool Development

The Trash Taxonomy Tool (TTT) is a database with a set of query tools and all previously mentioned relational tables accessible via an online application (wincowger.shinyapps.io/trashtaxonomy). The site was created using the shiny[106], dplyr[107], data.table[108], shinyjs[109], shinythemes[110], DT[111], shinyhelper[112], data.tree[91], and collapsibleTree[113], packages in R (4.0.5) and R Studio (1.4.1106). This site allows users to upload a comma-separated value (csv) file of their survey list to process using our alias and hierarchy framework. In technical terms, the TTT is a schema matching tool because it matches and maps schemas from trash surveys to a unified format[105]. The TTT first uses an alias lookup to match and map the user-provided survey classes to prime word keys. It then locates the prime word in the hierarchy and allows users to display all words more or less specific in their item and material columns. It finds all parent words when the less specific function is called and all child words when the more specific function is called. If the user provides a word that is not in the relational table system, a notification will return for that particular word. In this way, the users can view all materials and items in the hierarchy that are less or more specific than the words they used. More detailed documentation and a video tutorial can be found on the TTT website.

3.3.1.7 Relational Table Cleaning and Valdation

We cleaned our relational tables using several tests. We created basic queries to identify duplicated terms, remove them, and ensure that all relationship links

between the tables (Figure 3-1) were equivalent in both directions for the alias to hierarchy relationships. The material-item table keys are equivalent to the alias and misaligned class keys combined. For example, the material alias table's key column has the same terms as the key column in the material hierarchy table. We created a pipeline within our online tool to visually validate all the relational tables for nuanced relationships like semantic relationships within and between the tables. First, we upload the material-item relational table to the query tool, then return the relational table's results and visually assess the matches.

3.3.2 Assessment of the Current State of Trash Classification

3.3.2.1 Summary Statistics

We calculated summary statistics on each of the relational tables. The total number of classes was assessed by summing the number of unique words used within the survey lists (e.g., *fork or spoon* and *fork/spoon* are considered separate words). We assessed the number of unique classes by summing the unique prime aliases in the alias table (e.g., the two previously mentioned categories are joined to the same class). The number of levels of the hierarchies was assessed using the maximum number of levels of any given branch in the hierarchy tables. Diagrams were developed to demonstrate the depth and complexity of the hierarchical tables using the collapsibleTree[113] R package.

3.3.2.2 Factor Analysis

The similarities between the groups of survey types (organization, ecosystem, substrate) were assessed with multiple correspondence analysis (MCA), using FactoMineR[114] and FactoShiny[115]. We expected that the survey lists within similar classes (e.g., marine trash surveys) would use similar trash classes since they would have similar study goals. We split organization classes into research, nonprofit, and academic; ecosystems were split into marine, riverine, estuary, or land; substrates were split into beach, surface water, underwater, or roadside. First, we joined all classes used in the materials-items table to the alias tables. Second, we converted all classes to a matrix with zero denoting that the survey list did not have the class and one denoting that the survey list did, and one-hot encoded the material and item classes used in each survey list. The MCA's supplemental information (information not used to inform the model development) included the organization type, ecosystem type, and substrate type (Table 3-1). Confidence ellipses (95%) were plotted for each supplemental variable to determine if any of the group's categories were statistically unique from each other. Overlapping ellipses were described as statistically similar.

3.3.2.3 Comparability Analysis

We assessed the comparability of each survey list to all the others by calculating the one-way percent of overlapping items or materials after joining them both to the alias table:

$$Comparability\ Metric_{X,Y} = \frac{\Sigma\ Classess\ in\ sheet\ X\ equivalent\ with\ classes\ in\ sheet\ Y}{\Sigma\ All\ classes\ in\ sheet\ X} \quad (1)$$

where the *Comparability Metric*$_{X,Y}$ is a one-way test for how comparable survey X is with survey Y. The metric defines the proportion of the classes in survey list Y that are accounted for by the classes in survey list X after joining the lists to the alias table. We then averaged all comparability metrics for each survey by material and items independently and plotted them to identify the most comparable surveys and discuss strategies for creating a 100% comparable survey list. The comparability metric is a useful derivation to describe how much one survey accounts for the classes in another survey, a typical operation when merging trash survey lists.

Another way to compare trash surveys is to lump them together using the hierarchy. We used the hierarchy and alias tables to compare the Stormwater Monitoring Coalition (SMC) survey list with the NOAA survey list. First, we added randomly sampled trash counts (a standard trash survey method) between 1 and 10 for each trash class. We joined both surveys to the alias table and then to the hierarchical tables. We used the data.tree[91] package in R to sum up the hierarchies to demonstrate how the two surveys are related based on the hierarchy.

3.4 Results and Discussion

3.4.1 The State of Trash Taxonomy

3.4.1.1 Relational Table Summaries

Merging the material, item, and brand groups to their alias tables can inform us about the level of detail and potential applications for each group in use today. The alias lists condensed 87 classes to 25 unique materials, 1,138 items to 416 unique item classes, and 3,740 unique brand classes to 1,239 unique manufacturers. It is apparent that “material” is the most generic class used, “item” is more discretized, and “brand” has an even higher degree of subdivision. In survey development applications, reducing class choices to alias terms in the alias lists helps to make surveys more clear and data more consistent. If a user reduced classes to these alias terms before machine learning classification, they would improve their classification by clearly differentiating object classes and reduce labeling time.

Inspecting the hierarchy tables can provide insight into the depth of information in the trash taxonomy and improve description clarity. There are four levels (parent-child word relationships) for material classes and six levels for item classes in the hierarchical relational tables (Figure 3-2 and 3-3). The item hierarchy was more complex than the material hierarchy. We have not yet developed a hierarchy for brands, but we expect that one could be important for future developments. In an ideal hierarchical system, the terminal ends would encompass all possibilities of

their higher class. For example, *fiberglass* would encompass all possibilities of *glass* (Figure 3-3). However, that is not the case here since we are only characterizing the classes that surveys have made, and there are gaps in how trash surveys have characterized trash. Therefore, to accurately interpret the hierarchy, there is an implied *other* class as a subclass of each class wherever it is not explicitly made.

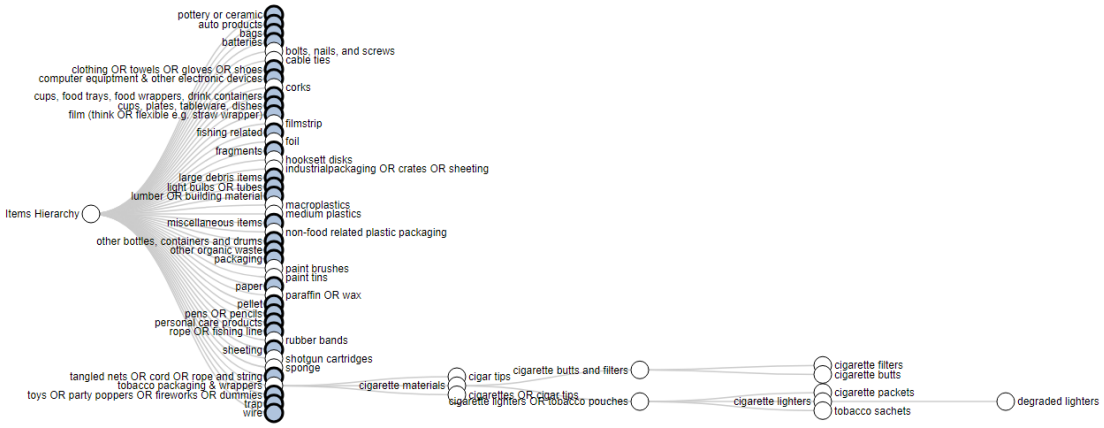

Figure 3-2: A subset of the Reingold-Tilford tree diagram of items hierarchy list. The entire hierarchy can be seen online at trashtaxonomy.shinyapps.io/trashtaxonomy. White circles have no subclasses, and blue circles have subclasses that are not already expanded in the display that could be expanded. At the far left of the tree is the most general classification and at the terminal end of each branch is the most specific classification. For example, “item” is the most general term that could be used to describe item classes.

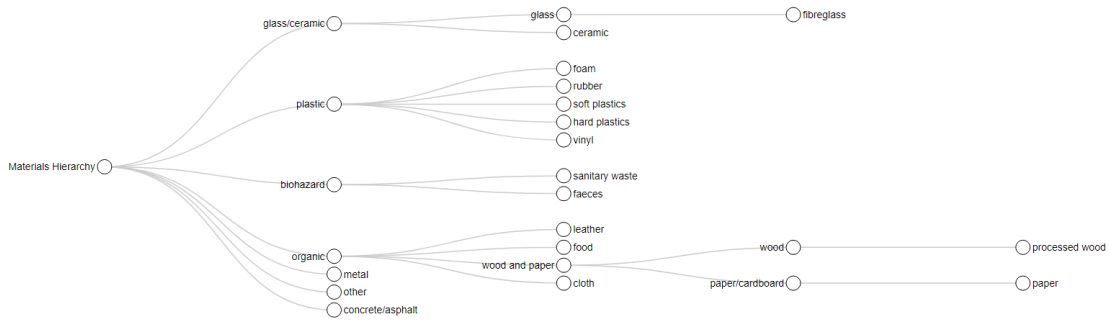

Figure 3-3: Reingold-Tilford tree diagram of materials hierarchy list displaying all hierarchical relationships among material words. At the far left of the tree is the most general classification and at the terminal end of each branch is the most specific classification. In the materials hierarchy, *plastic* is a subclass of material and *soft plastic* is a terminal end of the hierarchy and a subclass of *plastic*.

Out of 1509 material and item classes in the surveys, 392 did not fit our typology. We did not put them in our alias or hierarchical tables and instead made a separate misaligned class table. The main reason for misalignment was the categorization of trash by use, such as *fishing related* or *construction materials*. The challenge with these descriptors is they describe too broad of a range of material, item, and brand classes, so it is not clear how they would fit within the framework we have developed. For example, the class *smoking related* lumps item classes like *cigarette ends*, *tobacco packaging*, *matches*, *lighters*, and *pipes*, along with material classes like *plastic*, *organic*, *paper*, *metal*, and *glass*. Additionally, while one organization may choose to include *lighters* as a *smoking related* item, another organization may choose to put *lighters* in a *household item* use class. These descriptors could be useful for practitioners who want to conduct rapid assessments with lumped use-based descriptors, but the descriptors were too ambiguous to incorporate into our current system. We recommend that future

surveys designed to assess trash use class first start by describing the material and item classes and then build their use classes by summing observations of the material and item classes that fit their uses. These descriptors might be brought into alignment within the current system when a framework is developed that relates material-item-brand combinations to the use classes but would likely need a NoSQL nonrelational database schema due to all of the overlap. The list of descriptors that did not fit the typology can quickly filter less often used trash classes and ambiguous trash classes during data mining routines.

3.4.1.2 Factor Analysis of Survey lists

Survey lists are often described as being for a specific type of organization, ecosystem, or substrate. We tested whether those descriptors reflected differences in the suite of material class (46 survey lists) or item classes (52 survey lists) they describe using MCA (Table 3-1, Figure 3-4). No significant differences in material or item classes were found between survey lists by organization, ecosystem, or substrate type (Figure 3-4 and 3-5). This suggests that there is substantial overlap between the classes used in all types of surveys. In effect, there is not a large difference between a government survey and a nonprofit survey or between a marine survey and an inland survey when use classes are not considered.

Table 3-1: Group nests the types. Type is a subclass of information within each of the groups. Materials is the number of survey lists that fit within the type and have material classes. Items is the number of surveys that fit within the type and have item classes.

Group	Type	Materials (#)	Items (#)
Organization	research	28	34
	government	5	5
	non-profit	10	10
	multiple	2	2
	unknown	1	1
Substrate	sediment	11	13
	water	6	2
	multiple	2	2
	unknown	27	35
Ecosystem	inland	7	6
	marine	28	28
	multiple	11	17
	unknown	0	1

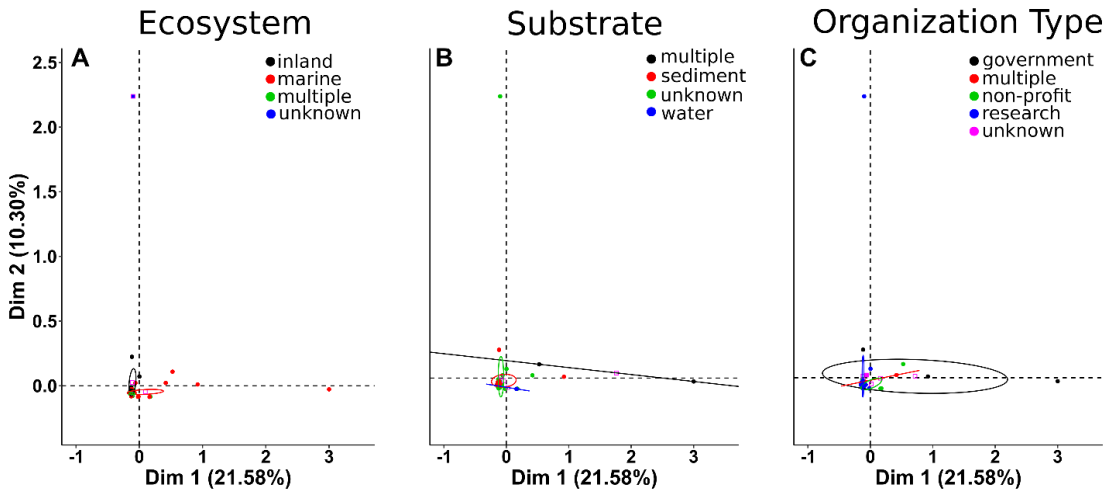

Figure 3-4: MCA results for comparison of A) Ecosystem, B) Substrate, and C) Organization survey descriptors on the basis of item classes. Each point represents a trash survey. The first and second dimensions of the MCA analysis account for 32% of the variance in item classes. Ellipses outline the 95% confidence interval for a given survey type. Overlapping groups do not significantly differ. The minimum number of data points required to form an ellipse is 2. Groups without ellipses only have one data point. The outliers are caused by groups that have few categories.

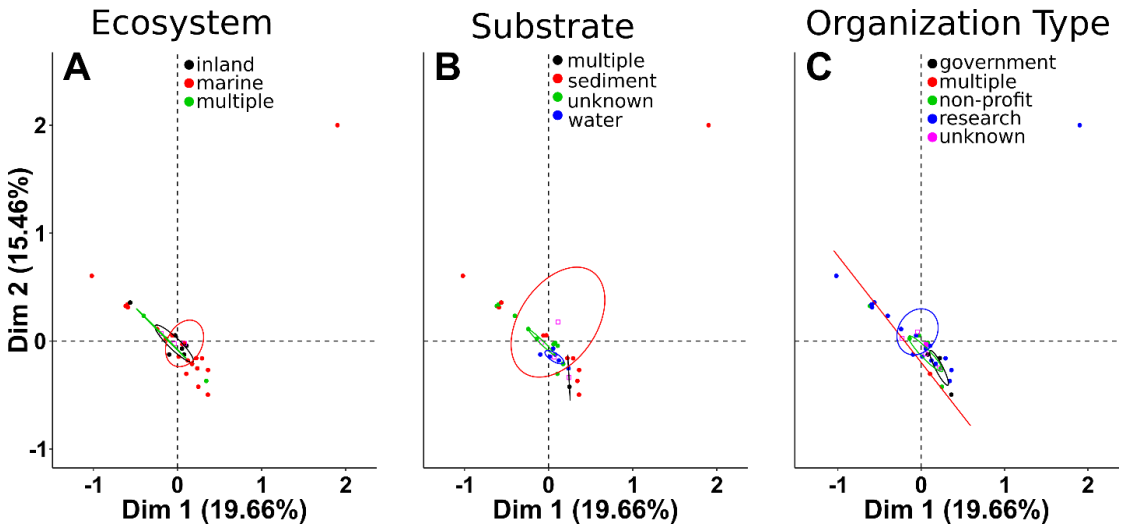

Figure 3-5: MCA results for comparison of A) Ecosystem, B) Substrate, and C) Organization survey descriptors on the basis of material classes. Each point represents a trash survey. The first and second dimensions of the MCA analysis account for 39.5% of the variance in material classes. Ellipses outline the 95% confidence interval for a given survey type. Overlapping groups do not significantly differ. The minimum number of data points required to form an ellipse is 2. Categories without ellipses only have one data point.

3.4.1.3 Comparability Analysis of Survey list

In total, 4,556 comparability metrics were derived between all combinations of surveys for item and materials (Supplemental Information). We found that the average comparability metric was 29.9% and 20.8% for all materials and items, respectively (Figure 3-6 and Table B-3). Some pairs of survey lists were 100% comparable for materials (562) and items (302). These lists could be compared directly without any inference or interpolation. Only 15 of the 114 surveys were moderately comparable (> 40%) on average, and 33 surveys were somewhat comparable (40 - 20%) in item classes. A majority of the survey comparisons were 0% comparable for material (2,470 pairs) and item (2,104 pairs) classes. In these

cases, lists pairs are incompatible for data aggregation and combination purposes at their current specificity level, a problem that cannot be rectified by the alias table alone.

None of the surveys are 100% comparable with all others. However, the surveys produced by NOAA, SMC, OSPAR, Project AWARE, JRC, Marine Conservation Society, and Vandervelde were among the highest comparability on average for material and item types. These surveys are potential candidates for adoption by new practitioners to enhance comparability. The JRC survey has the highest average for item classes of 49% comparability, and the Rech survey has the highest average for material classes of 60% comparability. If the material classes from Rech were used and the item classes from JRC survey were used in a survey, that survey would be the most comparable survey to all others currently presented. The ultimate goal is, of course, to achieve a 100% comparable survey (Figure 3-6).

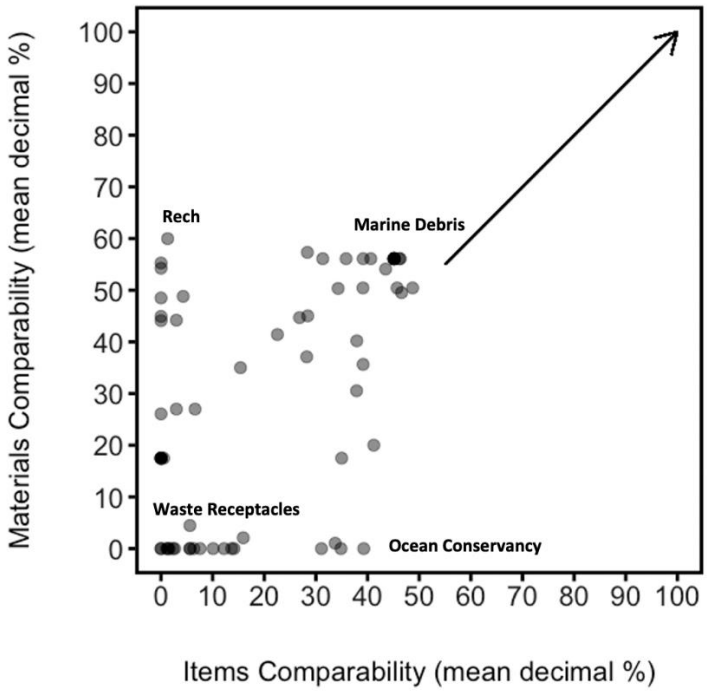

Figure 3-6: Average comparability for each survey list by item classes and material classes. The proportion represented the average percentage of classes in other lists that the list plotted has. The x axis is the average comparability of the item classes, and the y axis is the average comparability of the material classes. An arrow points toward where we aim for survey comparability to go in the future. Full list of comparability metrics for all survey lists in the SI (Table B-3).

How do we reach the goal of attaining more universally comparable surveys? The alias lists hold the answer. If a survey contains all of the prime words for material and item classes, it will be 100% comparable to all of the surveys included in this study based on equation 1. But how can we resolve the fact that there is an overlap in the definitions between many of the survey classes. The solution is to use the hierarchy as part of our classification routine. Essentially, every time a piece of trash is classified during a trash survey, the practitoner looks it up using the

hierarchy and chooses the most specific material and item classes (Figure 3-7). This allows for more general and more specific terms to be used simultaneously. Users can already do this on the TTT website using the collapsible trees on the reference table tab. Figure 3-7 demonstrates how the hierarchy can be used to drill down to the most specific material and item classes that can be used to describe the trash.

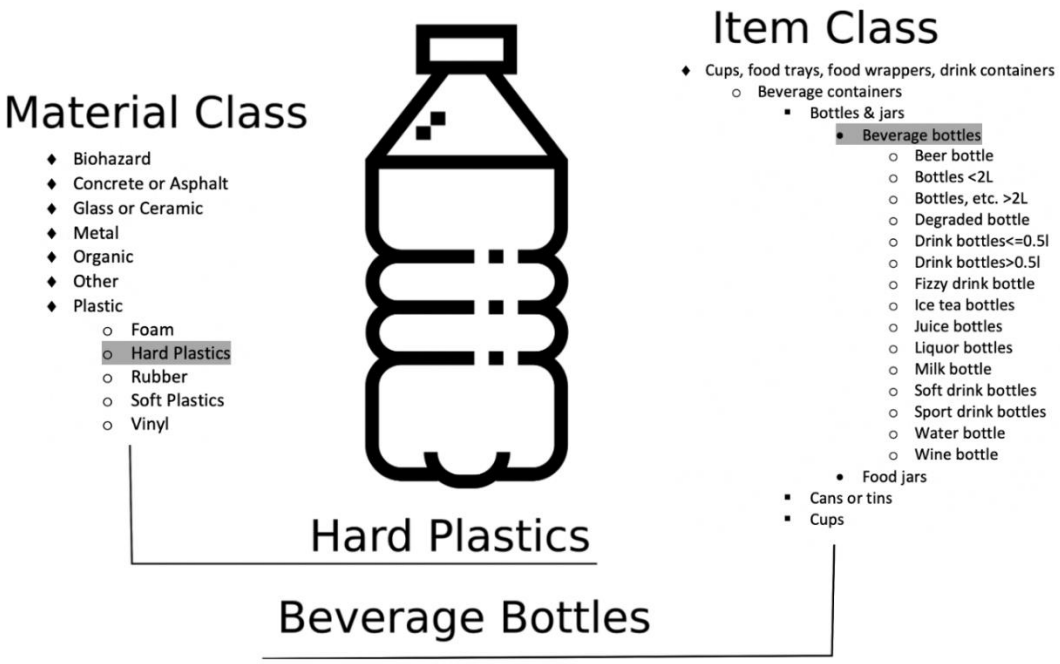

Figure 3-7: The object in the center is being classified using the material and item hierarchies on the TTT website. In this example of classifying an unlabeled plastic bottle, we can tell that it is made out of hard plastic and that it is a beverage bottle, but we cannot tell what type of beverage bottle it is, so it should be classified generically as a beverage bottle. The classes *hard plastic* and *beverage bottles* are chosen to best represent the object in as much detail as possible, without assuming beyond the specificity we can observe.

Comparison of slightly comparable datasets could be improved by utilizing the hierarchy in addition to the alias. However, we do not see a clear “best” or “better” path forward within several possible options to lump and split datasets at the present moment. One strategy is to lump the values. All trash classes will lump to the class *trash*, but in some cases, it is possible to lump to more specific classes (e.g., *forks* in one survey and *spoons* in another survey could lump to *utensils*) (Table 3-2). Another strategy to unify data is to split into more refined classes using the hierarchy tables, e.g., if one survey has *utensils* and the other survey has *forks*, *knives*, *spoons,* an attempt could be made to split the *utensils* class into more resolved classes. However, the analyst needs to have a way to infer what proportions the higher-level class should be split by to equal the values of the refined class. This problem has yet to be solved for trash classification. Splitting may often not be possible because it requires additional information beyond that in the survey lists. A challenge for lumping or splitting arises when a survey focuses on a particular set of items and materials but does not count the rest of the trash classes in an *other* class. The analyst then needs to infer the quantity and classes of trash that they did not characterize or only compare the quantities they did characterize to other studies. As a first step toward combining survey lists, we have attempted to solve the lumping problem using Table 3-2. This example demonstrates lumping counts from multiple surveys using different categories that are related by the hierarchy. We wrote an R script to do this automatically for any of the survey lists in the TTT. Although this demonstrates that survey lists can be

merged by lumping programmatically, limitations due to the method differences previously stated are likely to remain.

Table 3-2: Example of lumping analysis for SMC material classes with the NOAA material classes. Both data cards are first joined to the materials alias relational table, then to the hierarchical table. The final result can be plotted like this to show how a joined survey list could be lumped. The tree structure under Hierarchical Classes is tabbed to show finer levels of granularity in the descriptions. Count is the number of objects of that material type that the surveys observed. Total Sum is how those sums would lump given the hierarchy. The class missing counts the number of classes that were not integrated into the TTT. Zero indicates an accurate merge.

Hierarchical Classes	Count	Total Sum
• Trash	0	426
○ Glass or Ceramic	0	30
▪ Glass	30	30
○ Metal	42	42
○ Missing	0	0
○ Organic	0	51
▪ Cloth	25	25
▪ Wood	26	26
○ Other	85	85
○ Plastic	223	254
▪ Rubber	31	31

3.4.2 Applications of the Trash Taxonomy Tool

3.4.2.1 Practice Limitations

Efforts to use the TTT to classify certain types of trash and waste will remain challenging because of the complex nature of trash and trash survey operations. Classification using the TTT will continue to be influenced by users' objectives and

the users' interpretations. One example of challenges is found in efforts to classify trash that results from tobacco use (currently being added to the TTT). In the field of global tobacco control, the emerging class *tobacco product waste* is increasingly being used to encompass all products that contain tobacco leaf (e.g., cigarettes, cigars, smokeless tobacco, bidis, waterpipe tobacco) as well as all ancillary products and items used for the consumption of tobacco leaf (e.g., cigarette packaging, cigar wrappers, matches, matchboxes, lighters, smokeless tobacco tins, waterpipes and charcoal). *Tobacco product waste* constructed this way is thus a considerably heterogeneous class. For example, it includes cigarette butts with cellulose acetate plastic "filter" rods and lighters with butane residue. However, one can find definitions of *tobacco product waste* that exclude ancillary products and items. The TTT user's objectives in defining groupings of trash items (i.e., lumping versus splitting) will inevitably influence the application of the TTT, and the user's interpretations of trash items during survey operations will also to some degree shape classification. Nevertheless, it is possible that as practitioners use the TTT throughout the world, the application of the TTT will generate harmonized classification schema for such groups of products and those harmonized schema will become more solidified.

The use of hierarchy tables can also present challenges when practitioners are attempting to classify trash that results from the use of related products. For example, as electronic nicotine delivery systems (ENDS), commonly known as e-

cigarettes, have been introduced into markets throughout the world, some tobacco control experts have argued that e-cigarette products should be classified under the broad category of tobacco products. This would suggest that post-consumption waste from e-cigarette use should also be classified as *tobacco product waste*. Others have proposed that post-consumption waste from e-cigarette use should be defined as a separate class *e-cigarette product waste*[116]. Such distinctions in class can be important. While e-cigarette products share a commonality with cigarettes and other combustible tobacco products in that they deliver nicotine, e-cigarettes are distinct from combustible tobacco products in terms of function (i.e., producing aerosol rather than smoke) and materials (i.e, nicotine-containing e-liquid, metal casing, electronic circuitry, batteries, and plastic components rather than nicotine-containing tobacco leaf, tipping paper, plastic “filter” rods and glue). Recognizing that some tobacco companies are promoting their e-cigarette products as “clean” alternatives to cigarettes, one can argue that it is important to document environmental contamination from *e-cigarette product waste* as a separate class of trash. As practitioners use TTT, they will face challenges in determining what classifications are appropriate and useful globally. Despite these challenges, the use of hierarchy tables remains valuable for practical purposes. Distinctions in product function and trash materials are common, and some additional distinctions may be addressed in future iterations of TTT.

Some challenges may arise from the application of the alias tables in the TTT. Continuing with the example of *tobacco product waste*, a practitioner may have to decide whether menthol cigarettes can appropriately be defined as an alias class (synonym) of regular cigarettes. This may be problematic because, in some settings, there can be a public health social justice imperative to identify menthol cigarette butts and menthol packaging since historically and until now, tobacco companies have targeted teens with menthol cigarette advertising (to promote menthol cigarettes as “starter products”), and targeted US African American teens in particular[117]. So, on the basis of public health objectives a practitioner could reasonably wish to classify trash from menthol cigarette use separately and not define it as an alias of regular cigarettes. At high schools, practitioners may wish to define *menthol cigarettes* as a subset of *cigarettes* in a hierarchical structure rather than defining *menthol cigarettes* as an alias class of *cigarettes.*

These examples demonstrate some of the challenges practitioners may face when using a hierarchical and alias relational table system within the TTT to achieve global harmonization. Also, at the current stage of TTT development, we did not use material-item or item-brand tables to analyze the state of trash taxonomy. Future work should be done to describe the variability within these types of tables. There are several other limitations noted in section 3.2.1.1, which could also apply to some practitioners. Developing tables that describe the classification structure's objective may help to remedy some of these competing classification needs and

definitions of trash classes in the future. The TTT provides a platform within which practitioners around the world can conduct their own investigations while simultaneously discussing and rigorously deciding upon shared taxonomies.

3.4.2.2 Practitioner Collaboration

Adjusting current survey lists and developing new survey lists with a standardized trash taxonomy will facilitate more effective trash management. By adopting a shared trash taxonomy framework, organizations across sectors can work together to contribute to broader research and management applications. The TTT will allow new practitioners to join in ongoing efforts to collect trash data in a harmonized way. If practitioners use the TTT to generate comparable data across organizations and projects, it will be easier for those analyzing data from multiple datasets to 1) assess trends across space and time, 2) evaluate the effectiveness of prevention measures, and 3) identify new targets for mitigation.

Recent developments in trash taxonomic integration have been spurred by access to large and heterogeneous datasets with many different trash naming systems. Additionally, computer-assisted vision is now being used to classify trash in images[118]. Labeling images is labor-intensive and requires the development of a relational system for labels used. If the TTT is used to do the labeling, a single machine-learning system could produce an output that is comparable throughout all trash surveys we have assessed so far, rather than having to retrain staff and

relabel every new survey list. We have detailed many of these use cases and steps for tackling them in Table B-2.

3.4.2.3 Future of the Trash Taxonomy Tool

Trash taxonomy will continue to evolve as new materials and items are created and enter environments[119] and as researchers create new technologies for collecting data about trash and develop new ways of describing trash[120,121]. Our framework, relational tables, and source code will assist in developing and expanding the field of trash taxonomy. Extensions to the TTT can be included by directly collaborating with us on Github https://github.com/wincowgerDEV/TrashTaxonomy and submitting requests and feedback to https://github.com/wincowgerDEV/TrashTaxonomy/issues. The source code and data are licensed open access (CC by 4.0) attribution only. This analysis will need to be expanded to other languages in the future to accommodate differences in how different languages map the alias and hierarchy relationships. Translations are already starting to be done with cross-country trash databases like the pan European Marine Litter Database[122]. Future work on database development should prioritize nonrelational mapping structures between the classes, develop a reconciliation service in a standardized format[123], and assess the feasibility of incorporating semantic closeness and data value matching routines.[105]

There is still much work to be done on the fundamentals of trash taxonomy. Accurate brand identification is critical to ensuring the precise application of the principles of extended producer responsibility to hold manufacturers accountable for large loads of post-consumption trash and substantial environmental impacts that result from the use of their products. We suspect that it will take an ongoing large-scale effort to keep up with brand classes, and we applaud the work of Break Free From Plastic on this issue. Future work on brand classification within the TTT should include linking items, brands, and material combinations to identify the producers that ultimately should be responsible for the products they design and produce.

Several ongoing projects are using the TTT that will be assisting in future developments. NOAA Marine Debris is using the TTT to update their trash survey classes. The harmonized tables developed in this study are already being used to develop machine learning image classification in the Clean Currents Coalition so that the labels on trash items can be as restricted as possible without compromising the harmonizability of the dataset. The Trash Monitoring Playbook[124] suggested using the TTT to trash survey practitioners.

The widespread adoption of the TTT can harmonize global efforts to measure and document trash loads, trash types, and the extent of trash pollution in environments. The adoption of the TTT can also contribute to facilitating the

aggregation of datasets from trash surveys, improving comparisons of trash risk assessments, and illuminating pathways for future work on trash taxonomy. We hope that TTT will be used to support research designed to inform mitigation efforts and prevention efforts, particularly in the realm of policymaking. We recommend using the TTT to foster collaborative research that will generate scientific evidence for holding producers accountable, ultimately by supporting “upstream” policy initiatives that reduce trash pollution of environments, promote changes in consumer behaviors, and mandate changes in producer practices.

3.5 Data Availability Statement

The tables and code are open access to encourage users to update and improve on our relational framework (https://github.com/wincowgerDEV/TrashTaxonomy). The tables and Shiny app tool have a CC BY 4.0 license. This gives users permission to remix, copy, and commercialize with attribution. Our intent is for others to build on these tools and use them widely.

Chapter 4: Concentration discharge relationships of macroplastics

4.1 Abstract

River macroplastic flux is a critical metric for the management of plastic pollution. Continuous measurement of macroplastic concentration is not currently possible, so surveyors must predict concentrations during unobserved periods to calculate flux. We monitored macroplastic concentration in the Santa Ana River, a small coastal urban catchment with a losing river, a Mediterranean climate, and low flow conditions dominated by released wastewater effluent. Particles in samples were biased toward positively buoyant particles (98%). All negatively buoyant particles were removed from the samples to focus the study on macroplastic particles likely transported as surface load. We developed a strategy for predicting particle mass using particle projected area. Uncertainties were propagated throughout the analysis for model regressions, means, and sampling bias using bootstrap simulation. Particles were determined to be in surface load transport using the Rouse derivations. Floating macroplastic particle size distributions were statistically equivalent between lowflow and stormflow samples. Concentrations fell during the falling limb of one hydrograph and rose during the rising limb, suggesting clockwise hysteresis. A generalized additive model revealed that concentrations of macroplastic increased in response to small increases in discharge but decreased for the largest discharges. We predicted the annual mass flux of floating macroplastic at our sample location using mean concentrations

(27.4, 2.8-84.8 tonnes^{1}yr^{-1}) and the generalized additive model predictions (18.2, 2.9-222.2 tonnes^{1}yr^{-1}). These findings suggest that the main source of floating macroplastic was the channel and that surface transported macroplastics are predominantly supply-limited in rivers.

4.2 Introduction

Rivers are highly contaminated by plastic pollution and are the major conveyance of plastic from land to the ocean[35]. River plastic flux is a key variable in interpreting the magnitude of plastic to downriver ecosystems, the contamination at the study location, and changes in the magnitude of upriver plastic sources. Macroplastic (particles > 5 mm) are known to make up most of the mass of plastic in the environment and break down to form microplastic (particles < 5 mm)[33]. Therefore, rigorous estimates of river macroplastic flux are critical for addressing the global crisis of plastic pollution.

River macroplastic flux is typically quantified by multiplying river discharge ($m^{3}s^{-1}$) by macroplastic concentrations (count or mass$^{1}m^{-3}$). Continuous river stage (m) measurements are available in many locations within the United States and are periodically calibrated to discharge, velocity ($m^{1}s^{-1}$), depth (m), and other river flow characteristics by the United States Geological Service (USGS). However, there is currently no way to continuously monitor river macroplastic concentration. To

quantify macroplastic flux, one needs to make predictions about unobserved macroplastic concentrations.

Unobserved concentrations of fluvial particulate matter are often predicted using discharge hydrologic regime, hydrograph hysteresis, and rating curves fit to river discharge[125]. Changes in discharge reflect combined changes in the supply and transport of water to the monitoring stations and affect changes in the river's transport properties (e.g., turbulence, velocity, depth). Changes in both water supply and water transport properties can result in changes in the loading of particulates to the channel through changes in connectivity between sources and the channel. The ratio between the flux of water and the flux of particulates at any moment is reflected in the average concentration of the particulate in the flow. Multiple orders of magnitude of variability around the concentration discharge rating curves are typical, particularly in the small mountainous rivers characteristic of coastal California[126]. This variability is due in part to stochastic processes like storm sequence[127], spatio-temporal characteristics[128], and antecedent watershed conditions[129–131], which can result in variability in the processes controlling water and sediment delivery and routing[132]. Temporal structure to this variability can manifest in time-dependent concentration-discharge relationships, from hydrograph hysteresis[133] (i.e., different rising vs falling limb concentration-discharge relationships) to interdecadal scale trends[126,134]. The suspended load particle size distribution may shift with hydrologic mode and can be diagnostic of

sources and transport pathways of mineral sediment[135,136]. Investigation of temporal patterns in concentration-discharge relationships can provide insight into transport and supply processes and be used to refine flux estimation[131,132,137].

Early research on plastic pollution informed our study objectives. River macroplastic particle count to mass ratios are assumed constant in literature[138] despite changes in hydrological mode, suggesting stable particle size distributions. Our first aim is to test the hypothesis that macroplastic particle size distributions are stable regardless of hydrologic mode. Stormflow events have been observed to increase macroplastic concentration compared to lowflow[139]. Our second objective is to test whether hydrograph hysteresis or storm timing may play a role in these event to seasonal scale concentration discharge relationships. Rating curves have been observed between plastic concentration and discharge as decreasing[140], increasing or stable[141], and nonmonotonic[142], reflecting a similar diversity of rating curves to those seen in other particulate transport studies. Our third goal is to assess the macroplastic concentration-discharge rating curve in the Santa Ana River. Our final objective is to estimate the annual flux of macroplastic at our study location during the study year. In total, these objectives serve to inform science about transport processes of macroplastics in rivers and inform society about how best to manage macroplastic pollution.

4.3 Study Location

The Santa Ana River drains a small mountainous watershed (total area: 6900 km^2, area at sample site: 2341 km^2), experiences a hot, dry summer Mediterranean climate regime, with > 90% of its 61 cm of average annual precipitation occurring between October-April (Figure 4-1). The study location on the Santa Ana River was located where the river crosses the Van Buren Bridge in Riverside, CA which is 1.8 km downriver from USGS river gage 11066460. The main stem of the Santa Ana River in the vicinity of sample collection displays two major hydrologic regimes: low magnitude (mean daily discharge (par 60, stat 00003) = 1.8 $m^3\ s^{-1}$) flows supported entirely by wastewater discharge, and flashy storm flows (mean daily discharge: 14.0 $m^3\ s^{-1}$; and 2 year recurrence interval daily flow of 64.3 $m^3\ s^{-1}$) (Figure C-1). For most of the time, the middle reach of the Santa Ana is a losing river with discharge decreasing downriver unless fed by a stormflow event or at wastewater input points. The sampled reach is low gradient (slope = 0.004), sandy fine gravel bedded, and includes a vegetated riparian corridor that persists between flood control levees.

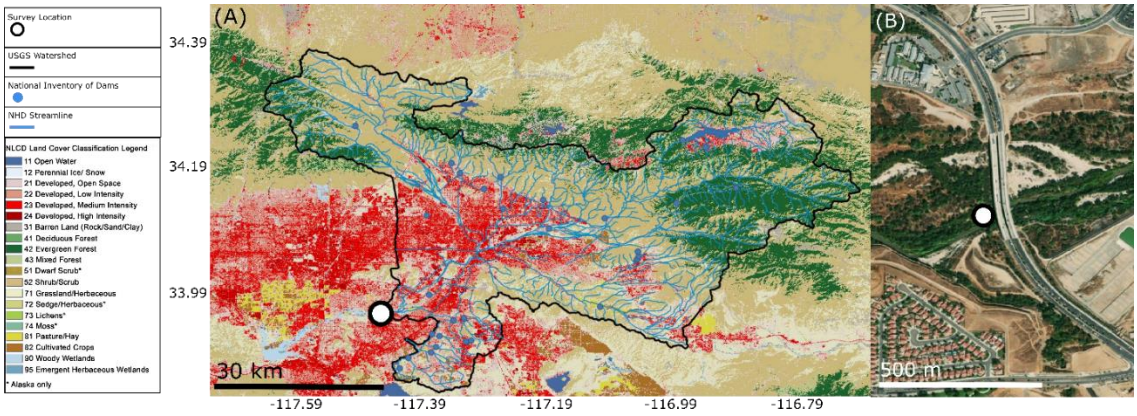

Figure 4-1: The watershed (A) and survey location (B) of this study. White dot is the location where the samples were taken. In (A) the basemap is the National Land Cover Dataset (NLCD) showing land cover types[143]. The landuse legend is adapted from fair use NLCD materials[144]. Stream centerlines are added from the National Hydrography Dataset in blue[145]. The Watershed boundary was delineated using Streamstats from the USGS[146]. The National Inventory of Dam[147] locations was plotted as blue dots. (B) Satellite imagery of the study reach is shown, and the survey location is downstream of the Van Buren Bridge in Riverside, CA.

Sources and fate of macroplastic at the study reach are dependent on the management of water and trash within the watershed and channel. A large amount of accumulated trash exists as standing stock within the channel riparian area[148], but there have not been previous studies on trash flux through the river. Potential sources of macroplastic to the channel are suspected to be runoff from upstream urban areas, direct dumping within the river, and waste from populations of unhoused people that live within the riparian area who do not have waste management services[148,149]. Urban runoff is actively mitigated via street sweeping and trash capture devices in storm drains[92,150]. However, to our knowledge, there are no mitigations implemented for removing the trash within the channel. The watershed upriver of the sample location is 31% developed land use. Immediately

adjacent and upriver of the sample location is the major metropolitan area of the Inland Empire, including Riverside and San Bernardino cities. Wastewater facilities that input to the Santa Ana have secondary or tertiary treatment before the wastewater is transferred to the channel. They are suspected to be a negligible source of macroplastic due to the filtration used during the treatment processes. Near the watershed's headwaters are mountains with primarily rural populations, but these sections are generally disconnected from the sampling reach due to dams at the foothills of many mountain tributaries and the losing nature of the river channel most of the year. Downriver of the study location is the Prado dam, which likely cuts off most trash flux from this reach to the ocean.

4.4 Methods

4.4.1 Field Methods

4.4.1.1 Macroplastic measurements

River macroplastic samples were collected in the Santa Ana River from the downriver side of the Van Buren bridge in Riverside, California (Figure 4-1 & 4-2). A steel box trawl (fabricated by Marcus Eriksen) with a square 0.16 m^2 intake and 5 mm mesh net was lowered from a bridge to the thalweg of the river using a portable crane (USGS Type A Crane with 3 Wheel Truck) attached to the trawl with rope and a boat shackle. On average, half of the net was submerged if the net was not resting on the river bed. To sample lowflows, we waded into the river and

set the net in the thalweg of the channel on the river bed. The total number of samples collected was limited to 20 due to the highly episodic, fast-moving, and high magnitude river flow in Southern California (Figure 4-3).

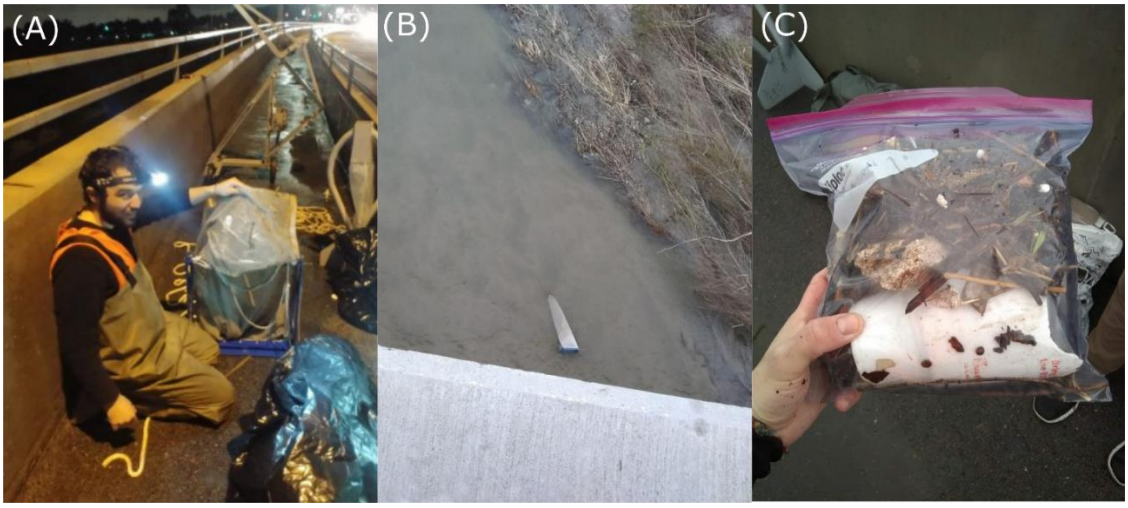

Figure 4-2: A) Sample collection apparatus and B) deployment from a bridge. The net has a 400 mm square aperture and a 5 mm mesh. C) An example of a sample that will be sorted for plastic visually.

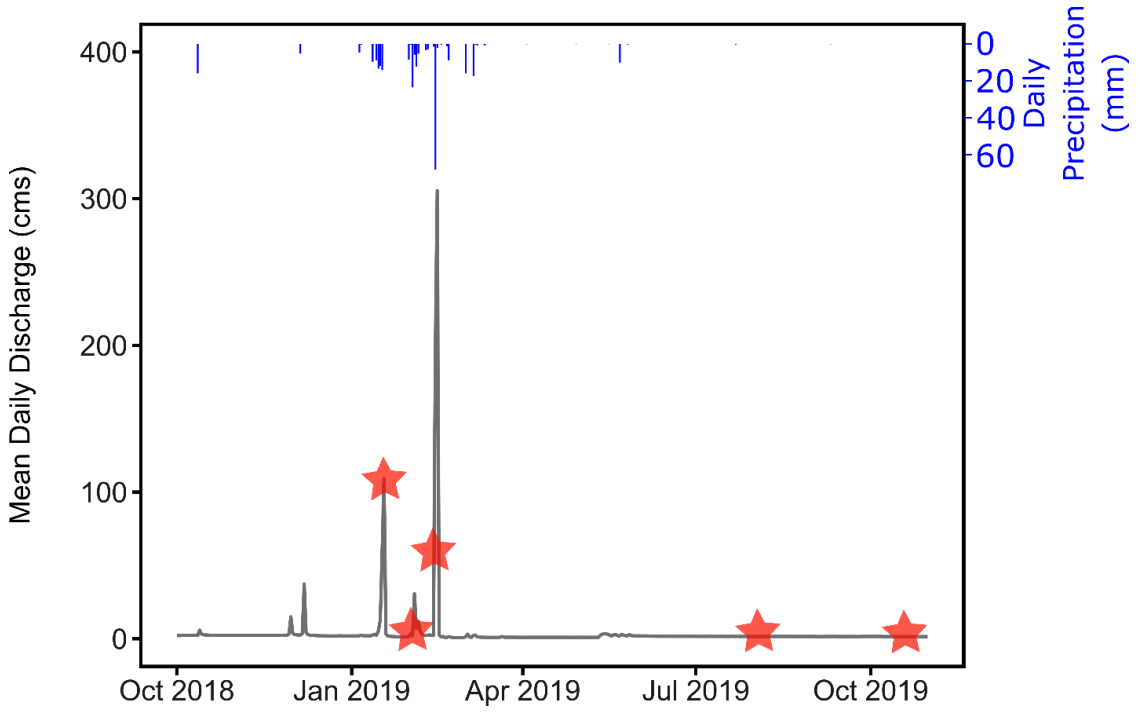

Figure 4-3: The hydrograph (mean daily average cubic meters per second) from October 1st 2018 to October 30th 2019. Red stars mark the days when samples were acquired. Hyetograph is inverted at the top with blue bars indicating the total daily precipitation in mm.

4.4.1.2 Hydrologic Measurements

All river hydrologic data were obtained from the USGS river gage 11066460, using the National Water Information System[151], located 1.8 km upriver from the macroplastic sampling location. Continuous stage data (15 min) (par 65) was acquired along with measurements of channel discharge (par 61), river velocity (par 55), channel cross-sectional area (par 82632), and channel width (par 4) from 2018-01-10 to 2020-04-21. The river cross-sectional area was divided by river width to estimate average river depth. USGS measurements were used to create rating curves using linear regression on $\log_{10}$ transformed stage and measured

variables. Log_{10} transformation bias was corrected using the approach of Ferguson [152]. The discharge rating curve was (log_{10}(discharge) = 5.1 * log_{10}(gage height) – 1.49, adjRSQ = 0.76, log_{10} correction = 1.09, $p = 10^{-16}$). The velocity rating curve was (log_{10}(velocity) = 1.24 * log_{10}(gage height) – 0.58, adjRSQ = 0.44, log_{10} correction = 1.02, $p = 10^{-9}$). The depth rating curve was (log_{10}(depth) = 2.67 * log_{10}(gage height) – 2.03, adjRSQ = 0.73, log_{10} correction = 1.03, $p = 10^{-16}$). Uncertainty in USGS rating curves was propagated using bootstrap simulation (resampling with replacement, n = 10,000) of the USGS measurements. River slope was estimated using the 1/9th arc-second digital elevation model from the National Elevation Dataset[153] and Google Earth. River shear velocity was estimated as the square root of average river depth times acceleration due to gravity times the river slope. Daily precipitation (Figure 4-3) was downloaded from Midwestern Regional Climate Center's cli-MATE application [82] for the KRAL airport weather station near the sample location.

4.4.2 Plastic particle characterization

Macroplastic particles were visually sorted from the samples and photographed with a scale in the image (Figure 4-4A). We used Image J[154] to quantify particle projected area (Figure 4-4B) for each particle using Image J's color thresholding, manual tracing, and particle size analysis routines (Figures 4-4A & 4-4B). Small artifact “particles” visible at the fringes of particles (Figure 4-4B) were removed by restricting the minimum particle size to 1 mm^2. Nominal particle size was estimated

as the square root of the particle projected area. Particles are well separated by this technique and outlined precisely.

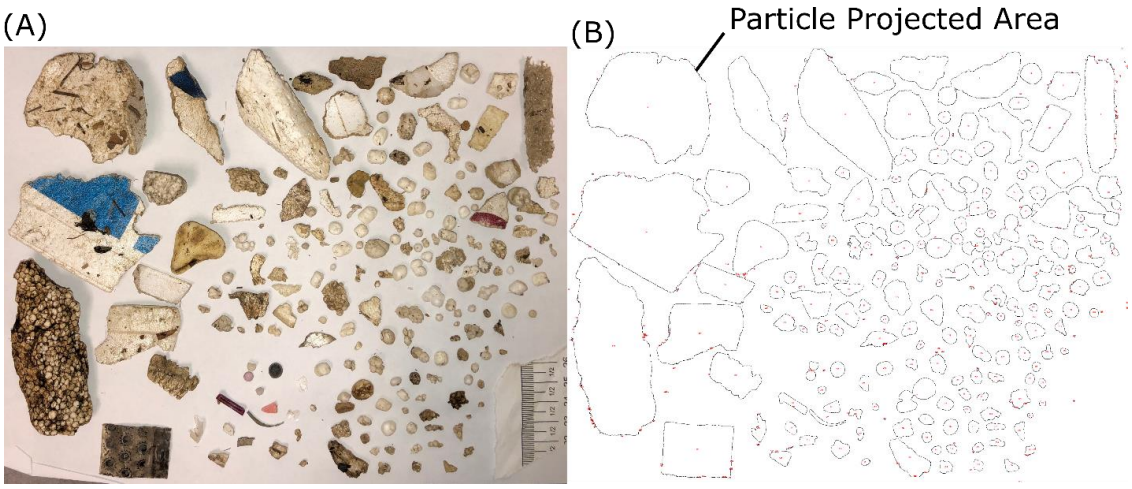

Figure 4-4: (A) Plastic particles extracted from samples in the Santa Ana River. (B) An outline image showing the traced projected surface area of each plastic particle.

All suspected plastic particles were subjected to a sink-swim test by placing them in fresh water from the lab de-ionized water faucet, agitating the particle until no surface bubbles were visible, and assessing if the particle floated or sank. All particles were labeled as settling or buoyant.

A subset of 88 out of 944 particle identities were validated using FTIR spectroscopy and 30 with Pyrolysis GCMS. The smallest particles of the samples were chosen for validation because they were the most likely to be misidentified [155]. For FTIR, a Thermo Nicolet 6700 ATR FTIR was used at 4/cm spectral resolution with daily background recording for the spectral range from 400-4000 wavenumbers (1/cm). Spectral analysis was done in Open Specy[46] with smoothing

conducted with a Savitzky-Golay filter with a window size of 12 points and a 3rd order polynomial, baseline correction conducted with the imodpolyfit routine using an 8th order polynomial, and a min-max normalization before identification. Identification was conducted using Pearson correlation and a 0.5 uncertainty threshold using the entire spectral range. In FTIR, three particles were identified as non-plastics, sixty-seven were identified as plastic, and eighteen could not be identified accurately using FTIR. In Pyrolysis, the CDS-2000 Pyroprobe pyrolyzer used a hydrogen reacting gas at a temperature of 750 C. The Agilent 6890N GC used a CDS-1500 Valved GC Interface oven program with a 320 C temperature and the hydrogen gas flow rate was 1.2 $ml^{1}min^{-1}$ in constant flow mode. The column characteristics were DB-5 (0.25 mm OD x 60 m L; 0.25 µ film thickness) fused-silica capillary column. The CDS-1500 GC Interface valve was closed after one min. The column oven temperature was initially held at 45°C for 2 min and then ramped to 320°C at $20°C^{1}min^{-1}$ rate. The column oven was held at 320°C for 19 min resulting in a total run time of 34.75 min. The MC electron Multiplier (EM) auto-tune voltage was adjusted by 200V above the auto-tune voltage. Data acquisition was performed in full-scan mode from 29-600 amu by using the Agilent ChemStation Software. The Injector and the Mass Spectrometer Transfer Line Heater were maintained at 320°C. The mass spectrometer Quadruple and Source temperatures were held at 150°C and 230°C. Pyrolysis identified 28 of the 30 particles as plastic.

Thirteen macroplastic particles from these samples with rising velocities were randomly chosen to measure rising velocities and reported on in another publication[56]. They were composed of expanded polystyrene, polyethylene, and polypropylene, and had powers roundness ranges from 2.2-5.9, Corey shape factor from 0.07-0.88, dimensionless diameter of 2.5-30.81, and rising velocities ranging from 0.221-1.69 m^1s^{-1}.

4.4.3 Estimating macroplastic concentrations and uncertainties

Three types of macroplastic concentrations (count or $mass^1$ $meter^{-3}$) were estimated, count, projected area, and mass concentrations along with their uncertainties. All three calculations required an estimate of sample water volume. Submerged net depth was set to 0.2 m (half of the net height) or the average river depth, whichever was smaller. We multiplied the depth of the submerged net by the width of the net (0.4 m) to get the submerged cross-section of the net. Uncertainty of submerged depth was incorporated by simulation for each sample using a uniform probability density function from 0.1 – 0.3 m. The average river velocity from the USGS rating curve (linear model on $\log_{10}$ transformed data with $\log_{10}$ bias correction) was multiplied by the submerged cross-sectional area and the sample duration to quantify the volume of water of the sample. River velocity rating curve uncertainties were incorporated into sample size uncertainty using bootstrap simulation of the model fit (resampling with replacement, n = 10,000).

We removed a subset of macroplastic particles from our observations that would have biased our results. Macroplastic particles can be transported in surface load, wash load, bed load, and rising or settling suspended load[156]. Surface sampling (conducted in this study) best measures surface load. Therefore, we wanted only to include particles that had a high likelihood of being in surface load transport (positively buoyant particles). We compared the freshwater settling plastics with the positively buoyant particles by size and count for all samples (Figure 4-5). We found that positively buoyant plastics were the most common plastic-type in the samples (98 %). We removed all settling particles from further analysis. We also noticed that the particle size distribution decreased in abundance around 5 mm in size, which corresponded to the net's mesh size. All particles smaller than 5 mm were removed from further analysis. We permuted all estimated shear velocities and all observed rising velocities of the particles. The largest mean Rouse number was -2.5, suggesting that most particles observed were in surface load transport. Therefore, we assumed that all particles in this study were transported at the surface of the water column. We used the depth-integrated average concentration estimate introduced by[35] and demonstrated by[156] to have a small level of bias for surface sampling particles in surface transport.

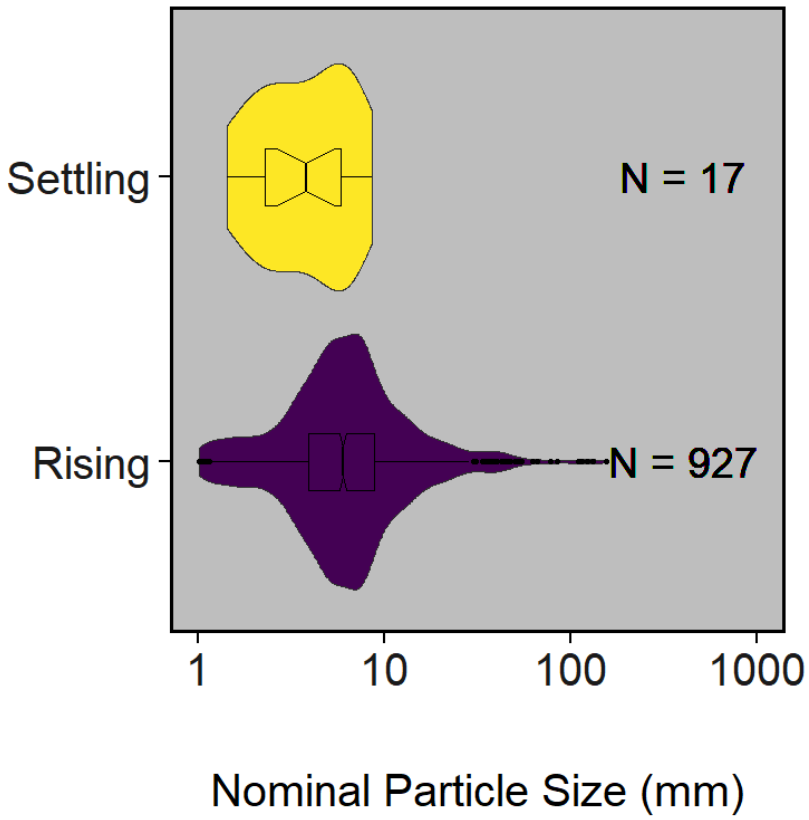

Figure 4-5: Nominal particle size distributions (the square root of the projected surface area) for settling and rising particles found in this study. Violin plots are centered with notched box plots within (95% confidence interval). Dots show points beyond 1.5 times the interquartile range.

Count, area, and mass concentrations were calculated by dividing the abundance by sample volume. Count concentration was calculated by counting the number of particles in the sample (after removing bias causing particles described in 3.2) and dividing it by the total sample volume. Count uncertainty (due to fragmentation from handling, missing particles, and inadequate sampling of particle counts) was estimated as up to ±10% of the sample count and was propagated using a uniform probability density function from 0 – 10%. Area concentration was calculated by

summing the projected surface area from all particles in the samples and dividing it by the sample volume. Area uncertainty was estimated in the same way as count uncertainty. We measured the mass of 124 of the suspected macroplastic particles imaged for particle size measurement. We derived a linear regression on $\log_{10}$ transformed data between the particle projected area and the mass of the particle ($\log_{10}$(particle mass (g)) = 1.13 * $\log_{10}$(particle area (mm^2) – 4, adjRSQ = 0.63, $\log_{10}$ correction = 1.36, $p < 10^{-16}$) (Figure C-2) and corrected for $\log_{10}$ transformation bias[152]. Then we used the regression to estimate the mass of all particles from our samples. Mass concentrations were computed by dividing the total mass of macroplastic by the sample volume. Mass uncertainty was computed in the same way as area and count uncertainties.

4.4.4 Statistical analysis

4.4.4.1 Lowflow and stormflow particle size distribution

Stormflow samples were separated from lowflow samples visually by using the slope change inflection points in the hydrograph. All particles from stormflow and lowflow samples were pooled to make two particle size distributions using empirical cumulative density functions. We used the two-sample Kolmogorov-Smirnov test to assess the null hypothesis that the particle size distributions of stormflow and lowflow were from the same distribution.

4.4.4.2 Hydrograph hysteresis and storm timing

We tested for hydrograph hysteresis and storm timing effects on the macroplastic concentration discharge relationship. To assess hysteresis, we connected the sample concentration-discharge values for each sampling day with a line, and drew an arrow indicating the relationship's direction through time. We assessed the relationship between the hydrograph domain (rising limb, falling limb) during each stormflow sampling event and the hysteresis. Stormflow periods were determined using the description in 3.5. The rising limb was separated from the falling limb by assessing whether the discharge increased (rising limb) or decreased (falling limb) at the sample time. Storm timing was assessed by plotting the 2018 water year discharge time series (October 1st 2018 - September 30th 2019) plus the month of October 2019 to include the final sample in the study. We described the likely relationships between the timing and magnitude of the stormflows and the concentration discharge relationships observed. Since only two stormflow events were sampled, we did not compute statistics on these trends and used them as a heuristic tool to identify future areas of study.

4.4.4.3 Macroplastic concentration-discharge rating curve

We assessed the concentration discharge rating curve for count and mass concentrations using generalized additive modeling with a smoothing spline. We tested the assumption of normality for $\log_{10}$ transformed concentrations using the Shapiro-Wilk test, and decided that we would use the assumption of normality for

the model (count concentration, W = 0.92 p = 0.08 | mass concentration, W = 0.97 p = 0.82). We fit the generalized additive model to log_{10} transformed macroplastic concentrations and discharge using a smoothing spline (k=7). We assessed our confidence in the model fit using the p-value (alpha = 0.05), and deviance explained.

4.4.4.4 Estimating annual mass flux

We tested two commonly employed techniques, mean concentration extrapolation and the concentration-discharge rating curve, for estimating the mass flux of macroplastic in water year 2018 at the site to assess the importance of uncertainties and concentration-discharge rating curves[126]. The continuous discharge of the water year 2018 was estimated from the continuous stage using a rating curve (section 3.1.2). Using mean concentration extrapolation, we estimated mass flux by assuming steady mean concentration using the mean mass concentration observed from our dataset. Total discharge for the water year 2018 was multiplied by the mean mass concentration to predict the annual flux. Using the generalized additive model rating curve, we predicted concentration for every discharge on record (15 min interval discharge). Mass flux was computed for every 15 min discharge interval and summed for the entire year. For both methods, confidence intervals were derived using 10,000 simulations with bootstrapped datasets for all data and models (resampling with replacement).

4.4.4.5 Data and code availability

All statistical tests and plots were written in reproducible R code, starting from raw data and ending with the outputs. The packages dataRetrieval[157], dplyr[107], ggplot2[158], mgcv[159], readxl[160], data.table[108], stringr[161], viridis[162], tidyr[163], MASS[164], and matrixStats[165] were used in the code. Data and code are shared open access on Open Science Framework (https://osf.io/mrey8/?view_only=46e4a0e91fbf4fff85d810c28c963665) to ensure the reproducibility and comparability of this research.

4.5 Results and discussion

4.5.1 Lowflow and stormflow particle size distribution

We tested for differences in the macroplastic particle size distributions during lowflow and stormflow. Smaller size classes were exponentially more abundant than larger sizes for both hydrologic regimes (Figure 4-6). A similar particle size distribution has been observed for microplastic particles[54]. There was a maximum distance between the two cumulative distribution functions of 0.080 (p-value = 0.66). The particle size distributions of macroplastic particles in stormflow and lowflow samples were statistically indistinguishable. There was also high goodness of fit (adjRSQ = 0.63) between particle mass and particle projected area observed in our study (Figure C-2). Van Emmerik et al.[140] assumed a constant count- mass ratio for macroplastic floating in rivers, which would be suspected if

the particle size distribution were also stable there. Assuming this stability continues in the future and is widespread, mean count-mass-area conversion ratios (common conversions in the field) should be constant regardless of discharge at a given site. Future work should compare the particle size distribution we found to distributions elsewhere to look for spatial variability.

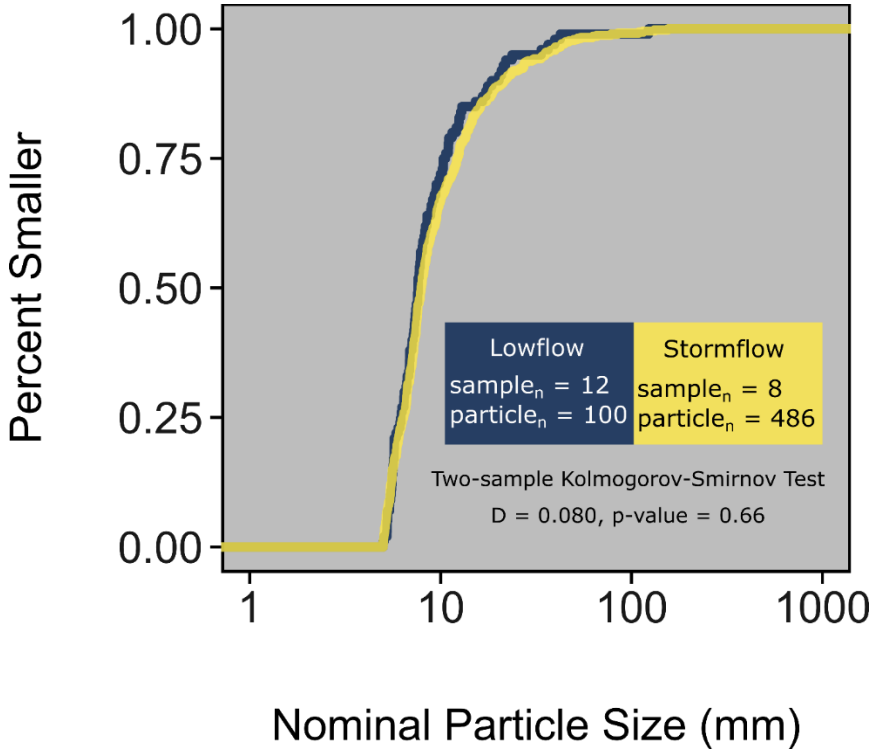

Figure 4-6: Empirical cumulative distribution functions for the nominal particle size (square root of particle projected surface area) of particles collected during stormflow and lowflow periods. Particle$_n$ refers to the total number of particles sampled during the respective transport mode. Sample$_n$ refers to the number of independent samples aggregated.

What can the observed uniform particle size distributions of macroplastic particles in riverflow tell us about watershed macroplastic pollution sources and transport processes? The particle size distribution is an expression of the source's particle

size distribution and the hydrologic transport characteristics at and above the sample location. Large, positively buoyant particles only need a minimum water depth to particle size ratio to become mobilized[166]. From a transportability perspective, it is unsurprising that we did not see a particle size preference because the river has an average depth of 0.16 m during lowflow conditions, which should mobilize the largest particle that can fit in the opening of our net (0.4 m). From a source fingerprint perspective, the water at our site is nearly 100 % wastewater effluent during lowflow conditions. Macroplastics during these lowflow conditions can only be sourced from the channel. A predominant source of macroplastics during stormflow may also be the river channel. Future inquiry into particle size distributions of surface transportable macroplastic particles in the channel bed, riparian area, and watershed would help us better understand differences in the particle size distributions between sources. Other quantifiable macroplastic fingerprints like probability density functions of shapes, colors, and polymer type may also assist source apportionment in future studies.

4.5.2 Hydrograph hysteresis and storm timing

We assessed the impact of hysteresis and storm timing on macroplastic concentration. Count concentrations ranged from 0.034 – 24 $num^{1}m^{-3}$ and had a median concentration of 0.25 $num^{1}m^{-3}$ and a mean of 1.89 $num^{1}m^{-3}$. Mass concentrations ranged from 0.00047 – 2.99 $g^{1}m^{-3}$ and had a mean concentration of 0.22 $g^{1}m^{-3}$ and a median of 0.016 $g^{1}m^{-3}$. Macroplastic concentrations rose during

the rising limb of one hydrograph and fell during the falling limb of another hydrograph (Figure 4-7). The same phenomenon was observed for mass concentrations (Figure C-3). Clockwise hysteretic behavior may be present for macroplastic particles, commonly found for natural mineral sediment[167]. Another macroplastic hydrograph sampling event in Northern California also observed clockwise hysteresis with macroplastic[168] with the largest macroplastic concentration transporting during the very beginning of the stormflow. Stenstrom & Kayhanian[169] also found that greater than 50% of litter flushes from roadsides during the first 2 hr of stormflow. Clockwise hysteresis can be described from source mobilization and transport processes. As discharge increases during the rising limb, it can mobilize available sources quickly and deplete them. By the time the falling limb happens, the river is no longer accessing new sources, and the old sources are already somewhat depleted, resulting in decreased concentration. This should particularly be the case for the positively buoyant macroplastic particles observed in this study because we expect that they will always be supply-limited since discharge conditions were always more than sufficient to effect transport. Another explanation can be provided by the transport rate of the macroplastic compared to the peak of the discharge[170]. Floating particles are transported at the highest velocity of the river because the surface is where the fastest velocities are in the river channel. If a floating macroplastic pulse was released simultaneously with a discharge pulse, one would expect the peak in macroplastic concentration to arrive before the discharge peak because the

average velocity of the discharge peak is likely slower than the surface velocity of the stream.

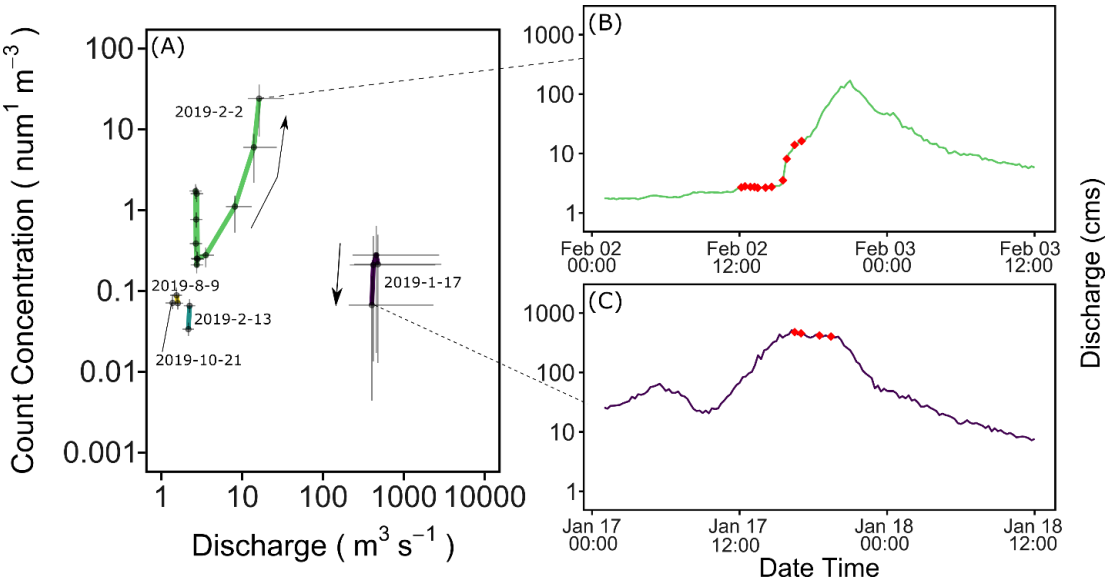

Figure 4-7: Concentration-discharge hysteresis for each sampling event. (A) Uncertainties from bootstrapped simulations are expressed as lines around the data points. Sampling events are uniquely colored, and hysteretic behavior is annotated using arrows to demonstrate the direction of the line during the sampling event. Dates are indicated nearest to each sampling event. The two storm hydrographs (B &C) are presented colored the same as the sampling event they are related to, and red dots are used to indicate the time a sample was taken.

A "first flush" event is common for many pollutants in Southern California, whereby high sediment concentrations are flushed during the first large storm event of the year. We found that an earlier storm event (1/17/2019) did not have higher concentrations than the later storm (2/2/2019). It is possible that we missed the first flush event since two stormflow events occurred before 1/17/2019 (Figure 4-3). It is also possible that the first flush event occurred on 2/2/2019 that we sampled. First flush events require a minimum storm magnitude threshold before

they initiate[171]. Future inquiry into first flush events for macroplastics should attempt to survey the first few hours of each stormflow of the year to standardize effects from hysteresis and better assess the role of storm timing.

4.5.3 Macroplastic concentration-discharge rating curve

Our results show a significant rating curve between discharge and concentration ($\log_{10}$(count concentration) = s($\log_{10}$(discharge)) – 0.47, $\log_{10}$ correction = 1.19, DE = 67 %, n = 20, p = 0.0002) (Figure 4-8). The same phenomenon was observed for mass concentrations (Figure C-4). The rating curve was nonmonotonic, with the highest macroplastic concentration in the center of the observed discharges and the lowest concentrations at the highest and lowest discharges. As discharge increased, it was able to tap into additional sources of macroplastic. However, the additional sources were outcompeted by water at the highest discharges, resulting in lower concentrations. In the Santa Ana River, the flow covers a larger region of the channel corridor between levees during higher flows and can access all available sources there. Increases in discharge thereafter increase the water volume but not the macroplastic input, which would result in a decrease in concentration. It is difficult to know if this relationship is driving the trend or if the trend is driven by the hysteresis discussed in section 4.2. A combination of both processes may be responsible. A recent study also observed a similar increasing trend with decreases in concentrations at the highest discharges[142]. However, increasing rating curves[168], decreasing[140], and no trend[141] between concentration

and discharge have been observed in other regions. At this time, we do not know what the primary driving force of variability is in concentration-discharge rating curves between watersheds.

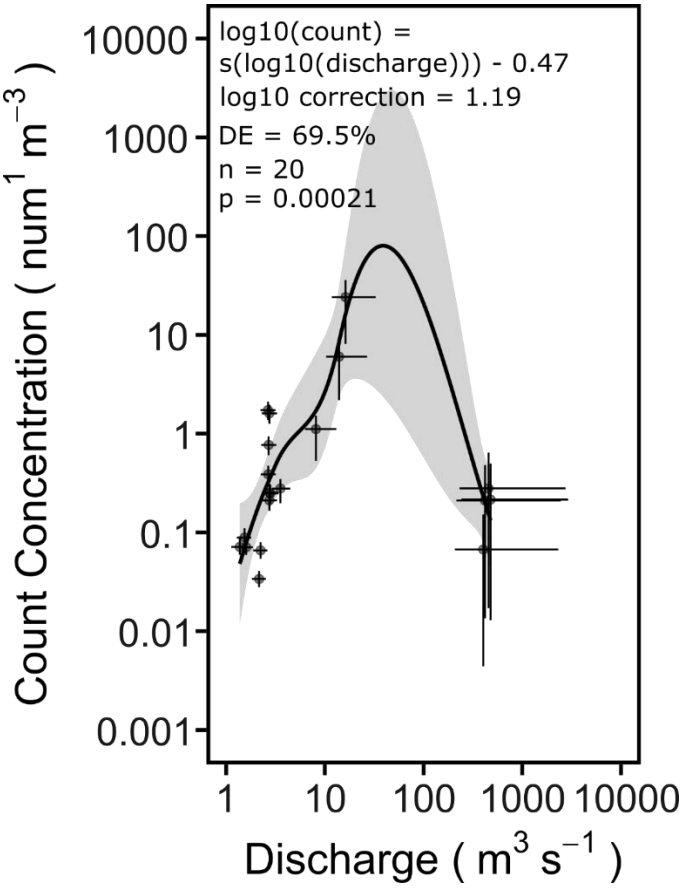

Figure 4-8: The generalized additive model on $\log_{10}$ transformed count concentration and discharge. In the top left corner, we provide the equation coefficients, number of observations, deviance explained, and p-value. Uncertainties for each data point's concentration and discharge values were bootstrapped and are provided as lines around each point.

4.5.4 Estimating annual macroplastic flux

We used two flux estimation strategies to assess the impact of accounting for the concentration-discharge rating curves we described in 3.3. The mean only annual

flux estimate was 27 (2.82-84.8) metric tonnes and the concentration-discharge rating curve estimate was 18.2 (2.9-222.2) metric tonnes (Figure 4-9). There is considerable overlap in the confidence intervals between the estimates. There was more uncertainty resulting from the model fit because we introduced the uncertainty of the generalized additive model into the estimate. Although the model was significant, accounting for measurement uncertainty revealed that we were less certain about the rating curve than the model alone would have suggested. This underscores the importance of robust uncertainty assessment in flux estimation strategies, which can change the interpretation of the suitability differences between models. At this time, we would recommend using the mean concentration to estimate flux since it is a simpler model. More data is required to assess the differences between these estimates. Future work should pursue the processes behind our preliminary findings of hydrograph hysteresis and nonmonotonic concentration-discharge relationships to decrease the uncertainty in those relationships for the Santa Ana River. Studies investigating fluxes elsewhere should assess whether similar relationships exist and account for them in their flux estimates accordingly.

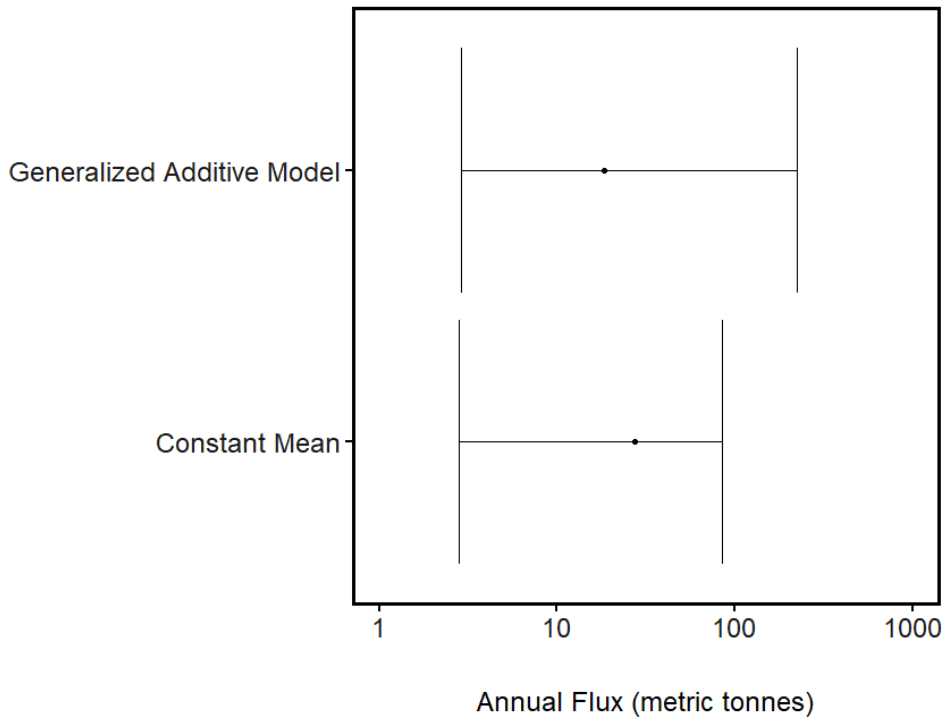

Figure 4-9: Total annual flux estimates (point) and uncertainties (whiskers) for estimating macroplastic flux using the Generalized Additive Model (18.2 (2.9-222.2) metric tonnes) (Figure 4-8) or the mean observed concentration (27 (2.82-84.8) metric tonnes).

4.6 Conclusions

Lowflow and stormflow samples had the same particle size distribution, suggesting that the main source of the macroplastic we observed was likely the channel. Hydrograph hysteresis seemed plausible with higher concentrations observed during the rising limb of the storm and lower concentrations observed during a near-peak falling limb, suggesting depletion of sources early in storms or quick mobility of macroplastic. Storm timing did not have an apparent effect on macroplastic concentration. Macroplastic concentrations were nonmonotonically related to discharge. The highest concentrations were observed in the mid

discharges, suggesting that macroplastic sources were most efficiently mobilized near the mid discharge, perhaps due to channel morphology. Water year macroplastic flux estimates made using mean concentration and the concentration-discharge rating curve were not statistically distinguishable. Mean concentration should be used at the current time to estimate flux but future studies should follow up on the findings revealed here to decrease the order of magnitude of uncertainty in our flux estimate and further investigate the dependency of macroplastics concentrations on time at the event to seasonal scale, and discharge. These phenomena may be particularly important in small, mountainous semi-arid systems such as the Santa Ana River.

Chapter 5: Open Spectroscopy

5.1 Abstract

Microplastic pollution research has suffered from inadequate data and tools for spectral (Raman and infrared) classification. Spectral matching tools often are not accurate for microplastics identification and are cost-prohibitive. Lack of accuracy stems from the diversity of microplastic pollutants, which are not represented in spectral libraries. Here, we propose a viable software solution: Open Specy. Open Specy is on the web (www.openspecy.org) and in an R package. Open Specy is free and allows users to view, process, identify, and share their spectra to a community library. Users can upload and process their spectra using smoothing (Savitzky–Golay filter) and polynomial baseline correction techniques (IModPolyFit). The processed spectrum can be downloaded to be used in other applications or identified using an onboard reference library and correlation-based matching criteria. Open Specy's data sharing and session log features ensure reproducible results. Open Specy houses a growing library of reference spectra, which increasingly represents the diversity of microplastics as a contaminant suite. We compared the functionality and accuracy of Open Specy for microplastic identification to commonly used spectral analysis software. We found that Open Specy was the only open source software, the only software with a community library, and Open Specy had comparable accuracy to popular software (OMNIC Picta and KnowItAll). Future developments will enhance spectral identification

accuracy as the reference library and functionality grows through community-contributed spectra and community-developed code. Open Specy can also be used for applications beyond microplastic analysis. Open Specy's source code is open source (CC-BY-4.0, attribution only) (https://github.com/wincowgerDEV/OpenSpecy).

5.2 Introduction

Spectroscopy is a critical step for polymer identification of microplastics[172,173]. Microplastics are plastic particles between 1 mm and 1 μm in size with various physical and chemical properties[174,175]. Raman and Fourier transform infrared (FTIR) spectroscopy are the most common techniques for identifying plastic particles in microplastic studies[176]. In environmental microplastic studies, plastic particles are extracted from an environmental matrix (e.g., sediment, water) using chemical and physical procedures. In some procedures, particles are filtered and the whole sample is analyzed using automated Raman or FTIR. Alternatively, particles are counted on a filter manually or extracted from a matrix, and individual particles are analyzed via Raman or FTIR. The spectra are first visually assessed for quality to determine if additional spectral measurements are necessary, then processed to amplify the signal-to-noise ratio and remove the presence of baseline signals, and finally matched using a reference library that contains plastic and non-plastic spectra.

Because microplastics are a diverse suite of contaminants[174], they require adaptable tools and extensive reference libraries for accurate matching. New specialized matching techniques that focus on peak regions of the reference spectra are shown to drastically outperform the standard techniques for microplastics research[177]. Open source software could be rapidly adapted to include this and other new techniques. Pure unweathered polymers are not commonly found in the environment[56,178]. Microplastic reference libraries should include many phases of particle degradation, additive mixtures, and colors for accurate matching[179,180], but only a small number of spectra are openly available. A recently published review on microplastics data analysis techniques found that more than half of research groups duplicated efforts by developing in-house spectral tools and matching libraries, but not sharing them with the wider scientific community[176]. We developed an open source tool, library, and community called Open Specy to satisfy these needs while improving functionality and accuracy for identifying plastic particles compared to commercial tools and libraries.

First, we describe the design of Open Specy and its supporting documentation. Then, we compare Open Specy's functionality to other spectroscopy software. Lastly, we validate Open Specy for microplastic analysis by comparing its accuracy to commercial spectroscopy software and outline how Open Specy will foster a scientific community and better spectral identification moving forward.

5.2 Experimental Section

5.2.1 Open Specy Features and Documentation

Open Specy users can view, process, identify, and share their IR and Raman Spectra (Figure 5-1). We created Open Specy in R (4.0.4)[181] using the RStudio IDE[182], with the shiny[106], ggplot2[158], smoother[183], dplyr[107], plotly[90], data.table[108], signal[184], shinyjs[109], shinythemes[110], shinyWidgets[185], shinyBS[186], digest[187], config[188], osfr[189], knitr[190], rmarkdown[191], testthat[192], mongolite[193], loggit[194], DT[111], rdrop2[195], hyperSpec[196], and hexView[197], libraries. Open Specy is online at www.openspecy.org and on CRAN as an R package[198] with extensive documentation, help guidance, and error guidance on the website. In the R package, the base functions in Open Specy can be accessed to expand the existing functionality for other use cases. The source code (written in R) and reference library materials are available on Github (https://github.com/wincowgerDEV/OpenSpecy) and Open Science Framework (OSF, https://osf.io/x7dpz/). The code and databases are version-controlled so that older versions can be retrieved by users who need to revive an older working session for any reason. We also thoroughly detailed step-by-step instructions for using the tool[199].

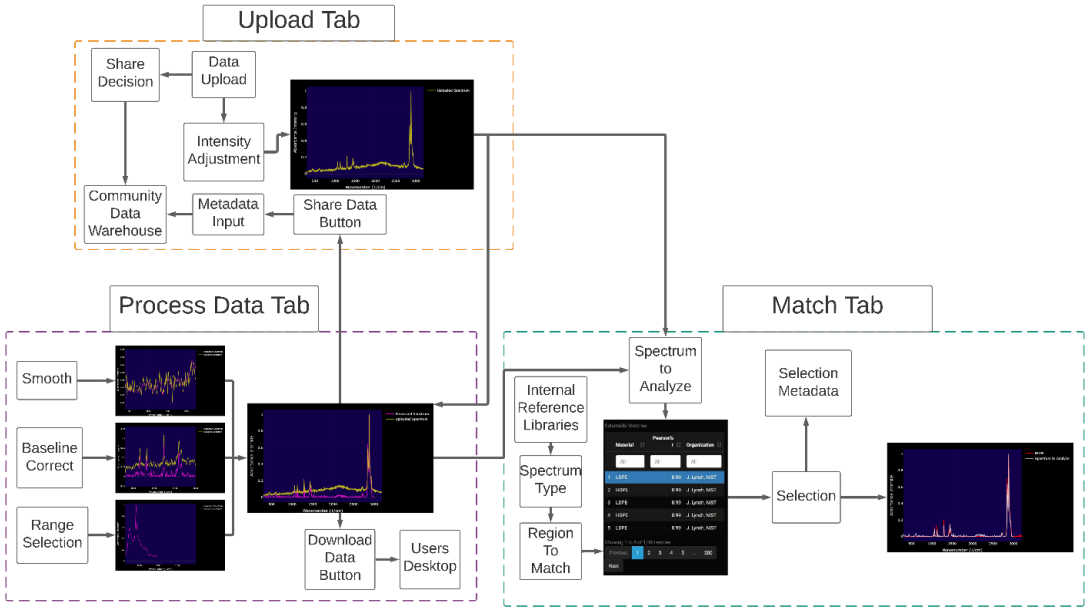

Figure 5-1. Workflow diagram for features and data pipeline in Open Specy. Interactive and updating version: https://lucid.app/lucidchart/invitations/accept/13cfe6c0-45c0-4e51-8c99-83711121c54c

A typical workflow for microplastic spectral identification in Open Specy consists of file upload, processing, and identification. Before upload, users select whether they want their uploaded data and session logs to be shared with the spectroscopy community or not. Shared data will help advance the tool and make users' work reproducible. Users can add metadata to make their uploaded data more useful. Metadata explanations are given in a live document (https://osf.io/bgdqf/) and in the tool. Any shared data with metadata will be vetted by experienced spectroscopy experts and added to the tool if it meets our quality requirements (https://osf.io/w9s43/). All shared data is automatically shared under a license of the user's choice and uploaded on OSF as funding allows (https://osf.io/rjg3c/). A

test spectrum can be uploaded in several formats (asp, csv, spa, spc, jdx, and 0). Once uploaded, a spectrum can be viewed in an interactive window with zoom, pan, screenshot, and layer on and off functionality.

Users can then process their spectrum using smoothing with Savitzky and Golay filter[200], and baseline correction with IModPolyFit[201]. We translated the script provided at https://github.com/michaelstchen/modPolyFit for IModPolyFit from MATLAB to R[202]. The IModPolyFit function iteratively finds the baseline by fitting a polynomial regression of the specified order to the whole spectrum. Many of the large peaks are identified on the first iteration because they stand above the fit and are ignored for further iterations. The iterative process finalizes once the difference between successive fits is minimal. The processed spectrum can be downloaded as a csv file.

Lastly, users can identify their spectrum to the onboard spectral library and interactively view the matches. The spectral library currently consists of a Raman library with 3696 spectra from RRUFF[203], 759 spectra from the Raman Open Database[204], 208 spectra from Cabernard et al.[205], 58 spectra from the Raman Spectroscopic Library UCL Chemistry[206], 44 spectra from the Open Specy community members Dora Mehn, Jennifer Lynch, and Claudia Cella, and 15 spectra from Horiba Scientific. The FTIR library consists of 325 spectra from Primke et al.[207], 272 spectra from Chabuka et al.[180], and 39 spectra from Thermo

Fisher Scientific. These spectra have all been manually adjusted to remove baseline and noise. A second version of each reference library was made by removing signal regions that are not the peaks as described in Renner et al. [177]. The user can choose to use the whole spectrum libraries or the peak spectrum libraries for identification. The matching procedure consists of a Pearson correlation between the chosen reference spectra and test spectrum. When matching is initiated, a grouped correction strategy first minimum-normalizes (intensity minus minimum intensity) over the whole spectrum or for each peak region depending on what the user specifies. The Pearson correlation coefficient is used directly as the hit quality index for ranking matches. The matches are returned in an interactive display that allows users to view matches individually alongside the test spectrum, and detailed metadata of any selected spectrum is displayed. To assess a good match, inspect peaks to ensure that the match has all of the same peaks with the same shape and the same height ratio. From our experience, when top matches are below 0.6 Pearson correlation coefficient, they should be suspected to be a result of incorrect preprocessing, poor quality spectra, or of a material type not currently in the reference library. User selections during preprocessing and matching are also logged to advance future developments of the application and ensure reproducibility of all manipulations to the spectra.

Ensuring accuracy through validation, inclusivity, and transparency are primary goals for our group. Validation is conducted on Open Specy whenever new spectra

or default settings are added to the library (https://osf.io/zcafk/). Validation must demonstrate greater than 80% accuracy for the whole procedure for these updates to be made to the tool. Currently, the validation statistics are above 90%. Anyone can use Open Specy free of charge. As Open Specy grows, these features will become more robust and numerous. Everyone is welcomed to collaborate with us to write publications, develop the tool, and share data. We have detailed a framework for collaboration in the Open Specy group (https://osf.io/q94dc/), and anyone is welcome to take the project and build something new with it that they publish themselves. Furthermore, we respond to any bug reports and feature requests from users as quickly as possible and track updates that are pushed to the web (https://github.com/wincowgerDEV/OpenSpecy/issues).

5.3 Results and Discussion

5.3.1 Review of the current tools

We searched for other Raman and FTIR spectroscopy spectral analysis tools and compared their base functionality to Open Specy (Table 5-1). We found that Open Specy has microplastic identification functionality that is not standard in all commercial spectroscopy software (e.g., standard OMNIC does not have a reference library and standard LabSpec cannot find a match to a library). Two other notable tools, siMPle[208] and Spectragryph[209], share their library spectra, are free to use, and are highly functional at processing spectra and spectral matching. siMPle was also developed with microplastic analysis in mind and was designed

to analyze full spectral maps from hyperspectral scanning devices[208]. Due to web hosting costs for large datasets, we have not yet implemented that functionality in Open Specy online. However, automation routines can be deployed using the R package functions from the Open Specy package, which could be iterated on a hyperspectral map or a large number of spectra. Only siMPle and Open Specy provided documented validation of the entire software routine for accurately identifying spectra. We suspect that the tools lacking validation documentation are undergoing validation, but the procedure is not transparent, which should be relevant to anyone using those tools. Most of the tools, including free tools like Open Specy and siMPle, offered users technical support. None of the spectral tools, besides Open Specy, made their source code available or had a crowdsourced library. Making the source code available will allow others to remix and reuse all the field components and subject the tool to perpetual peer review from users who identify software bugs as they arise and fix them. The crowdsourced library will make Open Specy competitive with commercial libraries, which rely heavily on pure materials for their reference spectra. Open Specy incorporates diverse spectra from diverse materials and already includes weathered materials to improve spectral identification accuracy for microplastic research[180]. The advancements brought by Open Specy are critical to the advancement of microplastic identification. Identifying microplastics accurately requires a maximum level of transparency and modularity in the tools.

Table 5-1. Meta-analysis of tool base functionality and utility for spectroscopy analysis software available today. Software tools are listed on the top axis. All software are assessed for basic functions/uses listed on the left axis. Tools are organized from most functions to least from left to right, and functions are organized from most common to least from top to bottom. “X” indicates that the tool has the functionality, and blank indicates the tool does not have the functionality.

	Open Specy[210]	siMPle[208]	Spectragryph[209]	KnowItAll[211]	OMNIC[212]	Essential FTIR[213]	Spec Tools[214]	FDM Search	Raman Tool Set[216]	LabSpec[217]
Process spectra	x	x	x	x	x	x	x		x	x
Find match to library	x	x	x	x	x	x		x		
Made for Raman and FTIR	x	x	x	x	x		x	x		
Technical support	x	x	x	x	x	x		x		x
Free	x	x	x				x		x	
Add spectra to library	x	x	x	x	x					
Nonplastic spectra in library	x	x	x	x						
Plastic spectra in library	x	x	x	x						
Spectral map analysis		x							x	x
Library data open access	x	x	x							
Environmentally weathered materials	x	x								
Documented Software QAQC	x	x								
Source code available	x									
Crowdsourced library	x									

5.3.2 Validation of Open Specy

We compared the material identification accuracy of Open Specy to OMNIC Picta software for FTIR and KnowItAll and ID Expert for Raman spectra using 50 highly validated plastic materials published in another manuscript[179]. The samples included 1 to 10 representatives of 9 polymer Raman spectra and 1 to 5

representatives of 14 different FTIR ATR polymers. The Raman and FTIR spectra from these test materials did not exist in any of the software tested. We processed the test spectra using baseline correction and smoothing techniques to amplify the signal-to-noise ratio in each software, then had the software identify the spectra using the standard matching procedure and assessed the top ten matches for a true positive result to the known identity of the spectra. If at least one of the spectra in the top ten matches was true, we accepted the software answer as true. A detailed explanation of the validation procedure and supporting data is available in the SI (https://osf.io/6yjmc/). We found that Open Specy currently outperforms KnowItAll (correct: Open Specy = 48/50, KnowItAll = 44/50) for Raman spectra, and slightly underperforms OMNIC Picta for FTIR spectra (correct: Open Specy = 48/50, OMNIC = 49/50). The Raman spectra misidentified in Open Specy were a polyethylene spectrum and a polyamide spectrum. The two misidentified FTIR spectra were polyethylene vinyl acetate and polyvinyl chloride. We are prioritizing additions of a greater diversity of these spectra in future releases of Open Specy and encourage community members to share references for these spectra. We expect that OMNIC Picta performed similarly to Open Specy because the Primkpe library[207], which has a diverse suite of consumer plastic materials relevant to microplastic research, was installed in OMNIC. Since Open Specy is an open source tool, we will be able to increase the accuracy over time using community shared spectra (https://osf.io/rjg3c/).

5.4 Conclusion

Over 2000 unique users have currently visited Open Specy, usage time on the website averages 250 hours per month, and nine peer-reviewed publications have already used and recommended Open Specy for microplastic spectral analysis[176,218–225]. We are dedicated to continual improvements in Open Specy, and we respond to all inquiries. In this way, the authors, their research groups, and the scientific community at large will support the development of a robust and ever-growing spectral identification and processing tool. There is a growing list of feature requests that we will respond to as time and funding allow (https://github.com/wincowgerDEV/OpenSpecy/issues). Immediate future developments will incorporate machine learning (in process, https://osf.io/bes7h/) and fusion matching approaches[180] to improve match accuracy and analysis simplicity. We made the source code for the tool entirely open source so that industry, scientists, and governments can develop and expand its functionality. We invite contributors to join us and have outlined how to contribute in the supporting documentation (https://osf.io/q94dc/).

5.5 Data Availability

All supporting information is cited throughout the manuscript as living documents, data, and source code, which will be indefinitely available on the OSF home page https://osf.io/3uatf/. These documents are downloaded into a zip file at the time of publication as part of the supplementary information but will not be perpetually

updated like the OSF page. The zip file structure follows the OSF page. Documents are grouped by use. Folder names follow the citations referenced throughout the manuscript. ReadMe text files are written in folders that need an additional explanation about the files contained within and their relationships. The ReadMe files follow the documentation on OSF.

Chapter 6: Concentration depth profiles of microplastics

6.1 Abstract

River flow is a major conveyance of microplastic (1-5000 μm) pollution from land to marine systems. However, current approaches to monitoring and modeling fluvial transport of microplastic pollution have primarily relied on sampling the surface of flow and assumptions about microplastic concentration depth profiles to estimate depth-averaged concentration. The Rouse profile was adapted to show that fluvial transport of microplastic pollution includes all traditional domains of transport (bed load, settling suspended load, and wash load), as well as additional domains specific to low-density materials with rising velocities in water (rising suspended load and surface load). The modified Rouse profile was applied to describe positively buoyant particle concentration depth profiles and compared to field observations to showcase the utility of this approach. A procedure was developed for assessing the uncertainty and bias from using a surface sample to estimate depth-averaged concentration while assuming either surface load or wash load concentration depth profiles. Both assumptions may introduce a large amount of uncertainty due to the range of suspended microplastic concentration depth profiles. Monitoring microplastic pollution and estimating the depth-averaged concentration of microplastics in fluvial systems would further benefit from broader adoption of depth-integrated sampling, characterization of particle concentration

depth profiles, and estimation of uncertainties in depth-averaged concentration based on the sampling approach.

6.2 Introduction

Plastic pollution in rivers threatens aquatic organisms, riverine ecosystem services, and human health at the global scale[226–228]. Macro-scale plastic particles (> 5 mm) are known to cause harm to animals through ingestion and entanglement[229], and there is increasing evidence for adverse ecosystem and human health impacts associated with microplastics (1 µm to 5 mm[230,231]) and even nanoplastic (< 1 µm) particles[232]. Microplastics are a diverse suite of contaminants with a wide range of shapes, sizes, colors, and chemical properties[174]. River discharge is also a dominant source of plastic pollution in the ocean[35,233,234], where hydrodynamic processes may transport plastic particles over vast distances and expand the scope of adverse impacts[235–237]. Large (factor of 10) differences between modeled and expected marine and fluvial plastic concentrations[35] have raised concerns that the transfer of fluvial microplastic pollution to the ocean may be dramatically misrepresented by current approaches that do not consider the range of fluvial microplastics concentration depth profiles[238–244]. Preliminary studies have indicated that microplastics may be transported differentially throughout the water column, but there has yet to be an analysis on how monitoring and flux estimation techniques may contribute to model disparities.

Current efforts to model and monitor microplastic concentration in rivers are negatively impacted by untested assumptions favoring a given concentration depth profile. For example, Besseling et al.[245] and Nizzetto et al.[246] modeled fluvial microplastic transport by assuming that microplastic particle density was greater than water, whereby microplastics travel with river flow only as wash load (uniformly distributed across the flow field), settling suspended load (increasing concentration with depth), or bed load (mostly transported along the river bed). Conversely, Lebreton et al.[35] and Miller et al.[247] characterized all microplastics as positively buoyant particles traveling at or near the surface (a region from the free surface to some depth below) of the river as surface load (transport only at the surface) or rising suspended load (increasing concentration toward the surface). Other monitoring-based studies assumed equally distributed concentrations of microplastic particles throughout the flow field (i.e., microplastics as wash load) regardless of particle size and the energetics of the flow field, evoking an assumption of neutral buoyancy[248,249]. The relatively few studies that have attempted to characterize variation in plastic particle concentrations across the flow field have documented transport as surface load[250], wash load[251,252], bed load,[253] and as a complex mixture of all concentration depth profiles[254]. This diversity of assumptions and observations highlights the need for a process-based approach to predict microplastic concentration depth profiles in rivers.

Concentration depth profiles in rivers are commonly predicted by the opposition of gravitational and turbulent forces, where particles with higher settling velocities

relative to the water's turbulent mixing are expected to display higher concentrations with depth[255]. Approaches to suspended particle (mineral sediment and organic matter) sampling have been refined to account for concentration depth profiles[256,257]. The Rouse profile model is often used as a heuristic and predictive tool[51,52]. Previous research on riverine concentration depth profiles has extensively validated the Rouse profile for predicting concentration depth profiles of negatively buoyant particles in natural systems (1.1-3.0 g ml^{-1})[258–261]. Microplastic particles have been observed to obey the same physical principles as natural particles commonly modeled with the Rouse profile[51,52]. Yet, microplastic particles span a wide range of densities higher, equal to, and less than that of water (0.022-2.2 g ml^{-1})[51,54,262]. Similar diffusivity equations to the Rouse profile have been used to describe the concentration depth profile of positively buoyant particles in the ocean[263], and a recent study incorporated positively buoyant macroplastic particle concentration depth profiles in rivers using the Rouse profile[264]. However, no study to date has applied the Rouse profile to positively buoyant microplastic particle transport in rivers. There is a need to demonstrate the Rouse profile application for predicting positively buoyant microplastic particle concentration depth profiles observed in the literature to inform transport monitoring and modeling.

Although microplastic particles are likely transported by river flow under a wide range of concentration depth profiles, many sampling efforts have focused on the surface of the water column[265] (from the surface to some fraction of the total flow depth) and estimated flux on assumptions about the concentration depth profile.

This sampling strategy will likely underrepresent microplastics near the river bed and overrepresent microplastics near the surface. Despite this approach's predominance, the field does not currently have a mechanism for describing the potential bias and uncertainty introduced by the range of potential concentration depth profiles.

We investigate three major questions. 1) What are the possible concentration depth profiles for microplastics in rivers? 2) How does the modified Rouse model compare to field observations of positively buoyant microplastics? 3) What is the potential range of bias and uncertainty introduced by current approaches to estimating average microplastic concentrations with surface samples?

6.3 Materials and Methods

6.3.1 Microplastic concentration depth profiles

We utilized a modified version of the Rouse profile[264] to predict the range of microplastic concentration depth profiles under theoretical and observed scenarios.

6.3.1.1 Theoretical basis for modified Rouse profile

Concentration depth profiles of particles in rivers are generated by the opposition of the rising or settling force of the particles (force accelerating particles toward the bottom or surface of the river) and the turbulent mixing force of the river (force

keeping particles in suspension). The Rouse number *P* (dimensionless) for settling particles is a non-dimensional representation of the concentration depth profile that describes the interaction between the particle settling velocity and vertical turbulent mixing:

$$P = \frac{w_s}{\beta k u_*} \quad (1)$$

where w_s (length per time) is the particle settling velocity, *k* (dimensionless) is the von Karman constant set to 0.4[266], u_* (length per time) is the shear velocity of the river, and β (dimensionless) is the parameter that adjusts the assumption of parabolic eddy diffusivity for the Rouse profile (equation 2) (assumed to be 1)[260]. The Rouse number has been used to describe the shape of the concentration depth profile of settling particles for over 80 years[255], and remains one of the simplest models to deploy with few parameters. Although there are many assumptions, this model has been demonstrated to produce a 0.75 – 1.5 predicted to observed ratio of Rouse number values for mineral sediment profiles in most natural systems[260]. By inputting negative values of w_s for particles with rising velocities, we derived the Rouse number of rising particles and generated the Rouse profile, a time-averaged transport equation, which describes the concentration depth profile with respect to a reference location and river depth:

$$\frac{C_a}{C_z} = \left(\frac{(h-a)}{a} \times \frac{z}{(h-z)}\right)^P \quad (2)$$

where C_a (quantity per volume) and C_z (quantity per volume) are the concentration of particles at depths *a* (length), *z* (length), where *z* is the reference location, and

h (length) is the total depth of the water. The Rouse profile is derived from first principles simplified by the assumptions of steady and uniform flow, equilibrium between upward/downward turbulence and particle settling or rising velocities, uniform channel geometry, parabolic eddy viscosity (where diffusion is greatest at the center of the channel)[267], uniform and constant Schmidt number of 1, and uniform and constant settling velocity[264].

In open channel flow, turbulent diffusion is often present throughout the water column and impacts the stratification of particle concentration between the river surface and bed[268]. Major components of hydraulic resistance that interact with the water column to induce turbulent mixing include the shear stress at the bed[269], channel bed grain roughness[269], bedforms[268], structures like bridges[270], vegetation[271,272], and wind shear stress at the river surface[273]. Turbulence dampening effects can also occur in rivers from the stratification of particles in the water column when particle concentrations are very high[274]. Here, we investigate turbulent mixing induced from the vertical velocity gradient generated by the no slip boundary condition at the river bed. Bed shear velocity is simple to estimate, is present in all rivers, and is often a dominant component of turbulence throughout the water column[273,275].

We derived shear velocity as:

$$u_* = \sqrt{ghs} \tag{3}$$

where u_* (length per time) is shear velocity, g (length per time squared) is the acceleration due to gravity, h (length) is mean water depth, and s (dimensionless) the water surface slope. This use of water depth instead of hydraulic radius assumes that the channel is much wider than it is deep. To derive the water depth for the river locations in this study, we fit a rating curve (general additive model with log-normal distribution) to observations by the United States Geological Survey USGS[151] between discharge and channel depth (calculated by dividing the channel cross-sectional area by channel width). To derive channel slope, we used Google Earth and ArcMap to measure river distance and a 1/9th arc second elevation digital elevation model from the National Elevation Dataset[153] to measure the downriver river surface elevation change.

We assigned names to Rouse number ranges for settling particles following those commonly stated in other sources[276] (Figure 6-1; Table 6-1) surface load, rising suspended load, settling suspended load, wash load, bed load, and immobile. We set thresholds based on the negative analog of settling particle domains for Rouse numbers of rising particles.

Table 6-1: Concentration depth profile domains are defined by Rouse number ranges with descriptions.

Concentration Depth Profile Domain	Rouse Number	Description
Immobile	$P > 7.5$	Particles are in contact with the river bed and not moving.
Bed load	$7.5 > P > 2.5$	Particles move primarily along the river bed by rolling, skipping and saltating along the bottom most portion of the flow field.
Settling Suspended Load	$2.5 > P > 0.8$	Particles are partially distributed throughout the water column with higher concentrations at the river bed.
Wash Load	$0.8 > P > -0.8$	Particles are equally distributed throughout the water column.
Rising Suspended Load	$-2.5 < P < -0.8$	Particles are partially distributed throughout the water column with higher concentrations at the surface of the river.
Surface Load	$P < -2.5$	Particles are traveling only at the surface of the river.

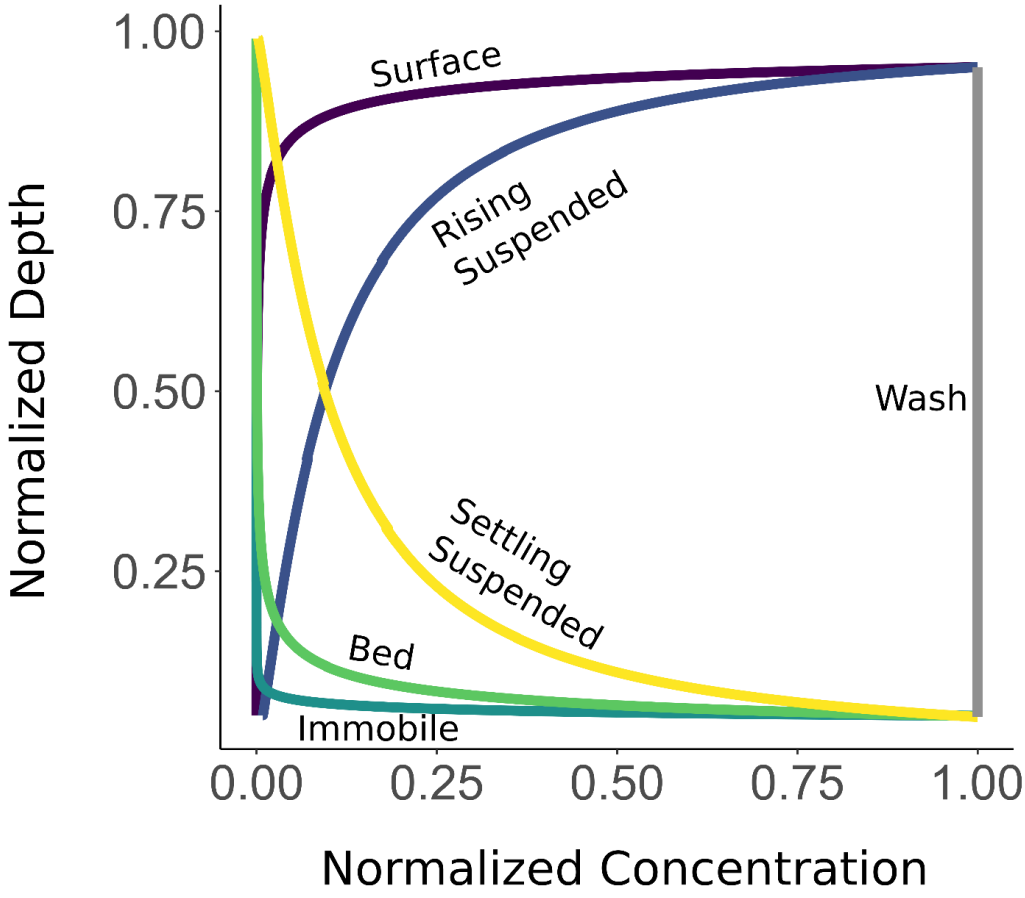

Figure 6-1: Normalized depth is min-max normalized h from equation 7. Normalized concentration on the x-axis is min-max normalized Ca from equation 7. This figure shows examples of boundary condition (Table 6-1) concentration depth profiles (equation 2). These are the boundaries for the concentration depth profile domains used throughout the study. The reference location for surface and rising suspended load was set to 0.95 (a reasonable surface sampling location). The reference location for immobile, bed, and settling suspended load was set to 0.05 (a typical bed load boundary). Colors correspond to Figure 6-3 and boundary conditions are marked with their corresponding domain name (Surface load (P = -2.5), Rising suspended load (P = -0.8), Wash load (P = 0), Settling suspended load (P = 0.8), Bed load (P = 2.5) and Immobile (P = 7.5)).

6.3.1.2 Predicting theoretical microplastic concentration depth profiles

To describe the global theoretical domains of microplastic transport, we used simplifying models. Rouse domains were calculated using the Rouse number

(equation 1) and thresholds for domain classification (Table 6-1). We defined the minimum and maximum u_* as 0.01 mm s^{-1} (e.g., a low gradient shallow river)[277] and 1000 mm s^{-1} (e.g., a high gradient deep river)[278]. These theoretical bounds are for rivers with clear water flow and a smooth boundary and bed. We then calculated the theoretical range of maximum and minimum particle settling and rising velocities. We considered that not all particles would be within the Stokes domain of the drag curve and employed a computational solution:

$$C_D = \frac{24}{Re} + \frac{2.6\left(\frac{Re}{5}\right)}{1+\left(\frac{Re}{5}\right)^{1.52}} + \frac{0.411\left(\frac{Re}{263000}\right)^{-7.94}}{1+\left(\frac{Re}{263000}\right)^{-8}} + \frac{0.25\frac{Re}{1000000}}{1+\frac{Re}{1000000}} \quad (4)$$

where a continuous drag curve is plotted as in Morrison[279] for all particle Reynolds numbers < 10^6, C_D (dimensionless) is the drag coefficient, and Re (dimensionless) is the particle Reynolds number. This drag curve only applies to spherical particles. Deviations from spherical particles will decrease the terminal rising or settling velocity[280,281] by increasing the drag coefficient so this method estimates the maximum terminal velocity range. The dimensionless group C_DRe^2 was then calculated as per Rhodes:[281]

$$C_D Re^2 = \frac{4}{3}\left(\frac{D_p^3 * \rho_f * abs(\rho_p - \rho_f) * g}{\mu^2}\right) \quad (5)$$

where D_p (length) is the particle diameter, g (length per squared time) is the acceleration due to gravity, ρ_p (mass per volume) is the particle density, ρ_f (mass per volume) is the fluid density, and μ (force times time divided by area) is the

dynamic viscosity of water (set to 20 °C). The range of theoretical plastic particle density (ρ_p) values was chosen to represent those found for settling and rising particles reported in the litterature:[51,54,262] ρ_p was set to 22 and 970 kg m^{-3} for rising particles and 1010 and 2200 kg m^{-3} for settling particles. Smaller particles generally have lower terminal velocities so we paired them with the density closest to water to find the lowest terminal velocity and larger particles with the furthest densities from water to find the highest terminal velocity. Microplastic particle diameter (D_p) was chosen to represent the smallest and largest particle characterized as "microplastic"[230,231] and set to 5 x 10^{-3} m for densities furthest from water and 1 x 10^{-6} m for densities closest to water. The intersection of the drag curve and the dimensionless group (a constant value with slope -2 in log-log space) specified the particle Reynolds number value used to calculate the rising or settling velocity:

$$w_s = \frac{Re' * \mu}{D_p * \rho_f} \quad (6)$$

where *Re'* (unitless) was the Particle Reynolds number found by the intersection of equations 4 and 5 and other units were previously mentioned in equation 5. After this calculation, terminal velocity w_s was set to negative (rising particles) or positive (settling particles).

6.3.1.3 Estimating observed microplastic concentration depth profiles

Concentration depth profiles were calculated using the Rouse number (equation 1) and thresholds for domain classification for observed microplastic particles[282]

(Table 6-1). The range of shear velocities was obtained from Baldwin et al.[283] with equation 3. Baldwin et al.[283] was used because it was an extensive microplastic pollution study found in our literature review, totaling 29 river systems, each with data available from the USGS sufficient to estimate shear velocity. The observed range of settling and rising velocities of microplastic particles were obtained from Waldschläger and Schüttrumpf[51]. The study conducted in Waldschläger and Schüttrumpf[51] measured the settling and rising velocities of a wide range of microplastic particle sizes (0.3-5 mm), shapes (foam, sphere, pellets, fibers, fragments), and polymers (EPS, PP, PE, PS, CoPA, PVC, PET).

6.3.2 Application to positively buoyant microplastic concentration depth profiles

As a preliminary test of model performance, we applied the Rouse profile to a subset of positively buoyant microplastic concentration depth profiles observed by Lenaker et al.[254] (Figure D-1). Lenaker et al.[254] measured microplastic concentration in rivers in the Great Lakes region using nets (1.5 m long by 100 cm wide by 40 cm high) at two depths (surface and ~0.5*depth) during six time points. Two of their study sites were chosen for testing because they had non-estuarine flow conditions and observations of foam particles. Eight paired samples (surface and subsurface) were collected in total at these sites, but here we only examine the six that contained foam particles. They counted and characterized microplastic particles by size (small microplastics, 0.333-1 mm, and large microplastics, 1-5 mm) and shape (foam, film, fragment, pellet/bead, fiber/line), and calculated

concentrations on the basis of sample particle counts and water volume estimated with the velocity area method. We transformed the sample concentrations to min-max normalized values for each sample pair (equation 7).

$$X_{norm} = \frac{(X - X_{min})}{(X_{max} - X_{min})} \quad (7)$$

Where X_{norm} (dimensionless) is the min-max normalized set, X (any dimension) is any set of numeric values, X_{min} is the minimum value in the set and X_{max} is the maximum value.

We limited this test to only foam particles in order to tightly constrain both density and shape. The foam microplastics that we have observed in the environment have been predominantly expanded polystyrene particles with similar densities and shapes[56]. The vast majority of "foam" particles in Lenaker et al.[254] were confirmed as polystyrene using FTIR, and confirmed as the expanded form of polystyrene by the authors (personal communication). Foam particles were assumed to have similar geometry and density to those identified as "expanded polystyrene foam" described by Waldschläger and Schüttrumpf[51] (expanded polystyrene foam particle sizes 0.8-5 mm). We derived a general linear model (slope = 0.047, intercept = 0.056, adjRSQ = 0.92 , p = $2.87*10^{-5}$, n = 9)(Figure D-2) between particle size and particle rising velocity for the particles in Waldschläger and Schüttrumpf[51] to estimate the rising velocity of the mean particle sizes in each size range defined by Lenaker et al.[254] (0.67 mm and 2.88 mm). The lower mean size

of foam in Lenaker of 0.67 mm was slightly smaller than the 0.8 mm particle size in the Waldschläger and Schüttrumpf[51] dataset, but we felt it was close enough to perform the extrapolation. We used this model instead of the approach in section 2.1 to estimate particle terminal velocities because the terminal velocities found in Waldschläger and Schüttrumpf[51] included influences due to particle geometry and surface roughness not included in the Reynolds number derivation. River shear velocity was computed using equation 6. The Rouse number was fit using the root mean squared error to the observations. The Rouse numbers of the predicted and observed profiles were ascribed to concentration depth profiles using Table 6-1. The number of times each concentration depth profile occurred for a size class at a given observation location were summed, and the results were compared.

6.3.3 Potential surface sampling bias and uncertainty

Studies use surface samples (a sample that extends from the surface to some depth below the surface) to calculate depth-averaged concentration under the assumption of a certain concentration depth profile (usually wash load or surface load). We examined the range of potential bias introduced by these assumptions under an idealized scenario model with variable surface sample depth and a range of possible concentration depth profiles.

6.3.3.1 Estimating the bias of surface sampling and assuming wash load

To calculate the potential bias introduced by assuming a wash load concentration depth profile, we derived a one-dimensional model to predict depth-averaged concentration by incorporating sampled depth and the Rouse profile (equation 2) in the unsampled region (Figure 6-2). We created the possible Rouse profiles using the range of Rouse numbers for suspended particles (P = -2.5 to 2.5). This range was determined as a possible range for suspended microplastic concentration depth profiles in section 2.1 and observed in discrete depth samples of total plastic by several studies[251,252,254]. All variables were min-max normalized (equation 7) so that they would be unitless. River depth h was set to 1, z was set to the center of the sampled depth d. Sampled depth d simulated a net opening that extends from the river's free surface down to the bottom of the net. d was varied from 0.99-0.05 at 0.01 intervals. We chose 0.99 and 0.05 normalized depths because it is realistic to sample between these depths for most rivers, the Rouse profile needs to be constrained between depths 1 and 0 (where modeled concentrations trend toward infinity), and the Rouse profile poorly models concentrations below ~0.05 depth[260]. C_a was estimated with C_z set to 1 for depths from 0.05 to the bottom of the sampled depth using the Rouse profile at 0.00001 intervals. Within the sampled depth d, C_a was set to C_z at 0.00001 depth intervals. C_z was used as the wash load estimate. We then averaged all C_a estimates and divided the depth-averaged concentration by the wash load estimate to determine potential bias. In this case, the bias is the

value that the assumed concentration would need to be multiplied by to equal our model's depth-averaged concentration.

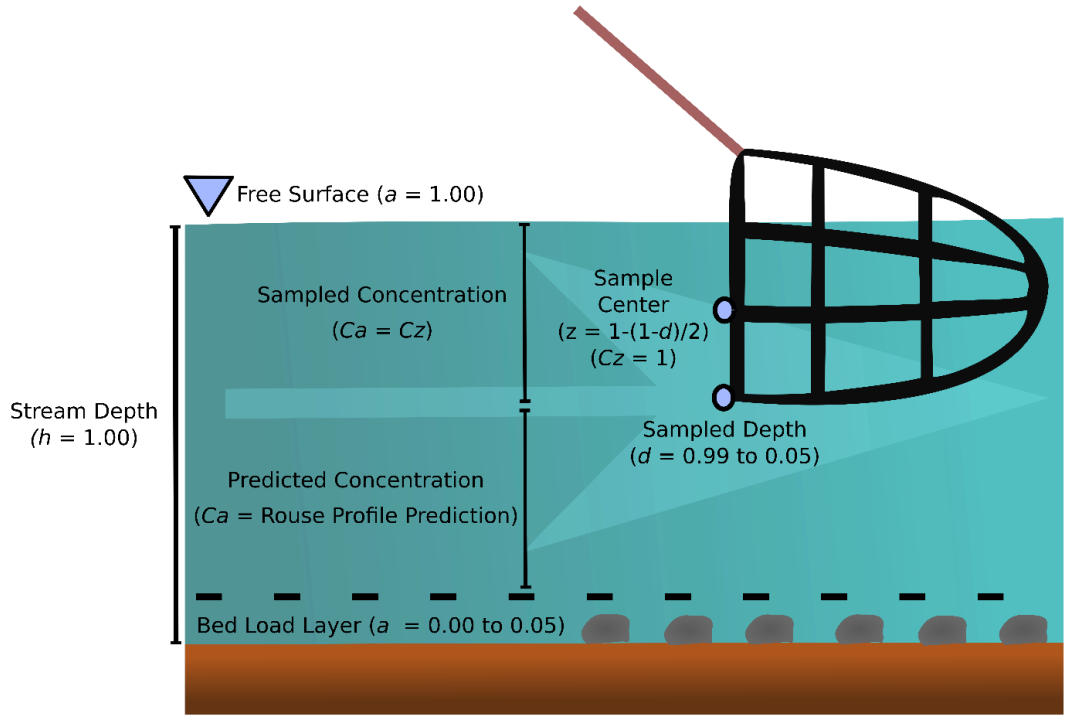

Figure 6-2: Visualization of the model setup and parameters used to estimate bias and uncertainty from surface samples. The variables listed are used in equation 2. C_a is the concentration estimate, z is the reference location, C_z is the reference concentration, d is the depth where the bottom of the net is, a is a location in the water depth, h is the depth of the water column. The depth layer from the bed up to 0.05 is not included because this model poorly describes bed load. An arrow points in the direction of flow.

6.3.3.2 Estimating the potential bias of surface sampling and assuming surface load

To be consistent with the approach used in other plastic pollution literature to estimate flux under the assumption of surface load, we closely followed the methods outlined in Lebreton et al.[35]. Their approach assumed that the

concentration found flowing through the net was the concentration representative of "surface plastics," and no plastic was transported below this surface load. The sample concentration was multiplied by the proportion of the river depth sampled to determine the depth-averaged concentration of plastic under the assumption. The same approach used in section 2.3.1 was used here to iterate through potential concentration depth profiles and sample depths and derive the potential bias introduced by this assumption.

6.3.3.3 Estimating uncertainty of surface sampling at varying sample proportions due to concentration depth profiles

Potential uncertainty was defined as the sum of the maximum overestimation and maximum underestimation bias, in $\log_{10}$ absolute value space from sections 2.3.1 and 2.3.2. Uncertainties do not vary between assumptions because they are constrained by the range of Rouse numbers tested (-2.5, 2.5), which was the same for each assumption setup in the model. We derived uncertainty estimates separately for rising particles, settling particles, and all particles, dependent on the proportion of the water column sampled (between 0.01 and 0.95).

6.3.3.4 Bias and uncertainty model assumptions

All assumptions carry over from those described for equations 1, 2, and 3. Since this is a 1D model, it does not account for concentration gradients across the river width. This model will best represent river conditions that are not rapidly changing

or ice-covered and long-duration samples. The model will best represent wide rivers with clear water flow and a smooth boundary. Lastly, bed load is not accounted for in the model, so bed load has to be ignored even though it is present.

6.3.4 Data analysis software and workflow

R studio with R version 4.0.1[284] was used to do data manipulation, analysis, and figure creation. Data was kept in the rawest form possible to record all manipulations in the R Code. Packages used include: ggplot2[158], dplyr[107], data.table[108], mgcv[285], stringr[161], readxl[160], tidyr[163], and viridis[162]. Several functions not available in any current packages were written in R. All code is shared along with raw data to make every step of the analysis reproducible (https://osf.io/azghy/).

6.4 Results and Discussion

6.4.1 Microplastic concentration depth profiles

We modeled the theoretical concentration depth profiles for microplastics in rivers and the observed case study of fluvial microplastic concentrations reported in Baldwin et al.[283] (Figure 6-3). While the range of the plot represents the extreme possibilities, the pink boxes are not extreme and are likely to be encountered in the real world. Recent experimental research[52] indicated critical shear velocities for microplastic particles between 1.41 mm s^{-1} and 15.2 mm s^{-1} – similar to the range of shear velocities at the threshold for motion that we found for the Baldwin

et al.[283] study conditions (Figure 6-3, lower pink box). Our results show that every concentration depth profile is possible under theoretical and observed ranges of common microplastic particle compositions and hydrologic conditions. One should not assume any particular concentration depth profile without additional information about particle and hydraulic characteristics or measurements of concentrations at various depths. This plot can also be used as a heuristic tool to provide a first estimate of which concentration depth profiles may be present in a given system. If a user knows the range of settling, rising, and shear velocities at their site (e.g., using equations 3-6 to get rough bounds), the user can draw bounding boxes around those regions on this figure to identify the potential concentration depth profiles of their particles.

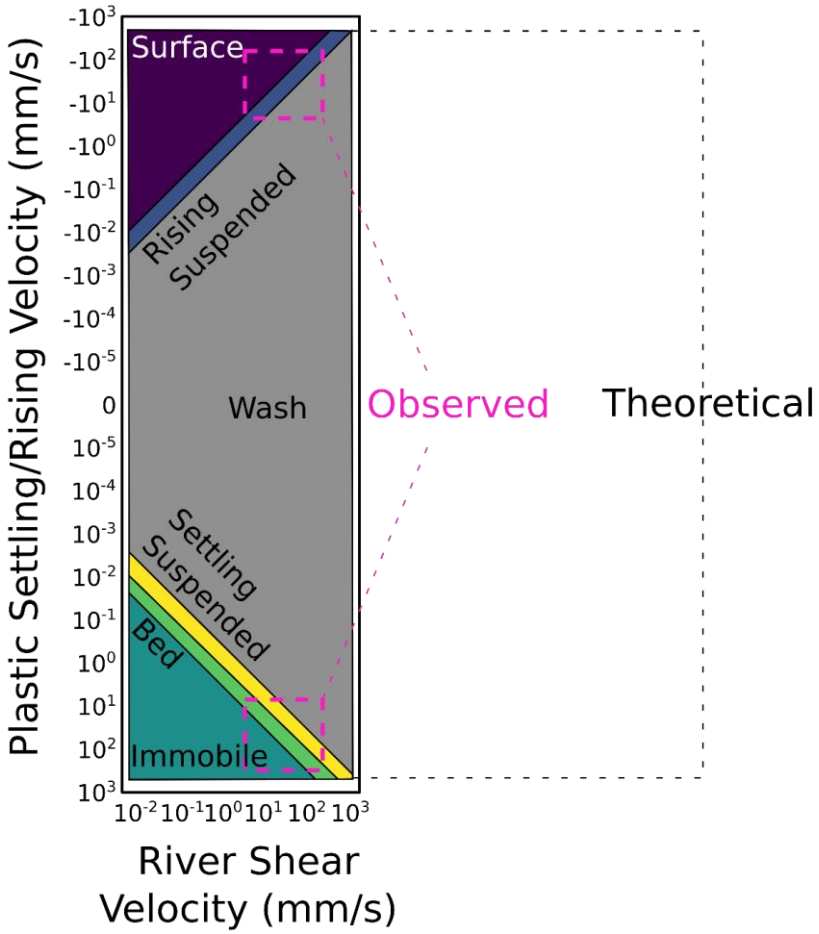

Figure 6-3: The full figure shows the range of theoretically possible microplastic settling and rising velocities and shear velocities of rivers using the Rouse model. Theoretical ranges used include microplastic particles from 0.001 to 5 mm with densities of rising particles of 22 and 970 kg m^{-3} and 1010 and 2200 kg m^{-3} for settling particles and low gradient rivers to high gradient rivers. Particles are assumed to be spherical in the theoretical case. Pink boxes show the range of settling and shear velocities of real microplastic particles measured by Waldschläger and Schüttrumpf[51] and real rivers Baldwin et al.[283]. The top pink box is for plastics PP, PE, EPS and the bottom pink box is for plastics PS, PVC, PET, and CoPA from Waldschläger and Schüttrumpf[51] and both boxes are for low gradient rivers near the great lakes from Baldwin et al.[283] (Figure D-1). Colored and labeled regions bin the concentration depth profiles of microplastic particles (Purple = Surface Load, Dark Blue = Rising Suspended Load, Gray = Wash Load, Yellow = Settling Suspended Load, Light Green = Bed Load, Teal = Immobile). Full definitions of concentration depth profiles are provided in Table 6-1 and Figure 6-1. Direct interpretation of areas on this plot as probabilities assumes log uniform distribution of settling and shear velocities.

6.4.2 Application to positively buoyant microplastic concentration depth profiles

We applied the Rouse profile to predict the concentration depth profiles of positively buoyant foam microplastic particles from Lenaker et al.[254] (Figure 6-4). Large microplastic particles (1-5 mm) were predicted to be in surface load in all six samples, which was in agreement with observations in all but 1 sample, in which they were transported as wash load. Small microplastic particles (0.333-1 mm) were predicted to be transported in rising suspended load in all five samples, but were observed to be in either surface load or wash load. Suspended load is a narrow transitionary domain (Rouse numbers 0.8-2.5) between wash load and surface load. Limited sampling at two depths[254] may have obscured the small microplastic particles' transitionary concentration depth profiles. Smaller positively buoyant particles have lower rising velocities in general, and we would expect them to be more evenly distributed with depth than larger particles with the same physical characteristics, which is suggested in the observations from Lenaker et al.[254] and in the model predictions. Particle densities, shapes, and surface characteristics may have been higher and more irregular, respectively than those tested in Waldschläger and Schüttrumpf[51] due to differences in extraneous matter association and weathering[56].

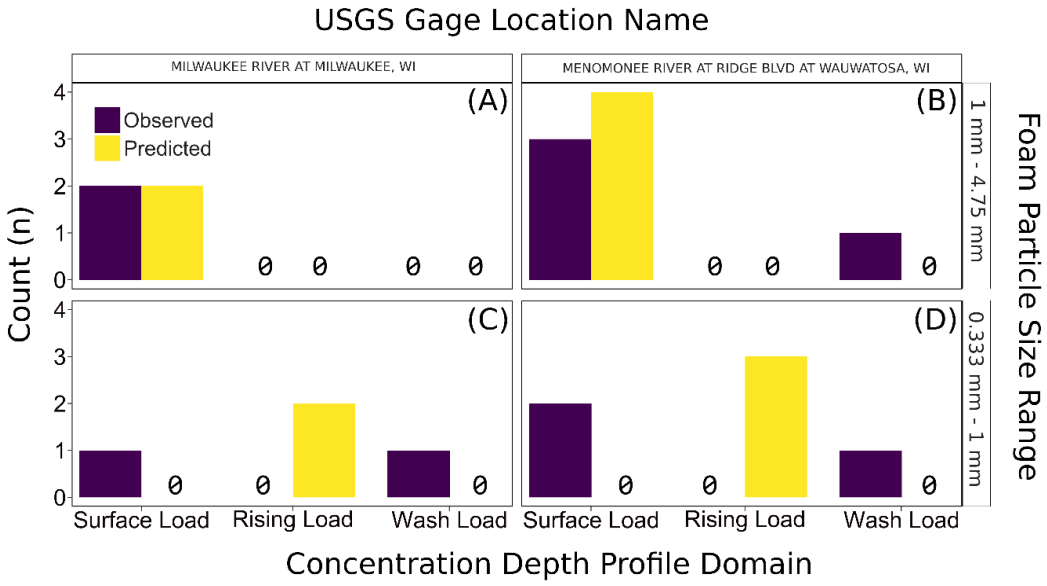

Figure 6-4: Predicted vs observed Rouse concentration depth profile domains for both sample locations (top axis) in Lenaker et al.[254] for large and small microplastic particles (right axis), delineating the number of times each concentration depth profile was present in a sample or prediction. Observed and predicted concentration depth profile domains for A) large microplastic particles (1 mm - 4.75 mm) at Milwaukee River and B) at Menomonee River. Observed and predicted concentration depth profile domains for small microplastic particles (0.333 mm - 1 mm) at C) Milwaukee River and D) Menomonee River. Full figures of concentration depth profiles for each sample are available in the SI (Figure D-3).

6.4.3 Potential surface sampling bias and uncertainty

These insights into fluvial transport of microplastic particles give rise to an important question: if samples are collected at the river surface, currently common practice[35,265], how much bias could be introduced by assuming wash load or surface load concentration depth profiles? Our model shows (Figure 6-3) that microplastic particles have the potential to travel as any concentration depth profile under river conditions and plastic conditions measured by microplastic researchers. Settling suspended load is likely to be poorly characterized by surface

samples. Microplastic traveling as bed load would not be observed in a surface sample taken above the bed load layer, and the surface load would be dramatically over-represented. However, any sample location in the water column represents microplastic traveling as wash load because the particles are evenly distributed across the flow field. Here we consider the concentration depth profiles of suspended and wash load particles with Rouse numbers between -2.5 and 2.5 (observed conditions, see Figure 6-3 and Lenaker et al.[254]), and estimate their difference from depth-averaged concentration estimates derived with surface samples using commonly assumed concentration depth profiles (Figure 6-5).

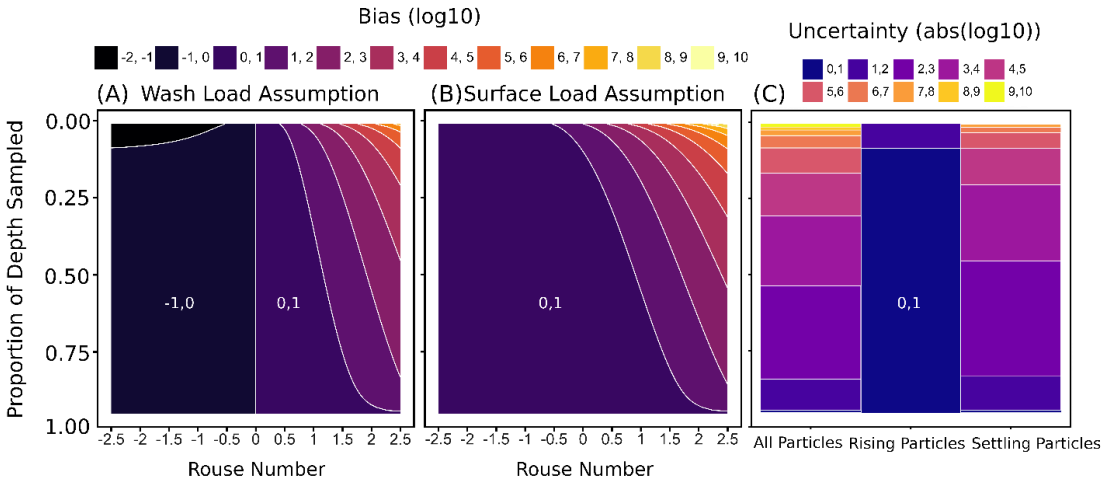

Figure 6-5: The proportion of river depth sampled (y-axis) ranges from 0.01 to 0.95, describing the proportion of the total water column sampled from the surface down. The Rouse number (x-axis for A and B) ranges from -2.5 to 2.5. Rouse numbers less than 0 are concentration depth profiles for particles with rising velocities, and Rouse numbers greater than 0 are concentration depth profiles for particles with settling velocities. Bias is the log10 value that the assumed concentration would need to be multiplied by to equal the modeled concentration. Bias greater than 0 indicates underestimation, and bias less than 0 indicates overestimations. A) The bias (log10) from using surface measurements to estimate depth-averaged concentration with the wash load assumption due to the proportion of depth sampled and the Rouse number. B) The bias (log10) in estimating depth-averaged concentration with a surface load assumption given the Rouse number and proportion of river depth sampled. C) Potential uncertainty (sum of the maximum and minimum log10 absolute value biases in A and B) of either assumption given the range of potential concentration depth profiles for all particles, rising particles, and settling particles for river depth sampled. Uncertainty can be understood as being from the possibility that microplastic particles of extremely high or low density and size cases (rising suspended load and settling suspended load) could be dominating the samples. Regions with bias or uncertainty less than an order of magnitude are marked using numbers in all three subfigures.

Our results show that surface sampling can cause a wide range of bias in estimating depth-averaged concentration in rivers due to concentration depth profiles (Figure 6-5). Under the assumption of wash load, surface samples will overestimate the depth-averaged concentration for positively buoyant profiles

(Rouse number < 0). In contrast, the surface load assumption can only result in underestimation for all concentration depth profiles. Surface sampling bias follows a similar shape and trend for both assumptions for settling profiles (Rouse number > 0). However, maximum underestimation is achieved with the surface load assumption when concentration depth profiles have positive Rouse numbers near 2.5 (i.e., strongly settling suspended particles). A minimum of zero bias is reached when the entire flow depth is sampled or when the Rouse number is zero using the wash load assumption. Uncertainty is generally the least for surface samples when only rising particles are considered. This is because surface samples represent positively buoyant particles relatively well.

Future surface monitoring efforts could consider limiting characterization to only freshwater positively buoyant particles to reduce uncertainty from surface samples. Samples could be subjected to a sink swim test or density separation to separate rising particles from settling particles[234] or particles could be characterized by polymer type and their density inferred[254]. Depth and width stratified sampling at a river cross-section (i.e., flow integrated sampling, currently the standard for representative sampling of natural fluvial suspended sediment) would also address the problem of sampling bias. However, depth and width stratified sampling presents physical and time constraints that may be prohibitive for many practitioners[286]. Another potentially useful approach is the characterization of the concentration depth profile during initial monitoring operations, followed by estimation using surface samples and assuming a percent

missed by the surface sample[287]. These findings can be used as a heuristic guide for planning sampling and understanding uncertainty due to suspended concentration depth profiles in future studies.

6.4.4 Future work

Future work should advance beyond the limitations of this modeling approach and its assumptions. Throughout the study, the model's hydraulic assumptions correspond to straight, wide channels with smooth boundaries (e.g., concrete) during times of relatively stable, clear, open water flow. Many natural systems have opposite characteristics[269,274], and these parameters could influence the turbulence in the river. The microplastic particles were modeled as spherical (section 2.1.2 only) and homogeneous and did not include effects from particle biofouling[288], aging[56], and aggregation[289], which differs from many common microplastic particles. All of these particle characteristics operate against our assumption of uniform and constant settling velocity[56]. Advancements on rising particle transport in rivers should incorporate other turbulence generating mechanisms like wind and vegetation and consider losses to the system like burial[290] and deposition[291]. This work, especially section 3.2, would benefit greatly from validation through controlled flume experiments to highly resolve observations of the relationship between river shear velocity and microplastic concentration depth profiles. Future studies should comprehensively examine turbulence (which changes through time and space), quantify the settling and rising

velocities of sampled particles, and monitor concentrations at more depths across the flow field and in more geographic locations. Our sample uncertainty evaluations assume representative, time-averaged sample collection that is hard to conduct accurately, and future work should assess the temporal component of sampling time in bias assessments[292]. The Rouse model is a 1D model, and future efforts should be made to resolve 2D and 3D effects, such as proximity to sources, where sources input (surface or subsurface), and mixing length scales through incorporation into hydrodynamic models. Comparing the biases and uncertainties from the assumptions and processes listed above to those presented in this study would improve prioritization of future research objectives. Future advancements on the uncertainty model would benefit from incorporating the probability density function of microplastic density, particle size and shape parameters, and river shear velocity to globally or regionally describe probable and average biases[54,293].

This study presents a precautionary tale about challenges involved in accurately monitoring plastic in river flow due to concentration depth profiles. We advocate for sampling and uncertainty estimation informed by transport processes. The methods and models we present will help researchers continue to develop robust methods to monitor and model microplastic transport and fate. The field of riverine microplastic pollution research has continued to progress rapidly and must now reconsider the transport complexity of this diverse suite of particulate pollutants.

Chapter 7: Conclusion

7.1 Advancements to watershed mass balances

In this dissertation, we focused on expanding the scientific understanding of anthropogenic litter transport processes operating on land and in rivers to inform the ultimate goal of advancing a watershed mass balance. We started by assessing how litter moves around on land to determine which transport processes were most responsible for bringing litter to the roadsides in the Inland Empire. Then we investigated the relationship between discharge and macroplastic concentration in the river to understand better how the Santa Ana river transports litter downstream. Last, we focused on microplastic concentration depth profiles to determine how microplastics behave in the water column of the river. We coalesce the major learnings here with a specific focus on how these findings might apply to an anthropogenic litter mass balance of the Santa Ana watershed (which drains much of the metropolitan area of the Inland Empire) and more broadly.

We learned that human transport was the primary process mobilizing receipts from their sale location to where they were littered on the Inland Empire roadsides we studied during predominantly dry periods. At one study location, we found the same standing stock during repeat surveys a year apart, suggesting that the change in standing stock on Inland Empire roadsides may be close to zero, which

has also been observed in other studies. It is possible that roadside storage is generally balanced by cleanup opperations and flux down storm drains.

We know from other work that runoff during stormflow is a major process transporting macroplastic from roadsides to river channels. However, we found that stormflow did not have a significantly different floating macroplastic particle size distribution than lowflow conditions and floating macroplastic concentrations seemed to increase most during the early stages of stormflow. Therefore, floating macroplastic is likely predominantly sourced from the stream channel during all flow conditions.

Once in the streamflow, particle properties and stream turbulence will dictate where particles reside in the water column. We found that sinking microplastic particles can be immobile in streamflow or any possible transport domain. The immobilization of particles increases channel storage. All of these findings may indicate that a large amount of roadside litter that goes to the Santa Ana channel is being stored within the channel and remobilized later.

These findings likely apply more broadly to small urban mountainous watersheds with Mediterranean climates around the world. These advances in our understanding of watershed transport processes of anthropogenic litter lead us to critical recommendations for future work.

7.2 Future work

Future studies should investigate channel storage to determine how much channel storage is happening in the Santa Ana river corridor. Roadside storage did not appear to be very large, and channel storage seemed to be an important source of litter in river flux in the Santa Ana River, even for buoyant macroplastic particles, a highly mobile fraction of total litter. This suggests that a large amount of channel storage is happening in the Santa Ana River. If so, then the river corridor may be an important sink for anthropogenic litter and an ecosystem highly impacted by anthropogenic litter in the watershed. The change of channel storage of anthropogenic litter could be investigated by monitoring the trash stored within the entire channel corridor for multiple years.

Future studies should decrease the uncertainties highlighted in this dissertation. We found that macroplastic concentration-discharge relationships in our study river were more complicated than a simple monotonic model, leading to an order of magnitude uncertainty in litter flux estimate. Floating particles may be more likely to be mobilized during the early stage of stormflow, making sinking particles relatively more abundant during later stormflow stages. Depth integrated sampling would benefit the analysis of that mechanism and may improve the analysis of the total flux, not just the floating component. Surface load transport and rising suspended load transport in rivers, described in Chapter 6, have not been thoroughly investigated in other studies. Experimental flume work should be

conducted to validate and calibrate the Rouse profile's predictions of surface transport and rising suspended transport. It is possible that processes at the stream surface, like surface tension, may impact the concentration depth profiles of rising particles.

Future studies should expand the methods we developed. The Trash Taxonomy and Open Specy are still early in development. The Trash Taxonomy needs to be simpler to use for practitioners. Right now, the barrier to entry is technical expertise in database management. We want to develop an intelligent system that takes in datasets in various formats and interprets them accurately. No other dataset exists like Open Specy's community database, and it is playing an important role in the advancement of spectral analysis for plastics pollution research. The labeled and unlabeled community shared spectra should be incorporated into a semisupervised artificial intelligence routine for analyzing spectra. We hope that the collaborative spirit within the anthropogenic litter research community continues to flourish and look forward to seeing what we learn together in the future.

References

(1) Nelson, C.; Botterill, D. Evaluating the Contribution of Beach Quality Awards to the Local Tourism Industry in Wales---the Green Coast Award. *Ocean Coast. Manag.* **2002**, *45* (2), 157–170.

(2) Suciu, M. C.; Tavares, D. C.; Costa, L. L.; Silva, M. C. L.; Zalmon, I. R. Evaluation of Environmental Quality of Sandy Beaches in Southeastern Brazil. *Mar. Pollut. Bull.* **2017**, *119* (2), 133–142.

(3) Andrady, A. L. Microplastics in the Marine Environment. *Mar. Pollut. Bull.* **2011**, *62* (8), 1596–1605. https://doi.org/10.1016/j.marpolbul.2011.05.030.

(4) Eriksen, M.; Lebreton, L. C. M.; Carson, H. S.; Thiel, M.; Moore, C. J.; Borerro, J. C.; Galgani, F.; Ryan, P. G.; Reisser, J. Plastic Pollution in the World's Oceans: More than 5 Trillion Plastic Pieces Weighing over 250,000 Tons Afloat at Sea. *PLoS One* **2014**, *9* (12), 1–15. https://doi.org/10.1371/journal.pone.0111913.

(5) Rochman, C. M. Plastics and Priority Pollutants: A Multiple Stressor in Aquatic Habitats. *Environ. Sci. Technol.* **2013**, *47* (6), 2439–2440.

(6) Lusher, A. Microplastics in the Marine Environment: Distribution, Interactions and Effects. In *Marine Anthropogenic Litter*; Bergmann, M., Gutow, L., Klages, M., Eds.; Springer International Publishing: Cham, 2015; pp 245–307.

(7) Gall, S. C.; Thompson, R. C. The Impact of Debris on Marine Life. *Mar. Pollut. Bull.* **2015**, *92* (1–2), 170–179.

(8) Wilcox, C.; Puckridge, M.; Schuyler, Q. A.; Townsend, K.; Hardesty, B. D. A Quantitative Analysis Linking Sea Turtle Mortality and Plastic Debris Ingestion. *Sci. Rep.* **2018**, *8* (1), 12536.

(9) Richardson, K.; Gunn, R.; Wilcox, C.; Hardesty, B. D. Understanding Causes of Gear Loss Provides a Sound Basis for Fisheries Management. *Mar. Policy* **2018**.

(10) Newman, S.; Watkins, E.; Farmer, A.; ten Brink, P.; Schweitzer, J.-P. The Economics of Marine Litter. In *Marine Anthropogenic Litter*; Springer, Cham, 2015; pp 367–394.

(11) Anderson, J. C.; Park, B. J.; Palace, V. P. Microplastics in Aquatic Environments: Implications for Canadian Ecosystems. *Environ. Pollut.*

2016, *218*, 269–280.

(12) Bucci, K.; Tulio, M.; Rochman, C. M. What Is Known and Unknown about the Effects of Plastic Pollution: A Meta-Analysis and Systematic Review. *Ecol. Appl.* **2019**, e02044.

(13) Barrows, A. P. W.; Christiansen, K. S.; Bode, E. T.; Hoellein, T. J. A Watershed-Scale, Citizen Science Approach to Quantifying Microplastic Concentration in a Mixed Land-Use River. *Water Res.* **2018**, *147*, 382–392.

(14) Coffin, S.; Dudley, S.; Taylor, A.; Wolf, D.; Wang, J.; Lee, I.; Schlenk, D. Comparisons of Analytical Chemistry and Biological Activities of Extracts from North Pacific Gyre Plastics with {UV-Treated} and Untreated Plastics Using in Vitro and in Vivo Models. *Environ. Int.* **2018**, *121*, 942–954.

(15) Setälä, O.; Fleming-Lehtinen, V.; Lehtiniemi, M. Ingestion and Transfer of Microplastics in the Planktonic Food Web. *Environ. Pollut.* **2014**, *185*, 77–83.

(16) Barboza, L. G. A.; Dick Vethaak, A.; Lavorante, B. R. B. O.; Lundebye, A.-K.; Guilhermino, L. Marine Microplastic Debris: An Emerging Issue for Food Security, Food Safety and Human Health. *Mar. Pollut. Bull.* **2018**, *133*, 336–348.

(17) Louis, G. E. A Historical Context of Municipal Solid Waste Management in the United States. *Waste Manag. Res.* **2004**, *22* (4), 306–322.

(18) Moore, S. M.; Cover, M. R.; Senter, A. A Rapid Trash Assessment Method Applied to Waters of the San Francisco Bay Region: Trash Measurement in Streams. *Measurement* **2007**, No. April.

(19) *Amendment to the Water Quality Control Plan for the Ocean Waters of California to Control Trash and Part 1 Trash Provisions of the Water Quality Control Plan for Inland Surface Waters, Enclosed Bays, and Estuaries of California*; 2015.

(20) California Regional Water Quality Control Board. Trash Total Maximum Daily Loads for the Los Angeles River Watershed. **2007**, 43.

(21) Mid Atlantic Solid Waste Consultants. *National Litter Survey*; 2009.

(22) Borrelle, S. B.; Ringma, J.; Law, K. L.; Monnahan, C. C.; Lebreton, L.; McGivern, A.; Murphy, E.; Jambeck, J.; Leonard, G. H.; Hilleary, M. A.; et al. Predicted Growth in Plastic Waste Exceeds Efforts to Mitigate Plastic Pollution. *Science (80-.).* **2020**, *369* (6510), 1515–1518.

(23) Torres, H. R.; Reynolds, C. J.; Lewis, A.; Muller-Karger, F.; Alsharif, K.; Mastenbrook, K. Examining Youth Perceptions and Social Contexts of Litter to Improve Marine Debris Environmental Education. *Environ. Educ. Res.* **2019**, *25* (9), 1400–1415.

(24) Wever, R.; van Onselen, L.; Silvester, S.; Boks, C. Influence of Packaging Design on Littering and Waste Behaviour. *Packag. Technol. Sci.* **2010**, *23* (5), 239–252.

(25) Schultz, P. W.; Bator, R. J.; Large, L. B.; Bruni, C. M.; Tabanico, J. J. Littering in Context. *Environ. Behav.* **2013**, *45* (1), 35–59.

(26) Bill Text - {AB-1884} Food Facilities: Single-Use Plastic Straws.

(27) California Department of; (CalRecycle), R. Single-Use Carryout Bag Ban (SB 270) Frequently Asked Questions. October 2016.

(28) Völker, C.; Kramm, J.; Wagner, M. On the Creation of Risk: Framing of Microplastics Risks in Science and Media. *Glob. Challenges* **2019**, *50*, 1900010.

(29) BASMAA. *Preliminary Baseline Trash Generation Rates for San Francisco, Technical Memorandum*; 2012.

(30) Cowger, W.; Booth, A.; Hamilton, B.; Primpke, S.; Munno, K.; Lusher, A.; Dehaut, A.; Vaz, V. P.; Liboiron, M.; Devriese, L. I.; et al. EXPRESS: Reporting Guidelines to Increase the Reproducibility and Comparability of Research on Microplastics. *Appl. Spectrosc.* **2020**, 0003702820930292. https://doi.org/10.1177/0003702820930292.

(31) Carpenter, E. J.; Smith, K. L. J. Plastics on the Sargasso Sea Surface. *Science (80-.).* **1972**, *175* (4027), 1240–1241. https://doi.org/10.1126/science.175.4027.1240.

(32) Moore, C. J.; Moore, S. L.; Leecaster, M. K.; Weisberg, S. B. A Comparison of Plastic and Plankton in the North Pacific Central Gyre. *Mar. Pollut. Bull.* **2001**, *42* (12), 1297–1300.

(33) L. Lebreton, B. Slat, F. Ferrari, B. Sainte-Rose, J. Aitken, R. Marthouse, S. Hajbane, S. Cunsolo, A. Schwarz, A. Levivier, K. Noble, P. Debeljak, H. Maral, R. Schoeneich-Argent, R. Brambini \& J. Reisser. Evidence That the Great Pacific Garbage Patch Is Rapidly Accumulating Plastic. *Sci. Rep.* **2018**, *8* (4666).

(34) Jambeck, J. R.; Geyer, R.; Wilcox, C.; Siegler, T. R.; Perryman, M.;

Andrady, A.; Narayan, R.; Lavender, K. Plastic Waste Inputs from Land into the Ocean. *Science (80-.).* **2015**, *347* (6223), 768–770. https://doi.org/10.1017/CBO9781107415386.010.

(35) Lebreton, L. C. M.; van der Zwet, J.; Damsteeg, J.-W.; Slat, B.; Andrady, A.; Reisser, J. River Plastic Emissions to the World's Oceans. *Nat. Commun.* **2017**, *8*, ncomms15611.

(36) Eerkes-Medrano, D.; Thompson, R. C.; Aldridge, D. C. Microplastics in Freshwater Systems: A Review of the Emerging Threats, Identification of Knowledge Gaps and Prioritisation of Research Needs. *Water Res.* **2015**, *75*, 63–82. https://doi.org/10.1016/j.watres.2015.02.012.

(37) Hoellein, T. J.; Rochman, C. M. The "Plastic Cycle": A Watershed-scale Model of Plastic Pools and Fluxes. *Front. Ecol. Environ.* **2021**, *19* (3), 176–183. https://doi.org/10.1002/fee.2294.

(38) Kawecki, D.; Nowack, B. {Polymer-Specific} Modeling of the Environmental Emissions of Seven Commodity Plastics As Macro- and Microplastics. *Environ. Sci. Technol.* **2019**, *53* (16), 9664–9676.

(39) Cowger, W.; Gray, A. B.; Schultz, R. C. Anthropogenic Litter Cleanups in Iowa Riparian Areas Reveal the Importance of Near-Stream and Watershed Scale Land Use. *Environ. Pollut.* **2019**.

(40) Meijer, L. J. J.; van Emmerik, T.; van der Ent, R.; Schmidt, C.; Lebreton, L. More than 1000 Rivers Account for 80\% of Global Riverine Plastic Emissions into the Ocean. *Sci Adv* **2021**, *7* (18).

(41) Kim, L. H.; Kang, J.; Kayhanian, M.; Gil, K. I.; Stenstrom, M. K.; Zoh, K. D. Characteristics of Litter Waste in Highway Storm Runoff. *Water Sci. Technol.* **2006**, *53* (2), 225–234.

(42) Van, A.; Rochman, C. M.; Flores, E. M.; Hill, K. L.; Vargas, E.; Vargas, S. A.; Hoh, E. Persistent Organic Pollutants in Plastic Marine Debris Found on Beaches in San Diego, California. *Chemosphere* **2012**, *86* (3), 258–263.

(43) Moore, C. J.; Lattin, G. L.; Zellers, A. F. Quantity and Type of Plastic Debris Flowing from Two Urban Rivers to Coastal Waters and Beaches of Southern California. *Rev. Gestão Costeira Integr.* **2011**, *11* (1), 65–73.

(44) Vriend, P.; Roebroek, C. T. J.; van Emmerik, T. Same but Different: A Framework to Design and Compare Riverbank Plastic Monitoring Strategies. *Front. Water* **2020**, *2*. https://doi.org/10.3389/frwa.2020.563791.

(45) Cowger, W.; Gray, A.; Christiansen, S. H.; DeFrond, H.; Deshpande, A. D.; Hemabessiere, L.; Lee, E.; Mill, L.; Munno, K.; Ossmann, B. E.; et al. Critical Review of Processing and Classification Techniques for Images and Spectra in Microplastic Research. *Appl. Spectrosc.* **2020**, *74* (9), 989–1010.

(46) Cowger, W.; Steinmetz, Z.; Gray, A.; Munno, K.; Lynch, J.; Hapich, H.; Primpke, S.; De Frond, H.; Rochman, C.; Herodotou, O. Microplastic Spectral Classification Needs an Open Source Community: Open Specy to the Rescue! *Anal. Chem.* **2021**, *93* (21), 7543–7548.

(47) Williams, A. T.; Simmons, S. L. Movement Patterns of Riverine Litter. *Water Air Soil Pollut.* **1997**, *98* (1), 119–139.

(48) Habib, D.; Locke, D. C.; Cannone, L. J. Synthetic Fibers as Indicators of Municipal Sewage Sludge, Sludge Products, and Sewage Treatment Plant Effluents. *Water Air Soil Pollut.* **1998**, *103* (1), 1–8.

(49) Walling, D. E. The Sediment Delivery Problem. *J. Hydrol.* **1983**, *65* (1–3), 209–237.

(50) Hager, W. H. Du Boys and Sediment Transport. *J. Hydraul. Res.* **2005**, *43* (3), 227–233.

(51) Waldschläger, K.; Schüttrumpf, H. Effects of Particle Properties on the Settling and Rise Velocities of Microplastics in Freshwater under Laboratory Conditions. *Environ. Sci. Technol.* **2019**, *53* (4), 1958–1966.

(52) Waldschläger, K.; Schüttrumpf, H. Erosion Behavior of Different Microplastic Particles in Comparison to Natural Sediments. *Environ. Sci. Technol.* **2019**, *53* (22), 13219–13227. https://doi.org/10.1021/acs.est.9b05394.

(53) Walling, D. E.; Moorehead, P. W. The Particle Size Characteristics of Fluvial Suspended Sediment: An Overview. In *Sediment/Water Interactions*; Springer, 1989; pp 125–149.

(54) Kooi, M.; Koelmans, A. A. Simplifying Microplastic via Continuous Probability Distributions for Size, Shape, and Density. *Environ. Sci. Technol. Lett.* **2019**, *6* (9), 551–557.

(55) Dibenedetto, M. H.; Ouellette, N. T.; Koseff, J. Transport of Anisotropic Particles under Waves. **2018**, *837*, 320–340.

(56) Waldschläger, K.; Born, M.; Cowger, W.; Gray, A.; Schüttrumpf, H. Settling

and Rising Velocities of Environmentally Weathered Micro- and Macroplastic Particles. *Environ. Res.* **2020**, *191*. https://doi.org/10.1016/j.envres.2020.110192.

(57) Rech, S.; Macaya-Caquilpán, V.; Pantoja, J. F.; Rivadeneira, M. M.; Campodónico, C. K.; Thiel, M. Sampling of Riverine Litter with Citizen Scientists--Findings and Recommendations. *Environ. Monit. Assess.* **2015**, *187* (6), 335.

(58) Araújo, M. C. B.; Costa, M. F. From Plant to Waste: The Long and Diverse Impact Chain Caused by Tobacco Smoking. *Int. J. Environ. Res. Public Heal.* **2019**, *16* (15).

(59) Müller, A.; Österlund, H.; Marsalek, J.; Viklander, M. The Pollution Conveyed by Urban Runoff: A Review of Sources. *Sci. Total Environ.* **2020**, *709*, 136125.

(60) Altman, R. The Myth of Historical Bio-Based Plastics. *Science (80-.).* **2021**, *373* (6550), 47–49. https://doi.org/10.1126/science.abj1003.

(61) Zylstra, E. R. Accumulation of Wind-Dispersed Trash in Desert Environments. *J. Arid Environ.* **2013**, *89*, 13–15.

(62) Mellink, Y. A. M.; van Emmerik, T.; Kooi, M.; Laufkötter, C.; Niemann, H. The Trash-Tracker: A Macroplastic Transport and Fate Model at River Basin Scale. **2021**. Preprint.

(63) Rochman, C. M.; Munno, K.; Box, C.; Cummins, A.; Zhu, X.; Sutton, R. Think Global, Act Local: Local Knowledge Is Critical to Inform Positive Change When It Comes to Microplastics. *Environ. Sci. Technol.* **2020**.

(64) Provencher, J. F.; Liboiron, M.; Borrelle, S. B.; Bond, A. L.; Rochman, C.; Lavers, J. L.; Avery-Gomm, S.; Yamashita, R.; Ryan, P. G.; Lusher, A. L.; et al. A Horizon Scan of Research Priorities to Inform Policies Aimed at Reducing the Harm of Plastic Pollution to Biota. *Sci. Total Environ.* **2020**, *733*, 139381.

(65) Wagner, T. P.; Broaddus, N. The Generation and Cost of Litter Resulting from the Curbside Collection of Recycling. *Waste Manag.* **2016**, *50*, 3–9.

(66) Schultz, P. W.; Bator, R. J.; Large, L. B.; Bruni, C. M.; Tabanico, J. J. Littering in Context: Personal and Environmental Predictors of Littering Behavior. *Environ. Behav.* **2013**, *45* (1), 35–59.

(67) De-la-Torre, G. E.; Rakib, M. R. J.; Pizarro, I.; Salinas, D. C. D. Occurrence

of Personal Protective Equipment ({PPE}) Associated with the {COVID-19} Pandemic along the Coast of Lima, Peru. **2021**, *774*, 145774.

(68) Roberts, K.; Phang, S.; Williams, J.; Hutchinson, D.; Kolstoe, S.; de Bie, J.; Williams, I.; Stringfellow, A. Lockdown Litter: A Critical Analysis of Global COVID-19 PPE Litter and Measures for Mitigation. **2021**. Preprint.

(69) Dutheil, F.; Baker, J. S.; Navel, V. {COVID-19} as a Factor Influencing Air Pollution? *Environ. Pollut.* **2020**, *263* (Pt A), 114466.

(70) Muñoz-Cadena, C. E.; Lina-Manjarrez, P.; Estrada-Izquierdo, I.; Ramón-Gallegos, E. An Approach to Litter Generation and Littering Practices in a Mexico City Neighborhood. *Sustain. Sci. Pr. Policy* **2012**, *4* (8), 1733–1754.

(71) Roper, S.; Parker, C. How (and Where) The Mighty Have Fallen: Branded Litter. *J. Mark. Manag.* **2006**, *22* (5–6), 473–487.

(72) Ballatore, A.; Verhagen, T. J.; Li, Z.; Cucurachi, S. This City Is Not a Bin: Crowdmapping the Distribution of Urban Litter. *J. Ind. Ecol.* **2021**, No. jiec.13164.

(73) Morales-Caselles, C.; Viejo, J.; Mart\'\i, E.; González-Fernández, D.; Pragnell-Raasch, H.; Ignacio González-Gordillo, J.; Montero, E.; Arroyo, G. M.; Hanke, G.; Salvo, V. S.; et al. An Inshore--Offshore Sorting System Revealed from Global Classification of Ocean Litter. *Nat. Sustain.* **2021**, *4* (6), 484–493.

(74) Landon-Lane, M. Corporate Social Responsibility in Marine Plastic Debris Governance. *Mar. Pollut. Bull.* **2018**, *127*, 310–319.

(75) Hapich, H.; Cowger, W.; Gray, A. B. Trash Taxonomy. 2020.

(76) Agriculture and Natural Resources, U. of C. CalLands https://callands.ucanr.edu/data.html.

(77) Census. QuickFacts https://www.census.gov/quickfacts/fact/table/riversidecountycalifornia/PST045219.

(78) Census. Census Planning Database 2015. 2021.

(79) OEHHA. Cal EnviroScreen https://oehha.ca.gov/calenviroscreen/report/calenviroscreen-30.

(80) Litterati. Litterati.org. 2021.

(81) Lynch, S. {OpenLitterMap.Com} -- Open Data on Plastic Pollution with Blockchain Rewards (Littercoin). *Open Geospatial Data, Softw. Stand.* **2018**, *3* (1), 6.

(82) MRCC. Cli-MATE. 2021.

(83) Statistics, B. of T. Trips by Distance https://data.bts.gov/Research-and-Statistics/Trips-by-Distance/w96p-f2qv.

(84) OpenRefine. Open Refine. 2021.

(85) Open Knowledge Foundation. Reconcile-Csv. 2021.

(86) Wijzer, K. *Kosten En Omvang Zwerfafval*; 2015.

(87) Ocean Conservancy. Trash Count to Mass Conversion https://osf.io/deg7p/. https://doi.org/10.17605/OSF.IO/DEG7P.

(88) Agostinelli, C.; Lund, U. {R} Package \texttt{circular}: Circular Statistics (Version 0.4-93). CA: Department of Environmental Sciences, Informatics and Statistics, Ca' Foscari University, Venice, Italy. UL: Department of Statistics, California Polytechnic State University, San Luis Obispo, California, USA 2017.

(89) Hussain, F.; Hussin, A. G.; Zubairi, Y. Z. On Development of Spoke Plot for Circular Variables. *Chiang Mai J. Sci.* **2010**, *37*, 369–376.

(90) Sievert, C. *Interactive Web-Based Data Visualization with R, Plotly, and Shiny*; Chapman and Hall/CRC, 2020.

(91) Glur, C. Data.Tree: General Purpose Hierarchical Data Structure. 2020.

(92) Riverside City. Street Sweeping Program https://riversideca.gov/streets/street-sweeping.asp.

(93) Pon, J. P. S.; Becherucci, M. E. Spatial and Temporal Variations of Urban Litter in Mar Del Plata, the Major Coastal City of Argentina. *Waste Manag. 32* (2), 343–348.

(94) Almroth, B. C.; Groh, K.; Walker, T. R.; Bergmann, M.; Allen, S.; Nerin, C.; Scheringer, M.; Fantke, P.; Muncke, J.; Green, D.; et al. *Statement on the Registration of Polymers under REACH and List of Signatures in Support*; 2021.

(95) Laist, D. W. Impacts of Marine Debris: Entanglement of Marine Life in Marine Debris Including a Comprehensive List of Species with

Entanglement and Ingestion Records. In *Marine Debris: Sources, Impacts, and Solutions*; Coe, J. M., Rogers, D. B., Eds.; Springer New York: New York, NY, 1997; pp 99–139.

(96) Vegter, A. C.; Barletta, M.; Beck, C.; Borrero, J.; Burton, H.; Campbell, M. L.; Costa, M. F.; Eriksen, M.; Eriksson, C.; Estrades, A. Global Research Priorities to Mitigate Plastic Pollution Impacts on Marine Wildlife. *Endanger. Species Res.* **2014**, *25* (3), 225–247.

(97) Sigler, M. The Effects of Plastic Pollution on Aquatic Wildlife: Current Situations and Future Solutions. *Water Air Soil Pollut. Focus* **2014**, *225* (11), 2184.

(98) Prata, J. C.; Silva, A. L. P.; Da Costa, J. P.; Mouneyrac, C.; Walker, T. R.; Duarte, A. C.; Rocha-Santos, T. Solutions and Integrated Strategies for the Control and Mitigation of Plastic and Microplastic Pollution. *Int. J. Environ. Res. Public Health* **2019**, *16* (13), 2411.

(99) Lebreton, L.; Andrady, A. Future Scenarios of Global Plastic Waste Generation and Disposal. *Palgrave Commun.* **2019**, *5* (1), 6.

(100) Kish, R. J. Using Legislation to Reduce One-time Plastic Bag Usage. *Econ. Aff.* **2018**, *38* (2), 224–239.

(101) Guild, E.; Mitsilegas, V. Immigration and Asylum Law and Policy in Europe. **2019**.

(102) Allen, K.; Cohen, D.; Culver, A.; Cummins, A.; Curtis, S.; Eriksen, M.; Gordon, M.; Howe, A.; Lapis, N.; Prindiville, M.; Thorpe, B.; Wilson S. *Better Alternatives Now, {BAN} List 2.0*; 2017.

(103) Fleet, D., Vlachogianni, T., Hanke, G. *A Joint List of Litter Categories for Marine Macrolitter Monitoring*.

(104) Ocean Protection Council. *California Ocean Litter Prevention Strategy: Addressing Marine Debris from Source to Sea*; 2018.

(105) Bellahsene, Z.; Bonifati, A.; Duchateau, F.; Velegrakis, Y. On Evaluating Schema Matching and Mapping. In *Schema Matching and Mapping*; Bellahsene, Z., Bonifati, A., Rahm, E., Eds.; Springer Berlin Heidelberg: Berlin, Heidelberg, 2011; pp 253–291.

(106) Chang, W.; Cheng, J.; Allaire, J. J.; Xie, Y.; McPherson, J. Shiny: Web Application Framework for R. 2020.

(107) Wickham, H.; François, R.; Henry, L.; Müller, K. Dplyr: A Grammar of Data Manipulation. 2020.

(108) Dowle, M.; Srinivasan, A. Data.Table: Extension of `data.Frame`. 2020.

(109) Attali, D. Shinyjs: Easily Improve the User Experience of Your Shiny Apps in Seconds. 2020.

(110) Chang, W. Shinythemes: Themes for Shiny. 2018.

(111) Xie, Y.; Cheng, J.; Tan, X. DT: A Wrapper of the JavaScript Library "DataTables." 2020.

(112) Mason-Thom, C. Shinyhelper: Easily Add Markdown Help Files to "shiny" App Elements. 2019.

(113) Khan, A. CollapsibleTree: Interactive Collapsible Tree Diagrams Using "D3.Js." 2018.

(114) Lê, S.; Josse, J.; Husson, F. {FactoMineR}: A Package for Multivariate Analysis. *J. Stat. Softw.* **2008**, *25* (1), 1–18. https://doi.org/10.18637/jss.v025.i01.

(115) Vaissie, P.; Monge, A.; Husson, F. Factoshiny: Perform Factorial Analysis from "FactoMineR" with a Shiny Application. 2021.

(116) Mock, J.; Hendlin, Y. H. Notes from the Field: Environmental Contamination from E-Cigarette, Cigarette, Cigar, and Cannabis Products at 12 High Schools - San Francisco Bay Area, 2018-2019. *MMWR Morb. Mortal. Wkly. Rep.* **2019**, *68* (40), 897–899.

(117) Lee, Y. O.; Glantz, S. A. Menthol: Putting the Pieces Together. *Tob. Control* **2011**, *20* (Supplement 2), ii1–ii7. https://doi.org/10.1136/tc.2011.043604.

(118) Pirika. Towards Litter-Free Cities https://en.research.pirika.org/.

(119) Prata, J. C.; Silva, A. L. P.; Walker, T. R.; Duarte, A. C.; Rocha-Santos, T. COVID-19 Pandemic Repercussions on the Use and Management of Plastics. *Environ. Sci. Technol.* **2020**, *54* (13), 7760–7765.

(120) Zhao, Z.; Kang, Y.; Magdy, A.; Cowger, W.; Gray, A. A Data-Driven Approach for Tracking Human Litter in Modern Cities. In *2019 IEEE 35th International Conference on Data Engineering Workshops (ICDEW)*; IEEE, 2019; pp 69–73.

(121) Kang, Y.; Zhao, Z.; Magdy, A.; Cowger, W.; Gray, A. Scalable Multi-Resolution Spatial Visualization for Anthropogenic Litter Data.

(122) Molina Jack, M. E.; Chaves Montero, M. del M.; Galgani, F.; Giorgetti, A.; Vinci, M.; Le Moigne, M.; Brosich, A. {EMODnet} Marine Litter Data Management at Pan-European Scale. *Ocean Coast. Manag.* **2019**, *181*, 104930.

(123) Delpeuch, A.; Pohl, A.; Steeg, F.; Sr., T. G. Reconciliation Service {API} https://reconciliation-api.github.io/specs/0.1/.

(124) Moore, S.; Hale, T.; Weisberg, S. B.; Flores, L.; Kauhanen, P. *California Trash Monitoring Methods and Assessments Playbook*; 2020.

(125) Walling, D. E. Assessing the Accuracy of Suspended Sediment Rating Curves for a Small Basin. *Water Resour. Res.* **1977**, *13* (3), 531–538.

(126) Gray, A. B. The Impact of Persistent Dynamics on Suspended Sediment Load Estimation. *Geomorphology* **2018**.

(127) East, A. E.; Stevens, A. W.; Ritchie, A. C.; Barnard, P. L.; Campbell-Swarzenski, P.; Collins, B. D.; Conaway, C. H. A Regime Shift in Sediment Export from a Coastal Watershed during a Record Wet Winter, California: Implications for Landscape Response to Hydroclimatic Extremes. *Earth Surf. Process. Landforms* **2018**, *43* (12), 2562–2577. https://doi.org/10.1002/esp.4415.

(128) Aguilera, R.; Melack, J. M. Concentration-Discharge Responses to Storm Events in Coastal California Watersheds. *Water Resour. Res.* **2018**, *54* (1), 407–424.

(129) Fisher, A.; Belmont, P.; Murphy, B. P.; MacDonald, L.; Ferrier, K. L.; Hu, K. Natural and Anthropogenic Controls on Sediment Rating Curves in Northern California Coastal Watersheds. *Earth Surf. Process. Landforms* **2021**, *46* (8), 1610–1628. https://doi.org/10.1002/esp.5137.

(130) Gray, A. B.; Pasternack, G. B.; Watson, E. B.; Warrick, J. A.; others. Effects of Antecedent Hydrologic Conditions, Time Dependence, and Climate Cycles on the Suspended Sediment Load of the Salinas River, California. *J.* **2015**.

(131) Warrick, J. A.; Rubin, D. M. Suspended-Sediment Rating Curve Response to Urbanization and Wildfire, Santa Ana River, California. *J. Geophys. Res.* **2007**, *112* (F2), F02018.

(132) Gray, A. B.; Warrick, J. A.; Pasternack, G. B.; Watson, E. B.; others. Suspended Sediment Behavior in a Coastal Dry-Summer Subtropical Catchment: Effects of Hydrologic Preconditions. *Geomorphology* **2014**.

(133) Williams, G. P.; Others. Sediment Concentration versus Water Discharge during Single Hydrologic Events in Rivers. *J. Hydrol.* **1989**, *111* (1), 89–106.

(134) Warrick, J. A.; Madej, M. A.; Goñi, M. A.; Wheatcroft, R. A. Trends in the Suspended-Sediment Yields of Coastal Rivers of Northern California, 1955–2010. *J. Hydrol.* **2013**, *489*, 108–123. https://doi.org/https://doi.org/10.1016/j.jhydrol.2013.02.041.

(135) Slattery, M. C.; Burt, T. P. Particle Size Characteristics of Suspended Sediment in Hillslope Runoff and Stream Flow. *Earth Surf. Process. Landforms J. Br. Geomorphol. Gr.* **1997**, *22* (8), 705–719.

(136) Li Yingxia; Lau Sim-Lin; Kayhanian Masoud; Stenstrom Michael K. Particle Size Distribution in Highway Runoff. *J. Environ. Eng.* **2005**, *131* (9), 1267–1276.

(137) Farnsworth, K. L.; Milliman, J. D. Effects of Climatic and Anthropogenic Change on Small Mountainous Rivers: The Salinas River Example. *Glob. Planet. Change* **2003**, *39* (1), 53–64. https://doi.org/https://doi.org/10.1016/S0921-8181(03)00017-1.

(138) van Emmerik, T.; van Oeveren, K.; Loozen, M.; Meijer, L. Measuring Plastic Transport in Rivers. In *Geophysical Research Abstracts*; 2019; Vol. 21.

(139) van Emmerik, T.; Tramoy, R.; van Calcar, C.; Alligant, S.; Treilles, R.; Tassin, B.; Gasperi, J. Seine Plastic Debris Transport Tenfolded During Increased River Discharge. *Front. Mar. Sci.* **2019**, *6*, 642.

(140) van Emmerik, T.; Kieu-Le, T.-C.; Loozen, M.; van Oeveren, K.; Strady, E.; Bui, X.-T.; Egger, M.; Gasperi, J.; Lebreton, L.; Nguyen, P.-D.; et al. A Methodology to Characterize Riverine Macroplastic Emission Into the Ocean. *Front. Mar. Sci.* **2018**, *5*, 372.

(141) Wagner, S.; Klöckner, P.; Stier, B.; Römer, M.; Seiwert, B.; Reemtsma, T.; Schmidt, C. Relationship between Discharge and River Plastic Concentrations in a Rural and an Urban Catchment. *Environ. Sci. Technol.* **2019**, *53* (17), 10082–10091. https://doi.org/10.1021/acs.est.9b03048.

(142) Haberstroh, C. J.; Arias, M. E.; Yin, Z.; Wang, M. C. Effects of Urban

Hydrology on Plastic Transport in a Subtropical River. *ACS ES&T Water* **2021**, *1* (8), 1714–1727. https://doi.org/10.1021/acsestwater.1c00072.

(143) Homer, C. G.; Dewitz, J.; Yang, L.; Jin, S.; Danielson, P.; Xian, G. Z.; Coulston, J.; Herold, N.; Wickham, J.; Megown, K. Completion of the 2011 National Land Cover Database for the Conterminous United States – Representing a Decade of Land Cover Change Information. *Photogramm. Eng. Remote Sensing* **2015**, *81*, 345–354.

(144) Multi-Resolution Land Characteristics Consortium, NLCD 2011 Legend https://www.mrlc.gov/data/legends/national-land-cover-database-2011-nlcd2011-legend.

(145) United States Geological Survey. National Hydrography Dataset. 2004.

(146) United States Geological Survey. StreamStats. 2016.

(147) Army Corps of Engineers. National Inventory of Dams. 2018.

(148) Moore, S.; Sutula, M.; Von Bitner, T.; Lattin, G.; Schiff, K. Southern California Bight 20 Regional Monitoring Program: Volume {III}. Trash and Marine Debris.

(149) Cowger, W.; Gray, A. B.; Schultz, R. C. Anthropogenic Litter Cleanups in Iowa Riparian Areas Reveal the Importance of Near-Stream and Watershed Scale Land Use. *Environ. Pollut.* **2019**, *250*. https://doi.org/10.1016/j.envpol.2019.04.052.

(150) California Regional Water Quality Control Board. NATIONAL POLLUTANT DISCHARGE ELIMINATION SYSTEM (NPDES) PERMIT AND WASTE DISCHARGE REQUIREMENTS FOR THE RIVERSIDE COUNTY FLOOD CONTROL AND WATER CONSERVATION DISTRICT, THE COUNTY OF RIVERSIDE, AND THE INCORPORATED CITIES OF RIVERSIDE COUNTY WITHIN THE SANTA ANA REGION. Order No. R8-2010-0033

(151) United States Geological Survey. National Water Information System data available on the World Wide Web (USGS Water Data for the Nation). https://doi.org/http://dx.doi.org/10.5066/F7P55KJN.

(152) Ferguson, R. I. River Loads Underestimated by Rating Curves. *Water Resour. Res.* **1986**, *22* (1), 74–76. https://doi.org/10.1029/WR022i001p00074.

(153) United States Geological Survey. 1/9th Arc-Second Digital Elevation Models (DEMs) - USGS National Map 3DEP Downloadable Data

Collection: U.S. Geological Survey. 2017.

(154) Schindelin, J.; Arganda-Carreras, I.; Frise, E.; Kaynig, V.; Longair, M.; Pietzsch, T.; Preibisch, S.; Rueden, C.; Saalfeld, S.; Schmid, B.; et al. Fiji: An Open-Source Platform for Biological-Image Analysis. *Nat. Methods* **2012**, *9* (7), 676–682. https://doi.org/10.1038/nmeth.2019.

(155) Kroon, F.; Motti, C.; Talbot, S.; Sobral, P.; Puotinen, M. A Workflow for Improving Estimates of Microplastic Contamination in Marine Waters: A Case Study from {North-Western} Australia. *Environ. Pollut.* **2018**, *238*, 26–38.

(156) Cowger, W.; Gray, A. B.; Guilinger, J. J.; Fong, B.; Waldschläger, K. Concentration Depth Profiles of Microplastic Particles in River Flow and Implications for Surface Sampling. *Environ. Sci. Technol.* **2021**, *55* (9), 6032–6041.

(157) De Cicco, L. A.; Lorenz, D.; Hirsch, R. M.; Watkins, W.; Johnson, M. DataRetrieval: R Packages for Discovering and Retrieving Water Data Available from U.S. Federal Hydrologic Web Services. U.S. Geological Survey: Reston, VA 2021. https://doi.org/10.5066/P9X4L3GE.

(158) Wickham, H. Ggplot2: Elegant Graphics for Data Analysis. **2016**.

(159) Wood, S. N. Fast Stable Restricted Maximum Likelihood and Marginal Likelihood Estimation of Semiparametric Generalized Linear Models. *J. R. Stat. Soc.* **2011**, *73* (1), 3–36.

(160) Wickham, H.; Bryan, J. Readxl: Read Excel Files. 2019.

(161) Wickham, H. Stringr: Simple, Consistent Wrappers for Common String Operations. 2019.

(162) Garnier, S. Viridis: Default Color Maps from “Matplotlib.” 2018.

(163) Wickham, H.; Henry, L. Tidyr: Tidy Messy Data. 2020.

(164) Venables, W. N.; Ripley, B. D. *Modern Applied Statistics with S*, Fourth.; Springer: New York, 2002.

(165) Bengtsson, H. MatrixStats: Functions That Apply to Rows and Columns of Matrices (and to Vectors). 2021.

(166) Braudrick, C. A.; Grant, G. E. When Do Logs Move in Rivers? *Water Resour. Res.* **2000**, *36* (2), 571–583.

(167) Rose, L. A.; Karwan, D. L.; Godsey, S. E. Concentration-Discharge Relationships Describe Solute and Sediment Mobilization, Reaction, and Transport at Event and Longer Timescales. *Hydrol. Process.* **2018**, *32* (18), 2829–2844.

(168) 5 Gyres, EOA inc. *Testing Trash ``Flux'' Monitoring Methods in Flowing Water Bodies*. 2016.

(169) Stenstrom, M. K.; Kayhanian, M. First Flush Phenomenon Characterization. California Department of Transportation. 2005.

(170) McDonnell, J. J.; Beven, K. Debates-The Future of Hydrological Sciences: A (Common) Path Forward? A Call to Action Aimed at Understanding Velocities, Celerities and Residence Time Distributions of the Headwater Hydrograph. *Water Resour. Res.* **2014**, *50* (6), 5342–5350. https://doi.org/10.1002/2013WR015141.

(171) Kim, L.-H.; Kayhanian, M.; Stenstrom, M. K. Event Mean Concentration and Loading of Litter from Highways during Storms. *Sci. Total Environ.* **2004**, *330* (1–3), 101–113.

(172) Brander, S. M.; Renick, V. C.; Foley, M. M.; Steele, C.; Woo, M.; Lusher, A.; Carr, S.; Helm, P.; Box, C.; Cherniak Cherniak, S. L.; et al. {EXPRESS}: Sampling and {QA/QC}: A Guide for Scientists Investigating the Occurrence of Microplastics Across Matrices. *Appl. Spectrosc.* **2020**, 3702820945713.

(173) Primpke, S.; Christiansen, S. H.; Cowger, W.; De Frond, H.; Deshpande, A.; Fischer, M.; Holland, E. B.; Meyns, M.; O'Donnell, B. A.; Ossmann, B. E.; et al. Critical Assessment of Analytical Methods for the Harmonized and Cost-Efficient Analysis of Microplastics. *Appl. Spectrosc.* **2020**, *74* (9). https://doi.org/10.1177/0003702820921465.

(174) Rochman, C. M.; Brookson, C.; Bikker, J.; Djuric, N.; Earn, A.; Bucci, K.; Athey, S.; Huntington, A.; McIlwraith, H.; Munno, K.; et al. Rethinking Microplastics as a Diverse Contaminant Suite. *Environ. Toxicol. Chem.* **2019**, *38* (4), 703–711.

(175) Hartmann, N. B.; Hüffer, T.; Thompson, R. C.; Hassellöv, M.; Verschoor, A.; Daugaard, A. E.; Rist, S.; Karlsson, T.; Brennholt, N.; Cole, M.; et al. Are We Speaking the Same Language? Recommendations for a Definition and Categorization Framework for Plastic Debris. *Environ. Sci. Technol.* **2019**, *53* (3), 1039–1047.

(176) Cowger, W.; Gray, A.; Christiansen, S. H.; DeFrond, H.; Deshpande, A. D.;

Hemabessiere, L.; Lee, E.; Mill, L.; Munno, K.; Ossmann, B. E.; et al. Critical Review of Processing and Classification Techniques for Images and Spectra in Microplastic Research. *Appl. Spectrosc.* **2020**, *74* (9). https://doi.org/10.1177/0003702820929064.

(177) Renner, G.; Schmidt, T. C.; Schram, J. A New Chemometric Approach for Automatic Identification of Microplastics from Environmental Compartments Based on FT-IR Spectroscopy. *Anal. Chem.* **2017**, *89* (22), 12045–12053.

(178) ter Halle, A.; Ladirat, L.; Martignac, M.; Mingotaud, A. F.; Boyron, O.; Perez, E. To What Extent Are Microplastics from the Open Ocean Weathered? *Environ. Pollut.* **2017**, *227*, 167–174.

(179) Munno, K.; De Frond, H.; O'Donnell, B.; Rochman, C. M. Increasing the Accessibility for Characterizing Microplastics: Introducing New {Application-Based} and Spectral Libraries of Plastic Particles ({SLoPP} and {SLoPP-E}). *Anal. Chem.* **2020**.

(180) Chabuka, B. K.; Kalivas, J. H. Application of a Hybrid Fusion Classification Process for Identification of Microplastics Based on Fourier Transform Infrared Spectroscopy. *Appl. Spectrosc.* **2020**, *74* (9), 1167–1183. https://doi.org/10.1177/0003702820923993.

(181) R Core Team. R: A Language and Environment for Statistical Computing. Vienna, Austria 2020.

(182) RStudio Team. RStudio: Integrated Development Environment for R. Boston, MA 2020.

(183) Hamilton, N. Smoother: Functions Relating to the Smoothing of Numerical Data. 2015.

(184) signal developers. {signal}: Signal Processing. 2014.

(185) Perrier, V.; Meyer, F.; Granjon, D. ShinyWidgets: Custom Inputs Widgets for Shiny. 2020.

(186) Bailey, E. ShinyBS: Twitter Bootstrap Components for Shiny. 2015.

(187) with contributions by Antoine Lucas, D. E.; Tuszynski, J.; Bengtsson, H.; Urbanek, S.; Frasca, M.; Lewis, B.; Stokely, M.; Muehleisen, H.; Murdoch, D.; Hester, J.; et al. Digest: Create Compact Hash Digests of R Objects. 2020.

(188) Allaire, J. J. Config: Manage Environment Specific Configuration Values.

2020.

(189) Wolen, A. R.; Hartgerink, C. H. J.; Hafen, R.; Richards, B. G.; Soderberg, C. K.; York, T. P. {osfr}: An {R} Interface to the Open Science Framework. *J. Open Source Softw.* **2020**, *5* (46), 2071. https://doi.org/10.21105/joss.02071.

(190) Xie, Y. Knitr: A General-Purpose Package for Dynamic Report Generation in R. 2020.

(191) Allaire, J. J.; Xie, Y.; McPherson, J.; Luraschi, J.; Ushey, K.; Atkins, A.; Wickham, H.; Cheng, J.; Chang, W.; Iannone, R. Rmarkdown: Dynamic Documents for R. 2020.

(192) Wickham, H. Testthat: Get Started with Testing. *R J.* **2011**, *3*, 5–10.

(193) Ooms, J. The Jsonlite Package: A Practical and Consistent Mapping Between JSON Data and R Objects. *arXiv:1403.2805 [stat.CO]* **2014**.

(194) Price, R. Loggit: Modern Logging for the R Ecosystem. 2021.

(195) Ram, K.; Yochum, C. Rdrop2: Programmatic Interface to the “Dropbox” API. 2020.

(196) Beleites, C.; Sergo, V. HyperSpec: A Package to Handle Hyperspectral Data Sets in R. 2020.

(197) Murrell, P. HexView: Viewing Binary Files. 2019.

(198) Cowger, W.; Steinmetz, Z. OpenSpecy: Analyze, Process, Identify, and Share, Raman and (FT)IR Spectra. 2021.

(199) Jessica Meyers, Jeremy Conkle, Win Cowger, Zacharias Steinmetz, Andrew Gray, Chelsea Rochman, Sebastian Primpke, Jennifer Lynch, Hannah Hapich, Hannah De Frond, Keenan Munno, B. O. Open Specy Standard Opperating Proceedure https://htmlpreview.github.io/?https://github.com/wincowgerDEV/OpenSpecy/blob/main/vignettes/sop.html (accessed Dec 4, 2020).

(200) Savitzky, A.; Golay, M. J. E. Smoothing and Differentiation of Data by Simplified Least Squares Procedures. *Anal. Chem.* **1964**, *36* (8), 1627–1639.

(201) Zhao, J.; Lui, H.; McLean, D. I.; Zeng, H. Automated Autofluorescence Background Subtraction Algorithm for Biomedical Raman Spectroscopy. *Appl. Spectrosc.* **2007**, *61* (11), 1225–1232.

(202) Ghosal, S.; Chen, M.; Wagner, J.; Wang, Z.-M.; Wall, S. Molecular Identification of Polymers and Anthropogenic Particles Extracted from Oceanic Water and Fish Stomach--A Raman Micro-Spectroscopy Study. *Environ. Pollut.* **2017**.

(203) Lafuente, B.; Downs, R.; Yang, H.; Stone, N. The Power of Databases: The RRUFF Project. In “Highlights in Mineralogical Crystallography”, Armbruster, T. & Danisi, RM, Eds. W. *Gruyter, Berlin, Ger.* **2015**, *1*, 30.

(204) El Mendili, Y.; Vaitkus, A.; Merkys, A.; Gražulis, S.; Chateigner, D.; Mathevet, F.; Gascoin, S.; Petit, S.; Bardeau, J.-F.; Zanatta, M.; et al. Raman Open Database: First Interconnected Raman{--}X-Ray Diffraction Open-Access Resource for Material Identification. *J. Appl. Crystallogr.* **2019**, *52* (3), 618–625. https://doi.org/10.1107/S1600576719004229.

(205) Cabernard, L.; Roscher, L.; Lorenz, C.; Gerdts, G.; Primpke, S. Comparison of Raman and Fourier Transform Infrared Spectroscopy for the Quantification of Microplastics in the Aquatic Environment. *Environ. Sci. Technol.* **2018**.

(206) Ian M. Bell, R. J. H. C. and P. J. G. C. I. L. Raman Spectroscopic Library http://www.chem.ucl.ac.uk/resources/raman/.

(207) Primpke, S.; Wirth, M.; Lorenz, C.; Gerdts, G. Reference Database Design for the Automated Analysis of Microplastic Samples Based on Fourier Transform Infrared ({FTIR}) Spectroscopy. *Anal. Bioanal. Chem.* **2018**.

(208) Primpke, S.; Cross, R. K.; Mintenig, S. M.; Simon, M.; Vianello, A.; Gerdts, G.; Vollertsen, J. {EXPRESS}: Toward the Systematic Identification of Microplastics in the Environment: Evaluation of a New Independent Software Tool ({siMPle}) for Spectroscopic Analysis. *Appl. Spectrosc.* **2020**, 3702820917760.

(209) Menges, F. Spectragryph https://www.effemm2.de/spectragryph/about.html.

(210) Cowger, W.; Steinmetz, Z.; Gray, A.; Hapich, H.; Rochman, C.; Lynch, J.; Primpke, S.; Herodotou, O. Open Specy www.openspecy.org.

(211) Wiley. KnowItAll https://sciencesolutions.wiley.com/knowitall-spectroscopy-software/.

(212) Scientific, T. OMNIC https://www.thermofisher.com/order/catalog/product/833-036200#/833-036200.

(213) Opperant LLC. Essential FTIR https://www.essentialftir.com/.

(214) Schlösser, M. Spec Tools http://spectools.sourceforge.net/software.html.

(215) Management, F. D. FDM Search Faster https://www.fdmspectra.com/FDM_SearchFaster_for_FTIR_and_Raman.html.

(216) Raman Tool Set https://sourceforge.net/projects/ramantoolset/.

(217) Horiba Scientific. LabSpec https://www.horiba.com/en_en/products/detail/action/show/Product/labspec-6-spectroscopy-suite-software-1843/.

(218) Amrutha, K.; Warrier, A. K. The First Report on the Source-to-Sink Characterization of Microplastic Pollution from a Riverine Environment in Tropical India. *Sci. Total Environ.* **2020**, *739*, 140377.

(219) Yokota, K.; Mehlrose, M. Lake Phytoplankton Assemblage Altered by Irregularly Shaped PLA Body Wash Microplastics but Not by PS Calibration Beads. *Water* **2020**, *12* (9), 2650.

(220) Battaglia, F. M.; Beckingham, B. A.; McFee, W. E. First Report from North America of Microplastics in the Gastrointestinal Tract of Stranded Bottlenose Dolphins (Tursiops Truncatus). *Mar. Pollut. Bull.* **2020**, *160*, 111677.

(221) Miller, E.; Sedlak, M.; Lin, D.; Box, C.; Holleman, C.; Rochman, C. M.; Sutton, R. Recommended Best Practices for Collecting, Analyzing, and Reporting Microplastics in Environmental Media: Lessons Learned from Comprehensive Monitoring of San Francisco Bay. *J. Hazard. Mater.* **2020**, 124770.

(222) Prata, J. C.; da Costa, J. P.; Fernandes, A. J. S.; others. Selection of Microplastics by Nile Red Staining Increases Environmental Sample Throughput by Micro-Raman Spectroscopy. *Sci. Total Environ.* **2021**.

(223) Sarkar, D. J.; Das Sarkar, S.; Das, B. K.; Praharaj, J. K.; Mahajan, D. K.; Purokait, B.; Mohanty, T. R.; Mohanty, D.; Gogoi, P.; Kumar V, S.; et al. Microplastics Removal Efficiency of Drinking Water Treatment Plant with Pulse Clarifier. *J. Hazard. Mater.* **2021**, *413*, 125347.

(224) Sparks, C.; Awe, A.; Maneveld, J. Abundance and Characteristics of Microplastics in Retail Mussels from Cape Town, South Africa. *Mar. Pollut. Bull.* **2021**, *166*, 112186.

(225) Sarkar, D. J.; Das Sarkar, S.; Das, B. K.; Sahoo, B. K.; Das, A.; Nag, S. K.; Manna, R. K.; Behera, B. K.; Samanta, S. Occurrence, Fate and Removal of Microplastics as Heavy Metal Vector in Natural Wastewater Treatment Wetland System. *Water Res.* **2021**, *192*, 116853.

(226) Adam, V.; Yang, T.; Nowack, B. Toward an Ecotoxicological Risk Assessment of Microplastics: Comparison of Available Hazard and Exposure Data in Freshwaters. *Environ. Toxicol. Chem.* **2019**, *38* (2), 436–447. https://doi.org/10.1002/etc.4323.

(227) Wagner, M.; Scherer, C.; Alvarez-Muñoz, D.; Brennholt, N.; Bourrain, X.; Buchinger, S.; Fries, E.; Grosbois, C.; Klasmeier, J.; Marti, T.; et al. Microplastics in Freshwater Ecosystems: What We Know and What We Need to Know. *Environ. Sci. Eur.* **2014**, *26* (1), 12. https://doi.org/10.1186/s12302-014-0012-7.

(228) Foley, C. J.; Feiner, Z. S.; Malinich, T. D.; Höök, T. O. A Meta-Analysis of the Effects of Exposure to Microplastics on Fish and Aquatic Invertebrates. *Sci. Total Environ.* **2018**, *631–632*, 550–559.

(229) Emmerik, T.; Schwarz, A. Plastic Debris in Rivers. *WIREs Water* **2020**, *7* (1). https://doi.org/10.1002/wat2.1398.

(230) Cox, K. D.; Covernton, G. A.; Davies, H. L.; Dower, J. F.; Juanes, F.; Dudas, S. E. Human Consumption of Microplastics. *Environ. Sci. Technol.* **2019**, *53* (12), 7068–7074. https://doi.org/10.1021/acs.est.9b01517.

(231) Karami, A.; Golieskardi, A.; Choo, C. K.; Larat, V.; Karbalaei, S.; Salamatinia, B. Microplastic and Mesoplastic Contamination in Canned Sardines and Sprats. *Sci. Total Environ.* **2018**, *612*, 1380–1386.

(232) Hernandez, L. M.; Xu, E. G.; Larsson, H. C. E.; Tahara, R.; Maisuria, V. B.; Tufenkji, N. Plastic Teabags Release Billions of Microparticles and Nanoparticles into Tea. *Environ. Sci. Technol.* **2019**, *53* (21), 12300–12310. https://doi.org/10.1021/acs.est.9b02540.

(233) Jambeck, J. R.; Geyer, R.; Wilcox, C.; Siegler, T. R.; Perryman, M.; Andrady, A.; Narayan, R.; Law, K. L. Marine Pollution. Plastic Waste Inputs from Land into the Ocean. *Science (80-.).* **2015**, *347* (6223), 768–771.

(234) Hurley, R.; Woodward, J.; Rothwell, J. J. Microplastic Contamination of River Beds Significantly Reduced by Catchment-Wide Flooding. *Nat. Geosci.* **2018**, *11* (4), 251–257.

(235) Lebreton, L. C.-M.; Greer, S. D.; Borrero, J. C. Numerical Modelling of

Floating Debris in the World's Oceans. *Mar. Pollut. Bull.* **2012**, *64* (3), 653–661.

(236) van Sebille, E.; Wilcox, C.; Lebreton, L.; Maximenko, N.; Hardesty, B. D.; van Franeker, J. A.; Eriksen, M.; Siegel, D.; Galgani, F.; Law, K. L. A Global Inventory of Small Floating Plastic Debris. *Environ. Res. Lett.* **2015**, *10* (12), 124006.

(237) Rochman, C. Microplastics Research—from Sink to Source. *Science (80-.).* **2018**, *360* (6384), 28–29.

(238) Buranyi, S. The Missing 99%: Why Can't We Find the Vast Majority of Ocean Plastic? *Guard.* **2019**.

(239) The Quest to Find the Missing Plastic | The Ocean Cleanup. *The Ocean Cleanup*. September 2019.

(240) Tramoy, R.; Gasperi, J.; Dris, R.; Colasse, L.; Fisson, C.; Sananes, S.; Rocher, V.; Tassin, B. Assessment of the Plastic Inputs From the Seine Basin to the Sea Using Statistical and Field Approaches. *Front. Mar. Sci.* **2019**, *6*, 151. https://doi.org/10.3389/fmars.2019.00151.

(241) Vriend, P.; van Calcar, C.; Kooi, M.; Landman, H.; Pikaar, R.; van Emmerik, T. Rapid Assessment of Floating Macroplastic Transport in the Rhine. *Front. Mar. Sci.* **2020**, *7*, 10.

(242) Schirinzi, G. F.; Köck-Schulmeyer, M.; Cabrera, M.; González-Fernández, D.; Hanke, G.; Farré, M.; Barceló, D. Riverine Anthropogenic Litter Load to the Mediterranean Sea near the Metropolitan Area of Barcelona, Spain. *Sci. Total Environ.* **2020**, *714*, 136807. https://doi.org/https://doi.org/10.1016/j.scitotenv.2020.136807.

(243) Wang, L.; Whiting, E. Buoyancy Optimization for Computational Fabrication. *Comput. Graph. Forum* **2016**, *35* (2), 49–58.

(244) Acha, E. M.; Mianzan, H. W.; Iribarne, O.; Gagliardini, D. A.; Lasta, C.; Daleo, P. The Role of the Rı́o de La Plata Bottom Salinity Front in Accumulating Debris. *Mar. Pollut. Bull.* **2003**, *46* (2), 197–202. https://doi.org/https://doi.org/10.1016/S0025-326X(02)00356-9.

(245) Besseling, E.; Quik, J. T. K.; Sun, M.; Koelmans, A. A. Fate of Nano- and Microplastic in Freshwater Systems: A Modeling Study. *Environ. Pollut.* **2017**, *220* (Pt A), 540–548.

(246) Nizzetto, L.; Bussi, G.; Futter, M. N.; Butterfield, D.; Whitehead, P. G. A

Theoretical Assessment of Microplastic Transport in River Catchments and Their Retention by Soils and River Sediments. *Environ. Sci. Process. Impacts* **2016**, *18* (8), 1050–1059.

(247) Miller, R. Z.; Watts, A. J. R.; Winslow, B. O.; Galloway, T. S.; Barrows, A. P. W. Mountains to the Sea: River Study of Plastic and Non-Plastic Microfiber Pollution in the Northeast USA. *Mar. Pollut. Bull.* **2017**, *124* (1), 245–251. https://doi.org/10.1016/j.marpolbul.2017.07.028.

(248) Schmidt, C.; Krauth, T.; Wagner, S. Export of Plastic Debris by Rivers into the Sea. *Environ. Sci. Technol.* **2017**, *51* (21), 12246–12253. https://doi.org/10.1021/acs.est.7b02368.

(249) Lechner, A.; Keckeis, H.; Lumesberger-Loisl, F.; Zens, B.; Krusch, R.; Tritthart, M.; Glas, M.; Schludermann, E. The Danube so Colourful: A Potpourri of Plastic Litter Outnumbers Fish Larvae in Europe's Second Largest River. *Environ. Pollut.* **2014**, *188*, 177–181. https://doi.org/10.1016/j.envpol.2014.02.006.

(250) Liedermann, M.; Gmeiner, P.; Pessenlehner, S.; Haimann, M.; Hohenblum, P.; Habersack, H. A Methodology for Measuring Microplastic Transport in Large or Medium Rivers. *Water* **2018**, *10* (4), 414.

(251) Dris, R.; Gasperi, J.; Rocher, V.; Tassin, B. Synthetic and Non-Synthetic Anthropogenic Fibers in a River under the Impact of Paris Megacity: Sampling Methodological Aspects and Flux Estimations. *Sci. Total Environ.* **2018**, *618*, 157–164.

(252) von Kunststoffen in der Donau in Österreich, U. Z. V. Plastik in Der Donau.

(253) Morritt, D.; Stefanoudis, P. V; Pearce, D.; Crimmen, O. A.; Clark, P. F. Plastic in the Thames: A River Runs through It. *Mar. Pollut. Bull.* **2014**, *78* (1), 196–200.

(254) Lenaker, P. L.; Baldwin, A. K.; Corsi, S. R.; Mason, S. A.; Reneau, P. C.; Scott, J. W. Vertical Distribution of Microplastics in the Water Column and Surficial Sediment from the Milwaukee River Basin to Lake Michigan. *Environ. Sci. Technol.* **2019**, *53* (21), 12227–12237. https://doi.org/10.1021/acs.est.9b03850.

(255) Rouse, H. Modern Conceptions of the Mechanics or Fluid Turbulence. *Trans. Am. Soc. Civ. Eng.* **1937**, *102* (1), 463–505.

(256) Hutchens, J. J.; Wallace, J. B.; Grubaugh, J. W. Transport and Storage of Fine Particulate Organic Matter. In *Methods in Stream Ecology*; Elsevier,

2017; pp 37–53. https://doi.org/10.1016/B978-0-12-813047-6.00003-6.

(257) Drummond, J. D.; Davies-Colley, R. J.; Stott, R.; Sukias, J. P.; Nagels, J. W.; Sharp, A.; Packman, A. I. Retention and Remobilization Dynamics of Fine Particles and Microorganisms in Pastoral Streams. *Water Res.* **2014**, *66*, 459–472. https://doi.org/10.1016/j.watres.2014.08.025.

(258) Osipov, V. I. Density of Clay Minerals. *Soil Mech. Found. Eng.* **2012**, *48* (6), 231–240.

(259) Edwards, T. K.; Glysson, G. D.; Guy, H. P.; Norman, V. W. *Field Methods for Measurement of Fluvial Sediment*; US Geological Survey Denver, CO, 1999.

(260) Leeuw, J.; Lamb, M. P.; Parker, G.; Moodie, A. J.; others. Entrainment and Suspension of Sand and Gravel. *Earth Surf. Process. Landforms* **2020**.

(261) Lamb, M. P.; de Leeuw, J.; Fischer, W. W.; Moodie, A. J.; Venditti, J. G.; Nittrouer, J. A.; Haught, D.; Parker, G. Mud in Rivers Transported as Flocculated and Suspended Bed Material. *Nat. Geosci.* **2020**, *13* (8), 566–570.

(262) Density of Plastics Material: Technical Properties Table. https://omnexus.specialchem.com/polymer-properties/properties/density

(263) Sundby, S. Factors Affecting the Vertical Distribution of Eggs. In *{ICES} Marine Science Symposia*; ices.dk, 1991; Vol. 192, pp 33–38.

(264) Zaat, L.-A. Below the Surface A Laboratorial Research to the Vertical Distribution of Buoyant Plastics in Rivers, Delft University of Technology, 2020.

(265) Waldschläger, K.; Lechthaler, S.; Stauch, G.; Schüttrumpf, H. The Way of Microplastic through the Environment - Application of the Source-Pathway-Receptor Model (Review). *Sci. Total Environ.* **2020**, *713*, 136584. https://doi.org/10.1016/j.scitotenv.2020.136584.

(266) Parker, G. 1D Sediment Transport Morphodynamics with Applications to Rivers and Turbidity Currents. *E-b. available Gary Park. Morphodynamics Web Page, last Updat. April* **2004**, *13*, 2006.

(267) Rijn, V. *Principles of Sediment Transport in Rivers, Estuaries and Coastal Seas*; 1993.

(268) Wiberg, P. L.; Smith, J. D. Velocity Distribution and Bed Roughness in

High-Gradient Streams. *Water Resour. Res.* **1991**, *27* (5), 825–838.

(269) Dingman, S. L. *Fluvial Hydraulics*; oxford university press, 2009.

(270) Yifan, Y.; Xiaozhou, X.; W., M. B.; W., S. T. Flow Redistribution at Bridge Contractions in Compound Channel for Extreme Hydrological Events and Implications for Sediment Scour. *J. Hydraul. Eng.* **2021**, *147* (3), 4021005. https://doi.org/10.1061/(ASCE)HY.1943-7900.0001861.

(271) Vargas-Luna, A.; Crosato, A.; Uijttewaal, W. S. J. Effects of Vegetation on Flow and Sediment Transport: Comparative Analyses and Validation of Predicting Models. *Earth Surf. Process. Landforms* **2015**, *40* (2), 157–176. https://doi.org/10.1002/esp.3633.

(272) Bennett, S. J.; Wu, W.; Alonso, C. V.; Wang, S. S. Y. Modeling Fluvial Response to In-Stream Woody Vegetation: Implications for Stream Corridor Restoration. *Earth Surf. Process. Landforms* **2008**, *33* (6), 890–909. https://doi.org/10.1002/esp.1581.

(273) Chu Chia R.; Jirka Gerhard H. Wind and Stream Flow Induced Reaeration. *J. Environ. Eng.* **2003**, *129* (12), 1129–1136.

(274) McLean, S. R. On the Calculation of Suspended Load for Noncohesive Sediments. *Journal of Geophysical Research*. 1992, p 5759.

(275) Jirka, G. H.; Brutsaert, W. Measurements of Wind Effects on {Water-Side} Controlled Gas Exchange in Riverine Systems. In *Gas Transfer at Water Surfaces*; Brutsaert, W., Jirka, G. H., Eds.; Springer Netherlands: Dordrecht, 1984; pp 437–446.

(276) Whipple, K. {IV}. Essentials of Sediment Transport. 2004.

(277) Makaske, B. Anastomosing Rivers: A Review of Their Classification, Origin and Sedimentary Products. *Earth-Sci. Rev.* **2001**, *53* (3), 149–196.

(278) Phillips, C. B.; Jerolmack, D. J. Self-Organization of River Channels as a Critical Filter on Climate Signals. *Science (80-.).* **2016**, *352* (6286), 694–697.

(279) Morrison, F. A. *An Introduction to Fluid Mechanics*; Cambridge University Press, 2013.

(280) Dietrich, W. E. Settling Velocity of Natural Particles. *Water Resour. Res.* **1982**, *18* (6), 1615–1626.

(281) Single Particles in a Fluid. In *Introduction to Particle Technology*; Rhodes,

M., Ed.; John Wiley & Sons, Ltd: Chichester, UK, 2008; pp 29–49.

(282) Baldwin, A. K.; Corsi, S. R.; Mason, S. A. Plastic Debris in 29 Great Lakes Tributaries: Relations to Watershed Attributes and Hydrology. *Environ. Sci. Technol.* **2016**, *50* (19), 10377–10385. https://doi.org/10.1021/acs.est.6b02917.

(283) Baldwin, A. K.; Corsi, S. R.; Mason, S. A. Plastic Debris in 29 Great Lakes Tributaries: Relations to Watershed Attributes and Hydrology. *Environ. Sci. Technol.* **2016**, *50* (19), 10377–10385.

(284) RStudio Team. RStudio: Integrated Development Environment for R. Boston, MA 2016.

(285) Wood, S. N. *Generalized Additive Models: An Introduction with R*, 2nd ed.; Chapman and Hall/CRC, 2017.

(286) Gray, J. R.; Glysson, G. D.; Edwards, T. E. Suspended-Sediment Samplers and Sampling Methods. *Sedimentation engineering: processes, measurements, modeling, and practise*. ASCE Publications: Reston, Virginia: USA 2008, pp 320–339.

(287) van Emmerik, T.; Strady, E.; Kieu-Le, T.-C.; Nguyen, L.; Gratiot, N. Seasonality of Riverine Macroplastic Transport. *Sci. Rep.* **2019**, *9* (1), 13549.

(288) Kooi, M.; Nes, E. H. van; Scheffer, M.; Koelmans, A. A. Ups and Downs in the Ocean: Effects of Biofouling on Vertical Transport of Microplastics. *Environ. Sci. Technol.* **2017**, *51* (14), 7963–7971.

(289) Zhang, H. Transport of Microplastics in Coastal Seas. *Estuar. Coast. Shelf Sci.* **2017**.

(290) Drummond, J. D.; Nel, H. A.; Packman, A. I.; Krause, S. Significance of Hyporheic Exchange for Predicting Microplastic Fate in Rivers. *Environ. Sci. Technol. Lett.* **2020**, *7* (10), 727–732. https://doi.org/10.1021/acs.estlett.0c00595.

(291) Hoellein, T. J.; Shogren, A. J.; Tank, J. L.; Risteca, P.; Kelly, J. J. Microplastic Deposition Velocity in Streams Follows Patterns for Naturally Occurring Allochthonous Particles. *Sci. Rep.* **2019**, *9* (1), 3740. https://doi.org/10.1038/s41598-019-40126-3.

(292) Stanton, T.; Johnson, M.; Nathanail, P.; MacNaughtan, W.; Gomes, R. L. Freshwater Microplastic Concentrations Vary through Both Space and

Time. *Environ. Pollut.* **2020**, *263*, 114481.

(293) Koelmans, A. A.; Redondo-Hasselerharm, P. E.; Mohamed Nor, N. H.; Kooi, M. Solving the Nonalignment of Methods and Approaches Used in Microplastic Research to Consistently Characterize Risk. *Environ. Sci. Technol.* **2020**, *54* (19), 12307–12315. https://doi.org/10.1021/acs.est.0c02982.

Appendix A – Chapter 2 supplemental information

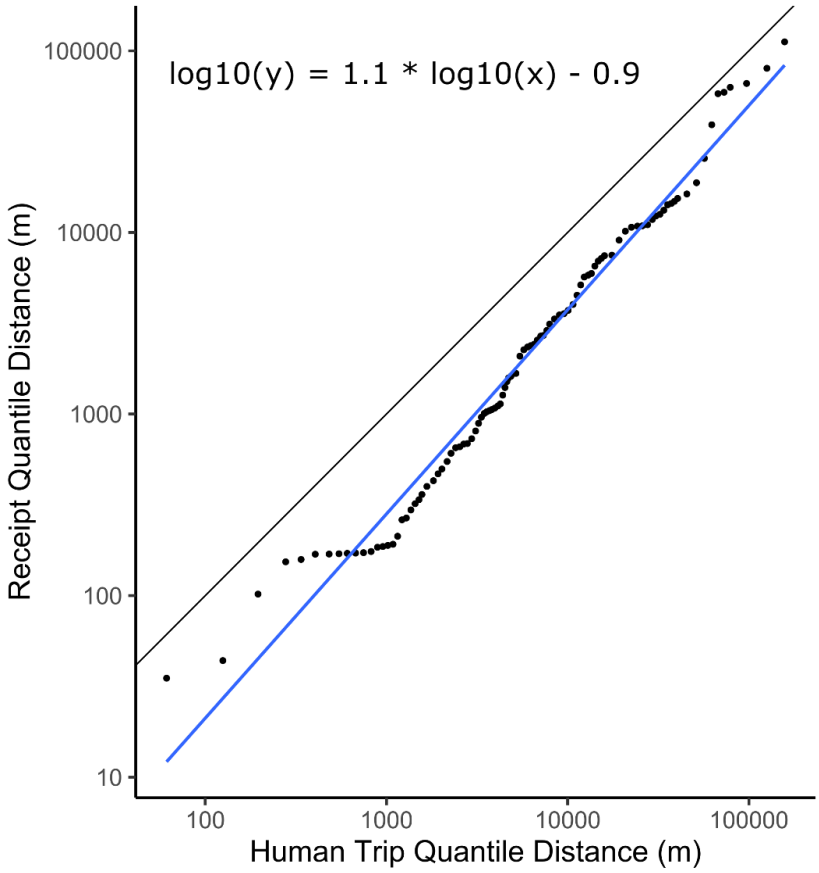

Figure A-1: Regression between paired quantile values for Human trip distances and Receipt transport distances. The equation for the blue line (the regression) is listed in the plot. Both axes and the equation are $\log_{10}$ scaled. The black line is a 1:1 line showing that the slope is similar between the paired quantiles, but there is an offset to smaller distances for the receipts.

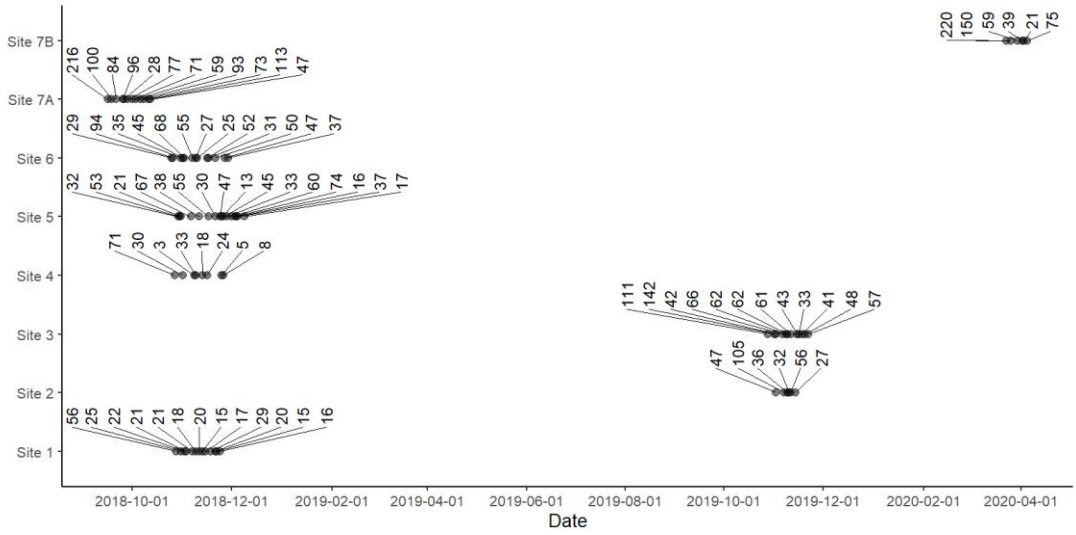

Figure A-2: Survey dates for at monitoring locations. Each point represents a survey. Total number of pieces of litter observed during the survey is plotted as a number connected to the survey date in order. Site 7 was repeated a year later and had a very similar initial standing stock of litter to the previous year (7A 2019: 216 pieces, 7B 2020: 220 pieces).

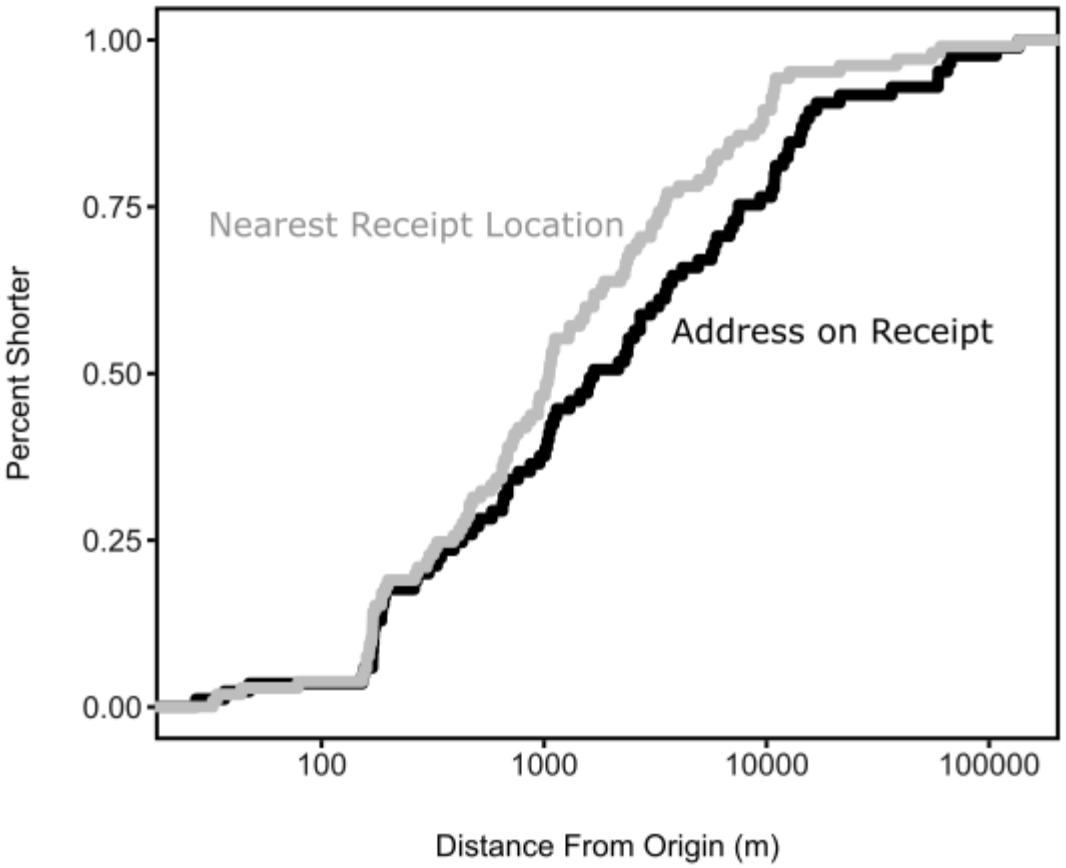

Figure A-3: Empirical cumulative distribution functions of the distance that receipts traveled from the sale location (black line) and the distance to the nearest possible sale location the receipt could have come from. People are not going to the nearest locations only to where the littering occurs they are also going to places slightly further, potentially along convenient paths during their daily commutes.

Appendix B – Chapter 3 supplemental information

Table B-1: Glossary definitions for terms used in the manuscript.

Term	**Definition**
Trash/Waste	Any object which no longer has a purpose.
Classification	Any type of system to describe trash
Harmonization	Facilitate comparative operations between existing and emerging surveys
Split	Separating one less spectific class into two or more more specific classes.
Lump	Taking two or more more specific classes and combining them into a less specific class that encompasses all.
Relational system	A system of connected relational tables
Relational table	A table with unique columns that contain a key term to be linked with terms in other relational tables in the relational system
Standardization	Prescribing one survey list, or a set of survey lists for different use cases
Class	A value used to describe a piece of litter (item, material, or brand)
Survey lists	List of classes used to describe trash in a list used when collecting samples
Survey type	A group of surveys based on ecosystem, organization, or Substrate focus.
Taxonomy	A suite of relational tables and tools that can be used to standardize and harmonize classification systems.

Table B-2: Some of the potential use cases of the Trash Taxonomy and the actions a user would need to achieve them.

Use Case	**Action**
Update a survey with more specific classes	Upload the current survey to the web tool. Click more specific items and materials. Choose from the options to replace less specific terms.
Create a brand new survey	Download the item and material hierarchy from the website and select words based on the needs of the study while avoiding overlapping terms. Add a class called "other" for things not in your list.
Expand the Trash Taxonomy	Download the misaligned class table and brand-item table and work on incorporating those classes into the framework.
Compare between the survey lists in this study	Download SI material in this study.
Combine two surveys using lumping.	Merge both surveys to the item and material hierarchies following the code shared in this publication.
Validate the web tool	Download material-item table from relational tables tab and upload to the query tool.

Table B-3: Average comparability metrics for each survey list (materials and items).

	Organization	Average Comparability Items (Proportion)	Average Comparability Materials (Proportion)
1	5gyres plastic beach microplastics protocol	0.07	0.27
2	aaas water diplomacy symposium list	0.45	0.56
3	abandoned and derelict vessels	0.00	0.17
4	baldhead island conservancy	0.45	0.56
5	blue ocean society for marine conservation	0.27	0.45
6	clean ocean access	0.34	0.01
7	cordeiro	0.06	0.04
8	corpus christi storm water runoff	0.45	0.56
9	cressida list english	0.02	0.00
10	debris items of local concern	0.06	0.00
11	deciduous trees	0.00	0.00
12	derelict crab trap list	0.00	0.17
13	derwent estuary list	0.36	0.56
14	dumping activities	0.03	0.00
15	exxpedition	0.39	0.56
16	fernandino	0.00	0.55
17	fish aggregating devices	0.00	0.17
18	fulbright vietnam project	0.28	0.37
19	ga sea turtle center	0.47	0.50
20	goal clean seas florida keys	0.46	0.56
21	gracia	0.03	0.44
22	icc data card	0.35	0.00
23	jrc	0.49	0.50

24	keep america beautiful	0.00	0.44
25	keep tampa bay beautiful	0.35	0.17
26	lee	0.04	0.49
27	lets do it world	0.46	0.50
28	marine conservation society	0.28	0.45
29	marine debris items	0.46	0.56
30	marine debris list	0.01	0.00
31	maryland department of the environment	0.14	0.00
32	mccormick	0.00	0.26
33	medical and personal hygiene	0.01	0.00
34	microplastics	0.03	0.27
35	nat geo source to sea expedition list	0.34	0.50
36	nelms	0.16	0.02
37	noaa	0.39	0.36
38	ocean and waterway activities	0.06	0.00
39	ocean conservancy	0.39	0.00
40	ocean conservancy icc list	0.41	0.20
41	oigman	0.00	0.45
42	open litter map	0.31	0.00
43	open ocean hourly observations	0.00	0.17
44	ospar	0.38	0.40
45	our ocean youth summit	0.01	0.17
46	project aware	0.39	0.50
47	rapid trash assessment	0.00	0.49
48	rech	0.01	0.60
49	rozalia project long list	0.41	0.56
50	rozalia project short list	0.31	0.56
51	sarasota dolphin research program debris team	0.45	0.56

52	seabin data collection	0.15	0.35
53	sea education association	0.45	0.56
54	shoreline and recreational activities	0.10	0.00
55	site assesment	0.06	0.00
56	smc	0.28	0.57
57	smoking related activities	0.02	0.00
58	sustainable seas trust	0.45	0.56
59	tetaitokerau debris monitoring project	0.44	0.54
60	the ocean race	0.38	0.31
61	tracking california's trash	0.14	0.00
62	usvi marine debris for noaa	0.45	0.56
63	vandervelde	0.23	0.41
64	vincent	0.00	0.17
65	waste receptacles	0.00	0.00
66	williams	0.12	0.00
67	willis	0.00	0.54
68	zylstra	0.08	0.00

Appendix C – Chapter 4 supplemental information

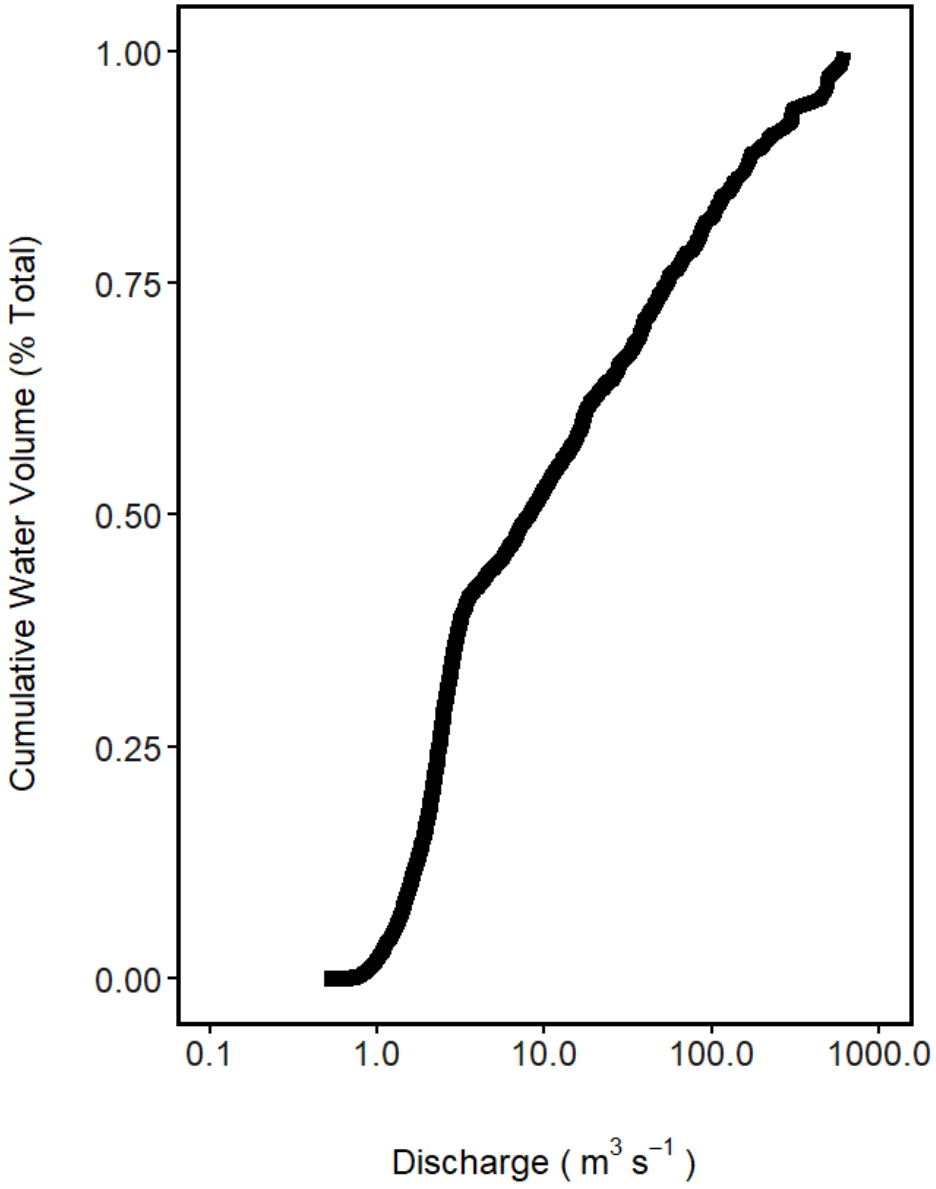

Figure C-1: Cumulative water flux m^3 by discharge (m^3s^{-1}) at the sample location from 1990-1-1 to 2019-12-31.

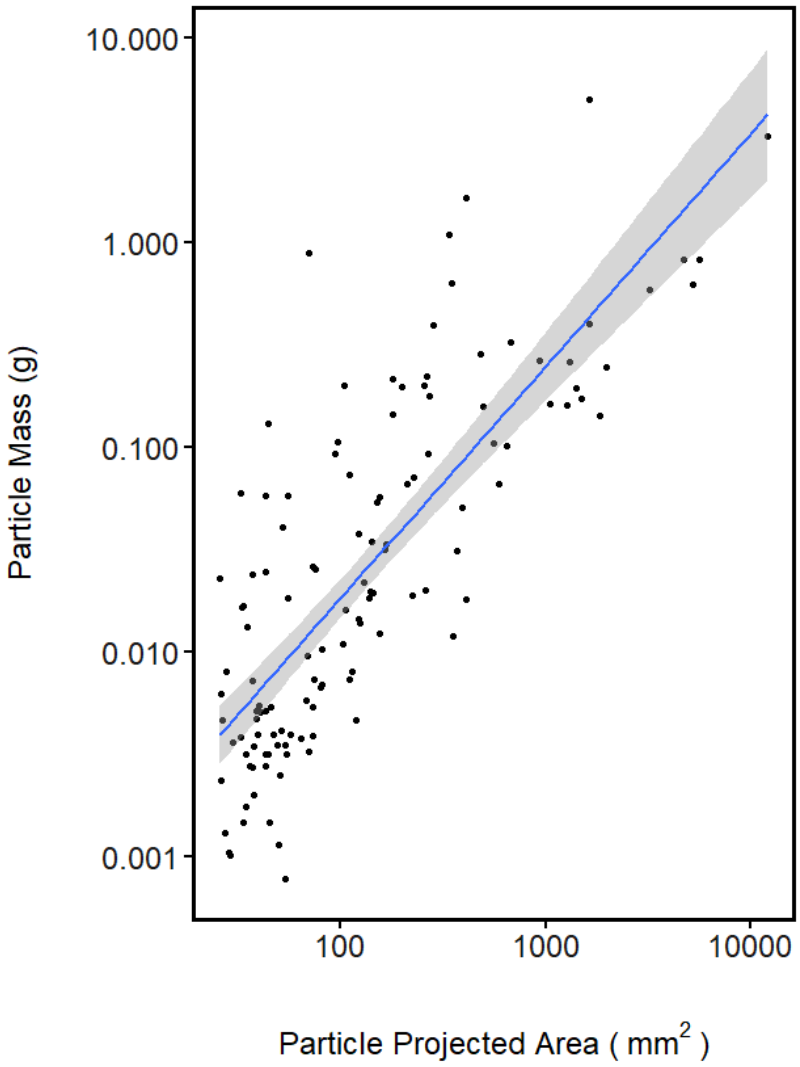

Figure C-2: Particle Mass (g) to projected Area (mm^2) linear relationship on log_{10} transformed data.

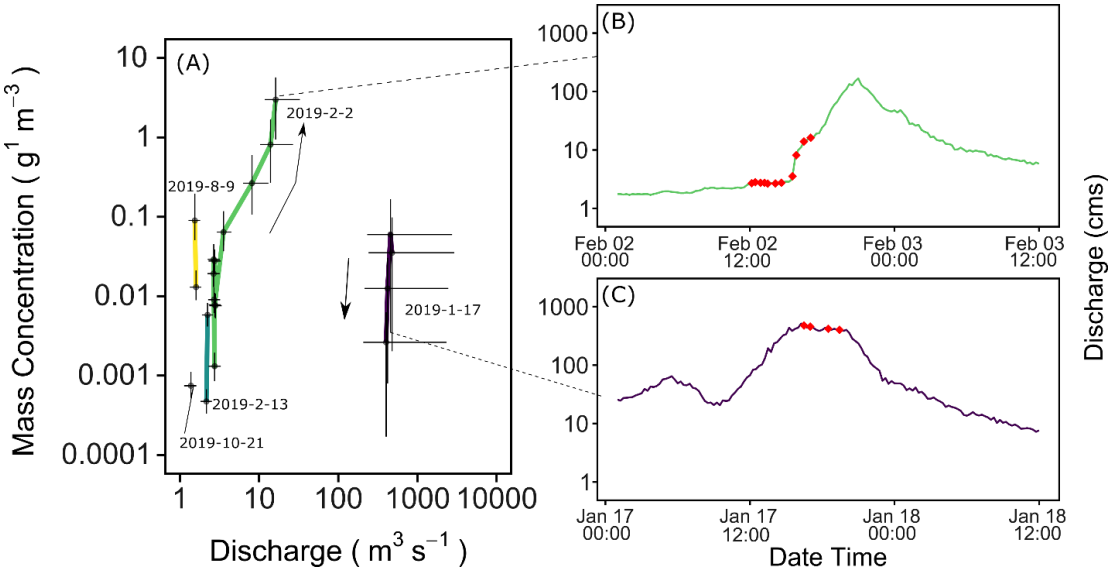

Figure C-3: Mass concentration hysteresis analysis. (A) lines around the points indicate bootstrapped uncertainties. Each sampling day has its of color and a line connects the samples by time of sampling. An arrow indicates the direction the concentration line is going through time. (B) Hydrograph during February 2nd event with sample times plotted as red dots on the hydrograph. (C) Hydrograph during January 17th event with sample times plotted as red dots on the hydrography.

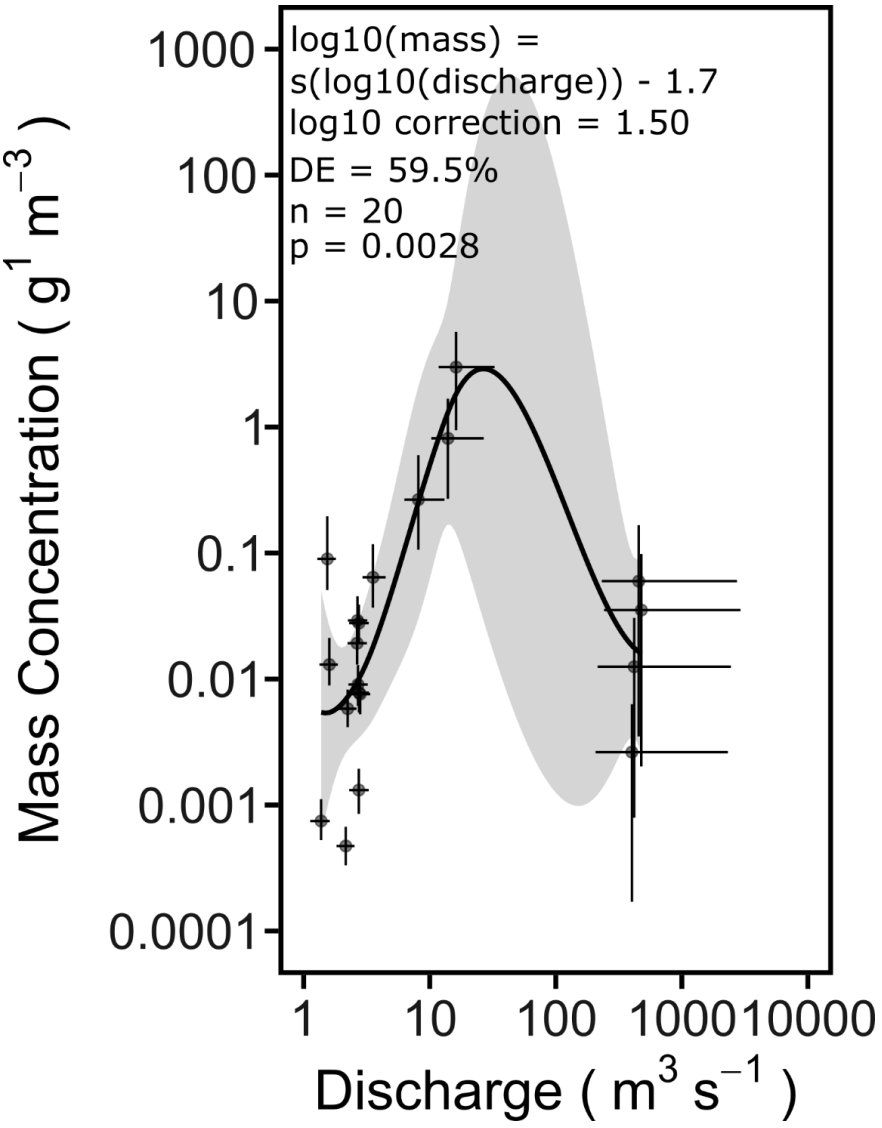

Figure C-4: Generalized additive model using discharge to predict mass concentration. Deviance explained, sample size, and p value for the smooth term are given. Uncertainties were bootstrapped around each observation and uncertainty range in discharge and concentration is given for each observation.

Appendix D – Chapter 6 supplemental information

Figure D-1: Central map of the United States with pull outs at sampling locations (green circles) in Lenaker et al. [254] (USGS sites 40870837 -S1A1- 4087000 -S1A2-). Northing arrows and scale bars in bottom right hand corner of each pop out.

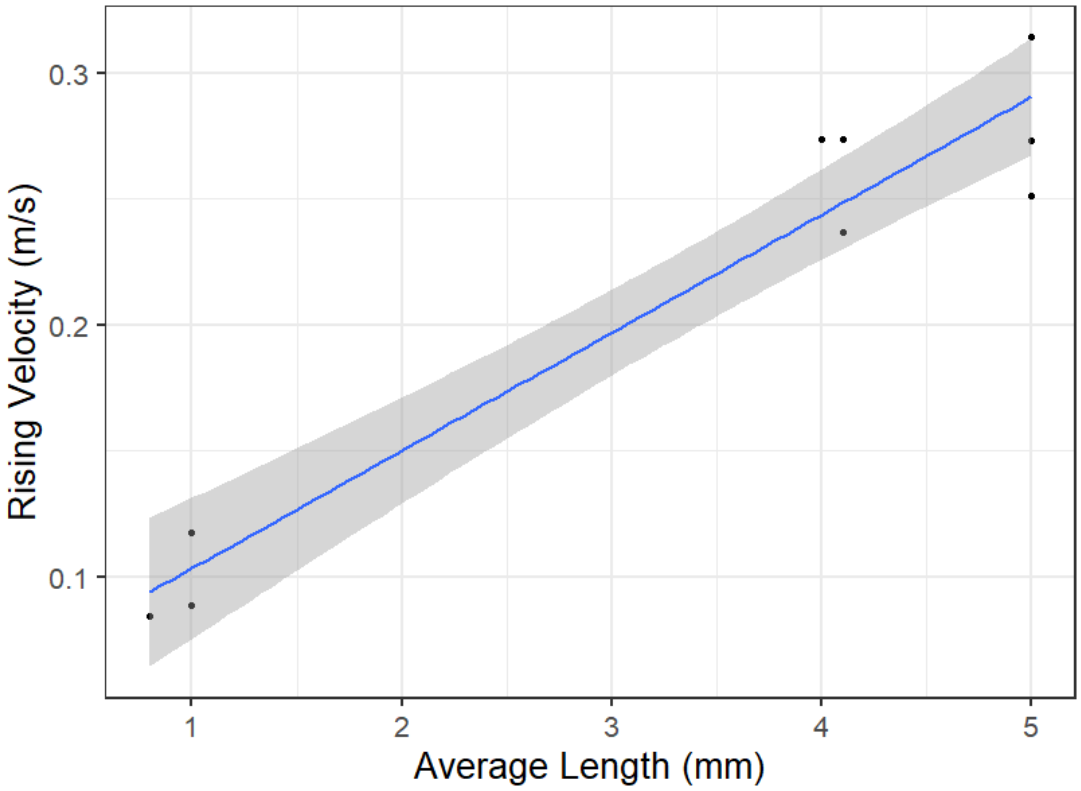

Figure D-2: General linear regression between particle size and rising velocity for foam particles from Waldschläger and Schüttrumpf.[51]

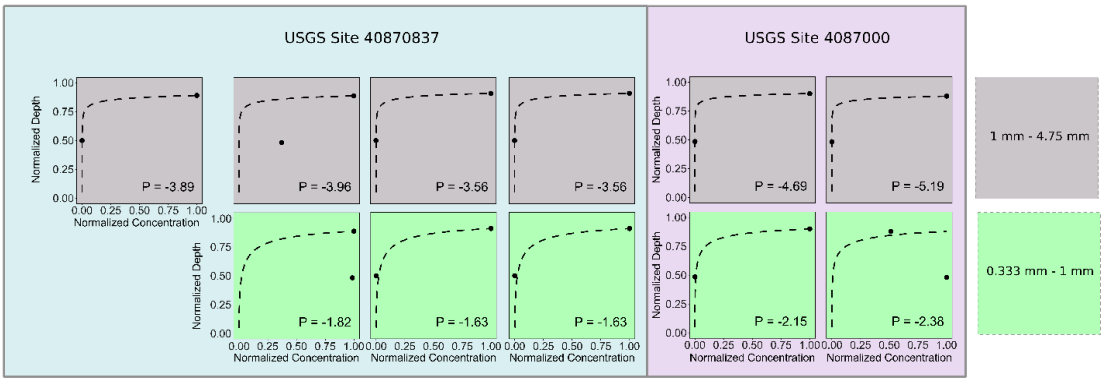

Figure D-3: Measured concentration depth profiles of foam particles at two locations (top axis) binned by particle size (right axis) using data from Lenaker et al.[254] (black dots). The black dashed line denotes the modeled Rouse profile concentration depth profile. Concentration and depth are maximum normalized (equation 7). Paired samples are directly above one another.